

Functional Tissue-based Therapy Response Prediction for Breast Cancer Patients



Titia Meijer

Functional Tissue-based Therapy Response Prediction for Breast Cancer Patients

Functionele weefsel-gebaseerde therapierespons voorspelling voor
borstkanker patiënten

Titia Geertje Meijer

ISBN: 978-94-6380-873-6
Printed by: ProefschriftMaken.nl
Cover: shutterstock.com
Lay-out: Dennis Hendriks / ProefschriftMaken.nl

© 2020, Titia Meijer

All rights reserved. No part of this thesis may be reproduced or transmitted in any form or by any means, electronically, mechanically, including photocopying, recording or by any information storage and retrieval system, without written permission of the author.

Functional Tissue-based Therapy Response Prediction for Breast Cancer Patients

Functionele weefsel-gebaseerde therapierespons voorspelling voor
borstkanker patiënten

Proefschrift

ter verkrijging van de graad van doctor aan de
Erasmus Universiteit Rotterdam
op gezag van de rector magnificus
Prof.dr. R.C.M.E. Engels
en volgens het besluit van het College voor Promoties.
De openbare verdediging zal plaatsvinden op

28 oktober om 11:30 uur

Titia Geertje Meijer

geboren op 22 november 1989
te Zwolle

Promotor:

Prof. dr. R. Kanaar

Co-promotoren:

Dr. A. Jager

Dr. D.C. van Gent

Overige leden leescommissie:

Dr. C.H.M. van Deurzen

Prof. dr. J.W.M. Martens

Prof. dr. M.A.T.M. van Vugt

List of content

Chapter 1	Introduction	1
Chapter 2	<i>Ex vivo</i> tumor culture systems for functional drug testing and therapy response prediction	13
Chapter 3	Functional <i>ex vivo</i> assay reveals homologous recombination deficiency in breast cancer beyond BRCA gene defects	37
Chapter 4	Direct <i>ex vivo</i> observation of homologous recombination defect reversal after DNA damaging chemotherapy in metastatic breast cancer patients	69
Chapter 5	RECAP identifies homologous recombination deficiency in breast cancers undetected by DNA-based BRCAness tests	95
Chapter 6	<i>Ex vivo</i> tissue-based cisplatin testing on metastatic breast cancer biopsies	125
Chapter 7	Functional homologous recombination screening of breast and ovarian cancer cell lines	157
Chapter 8	Summary, general discussion and future perspectives	187

A large, dark, textured splash of ink or paint on a white background. The splash is irregular and has a rough, layered appearance, with various shades of gray and black. The text "Chapter 1" is centered in white, bold, sans-serif font.

Chapter 1

Introduction

Introduction

Breast cancer

Breast cancer (BC) is the most common malignancy in women with the second highest cancer related mortality rate ^[1]. BC is a heterogeneous disease and comprises different subtypes defined by immunohistochemistry: estrogen receptor (ER) and/or progesterone receptor (PR) positive BC, BC with human epidermal growth factor receptor 2 (HER2) amplification and triple negative breast cancer (TNBC), which is characterized by the absence of expression of ER/PR/HER2. Another method for categorizing BC is by their distinct molecular patterns, which classifies BC into five intrinsic subtypes with variable clinical outcomes: luminal A, luminal B, HER2 over-expression, basal and normal-like tumors ^[2,3].

Most BCs occur sporadically, but in approximately 15-20% of the cases there is a positive family history for the disease ^[4]. These so-called familial BCs often have germline mutations in one of several BC susceptibility genes (*BRCA1*, *BRCA2*, *CHEK2*, *PALB2*, *PTEN*, *TP53* and *ATM*)^[5]. However, in more than half of the familial BC cases these genes remained unaffected, thus the underlying genetic variation causing the increased BC risk remains unknown. Approximately 3% of all BC cases are due to germline mutations in *BRCA1/2* ^[6], and in TNBC this percentage is even 10-20% ^[7].

Prediction of therapy response

Various systemic therapies, ranging from classic chemotherapy to personalized targeted treatments, are available for BC treatment. Proper selection of patients who are most likely to benefit from these treatment regimens is of utmost importance. Biomarker-driven research has yielded strong predictive biomarkers that correlate with patient response to a certain drug. For example, the monoclonal antibody trastuzumab, targeting HER2, dramatically improved survival for patients with BC overexpressing HER2 ^[8]. However, predictive biomarkers for classic chemotherapies do not yet exist.

Besides specific molecular markers (e.g. *EGFR* mutation status in non-small cell lung cancer ^[9], *BRCA* mutation status in BC ^[10]), the field of biomarker discovery has moved to genomic, transcriptional and proteomic predictive signatures ^[11-13]. More recently, whole-genome sequencing was exploited to characterize individual patients and predict therapy response ^[5, 14-17]. However, validation of these biomarkers and subsequent integration in the diagnostic process are major bottle-necks that require extensive research. For example, there are concerns regarding turn-around time of the generation of these biomarkers, what to do with variants of unknown significance, whether the tests detect historic events or reflect real-time tumor characteristics and how to cope with complex data analyses.

BRCA and Homologous Recombination

Germline *BRCA1/2* mutation status is the predictive biomarker for PARP inhibitor treatment [18-20]. The *BRCA1/2* genes are essential for the repair of DNA double strand breaks (DSB) through the homologous recombination (HR) pathway. If the DSBs are left unrepaired, this will lead to genomic instability and eventually cell death [21]. The HR pathway ensures error-free repair of DSBs during S- and G2-phase of the cell cycle [22] (Figure 1). RAD51 is one of the proteins involved in this pathway and forms a nucleoprotein filament around the single-stranded DNA flanking the DSB, promoting the strand exchange with the sister chromatid for the repair (Figure 1). In HR deficient (HRD) tumors the HR pathway is not capable of repairing the DSBs. Besides germline *BRCA1/2* mutations, HRD can also be caused by somatic *BRCA1/2* mutations and *BRCA1* promoter hypermethylation, as well as via other mechanisms than loss of *BRCA* (e.g. PALB2 inactivation [23]). It has been shown that BRCA deficient tumors respond well to PARP inhibitor treatment [18, 19], which works via the concept of synthetic lethality.

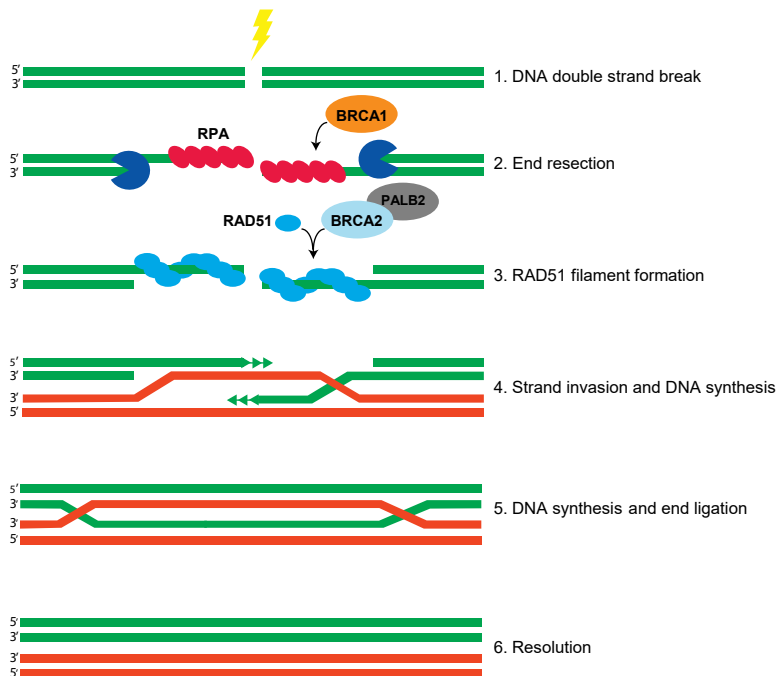


Figure 1: The homologous recombination (HR) pathway ensures error-free repair of DSBs. HR occurs during S and G2 phase of the cell cycle, as the sister chromatid is then present to serve as a template to faithfully restore the DNA. When a DSB has arisen, due to irradiation or DSB causing chemotherapy, the first step towards DNA repair via the HR pathway is end-resection, resulting in single-stranded DNA through 5'-3' exonucleolytic activity. During this step, multiple proteins are involved, including BRCA1. This single-stranded DNA is coated by RPA, which is subsequently replaced by RAD51. RAD51 loading on the DNA is mediated by BRCA2 and PALB2. RAD51 forms a nucleoprotein filament around the single-stranded DNA, which allows strand invasion of the sister chromatid and D-loop formation. Lastly, the invading 3' strand is elongated by DNA polymerases and the DSB is resolved. The HR pathway is comprised of multiple sub-pathways [34], and for simplicity only one (the DSBR model [35]) is schematically depicted here.

Synthetic lethality and PARP inhibition

Synthetic lethality occurs when there is a combination of two deficiencies, while only one of these deficiencies is still compatible with life. More specifically, in case of PARP inhibition, the combination of HRD and inhibition of the PARP enzyme leads to specific tumor cell killing (Figure 2). The PARP enzyme is involved in DNA repair of DNA single strand breaks (SSB). Through PARP inhibition, SSBs are not repaired as efficiently anymore and upon DNA replication these SSBs are converted to DSBs, which require the HR pathway for their repair^[24, 25]. In addition, PARP inhibition leads to trapping of PARP molecules on the DNA, thereby preventing DNA replication and transcription, leading to cell death. In tumor cells of *BRCA1/2* gene mutation carriers both *BRCA* alleles are affected, leading to HRD, which in combination with PARP inhibition leads to specific cell death. In healthy cells of *BRCA1/2* gene mutation carriers only one of the two alleles is affected, leaving the HR pathway intact and consequently the healthy cells remain unharmed as synthetic lethality does not occur (Figure 2). Thus, PARP inhibitors offer an elegant and targeted treatment for HRD tumors.

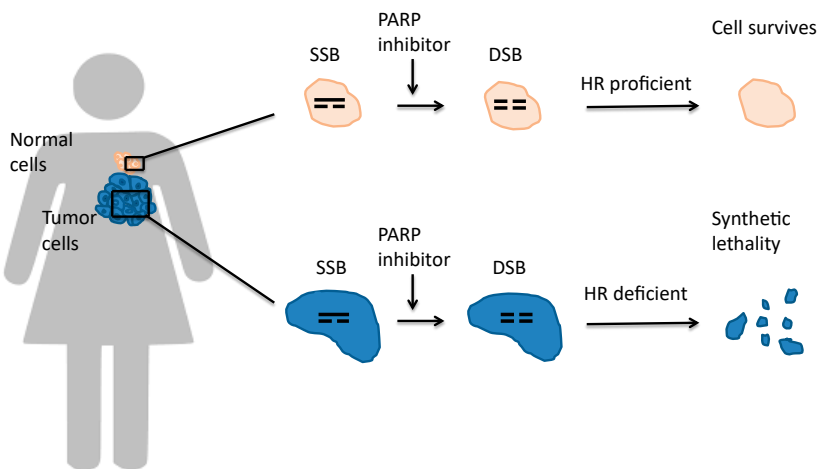


Figure 2: Mechanism of PARP inhibition. Single strand DNA breaks (SSBs) occur frequently and require Poly(ADP-ribose) polymerase I (PARP-I) for efficient repair. Upon treatment with a PARP-inhibitor, the SSBs repair is attenuated and as a consequence unrepaired SSBs convert into double strand DNA breaks (DSBs) upon DNA replication. These DSBs require the HR pathway for their repair. However, if the HR pathway is not properly functioning (i.e. HR deficiency), the DSBs cannot accurately be repaired and will accumulate, leading to cell death.

Germline *BRCA1/2* mutation status is currently the only predictive biomarker for PARP inhibitor treatment. However, the population of BC patients who could benefit from PARP inhibitor treatment can be enlarged through patient selection based on the HRD status of the tumor, instead of germline *BRCA* mutation status. Various HRD tests have been developed to identify HRD tumors in addition to germline *BRCA* mutated tumors^[15, 26-28].

In this thesis, the REpair CAPacity (RECAP) test is presented, a functional assay exploiting the formation of RAD51 foci in proliferating cells after *ex vivo* irradiation of fresh BC tissue [27, 29, 30].

Tissue-based functional analyses

As therapy response often cannot be predicted accurately by a single genetic marker only, alternative ways of patient stratification are needed. Beyond mutational status, many other factors influence tumor behavior and therapy response, for example epigenetic factors and the tumor microenvironment [31, 32]. For instance, although HER2 amplification is a strong predictive marker of response to trastuzumab in BC patients, its predictive value in gastric cancer is much weaker [33]. Therefore, the current difficulty to translate genetic information to tumor behavior necessitates development of tools to select patients for therapies based on tumor phenotype rather than genotype. *Ex vivo* assays that predict therapy response may fill this knowledge gap.

Prediction of individual treatment responses by functional *ex vivo* assays require a viable sample from the tumor, which is then cultivated in the laboratory and exploited for drug screening or other *ex vivo* functional testing. The model systems derived from viable tumor samples should closely resemble the *in vivo* tumor characteristics and microenvironment. A broad spectrum of model systems, ranging from classic 2D monolayer culture techniques to more experimental 'cancer-on-chip' procedures, are discussed in chapter 2. Organotypic tissue slices are the model system used for the functional *ex vivo* assays described in this thesis.

The aims and scope of this thesis

The general aim of this thesis is to improve biomarker development and therapy response prediction for BC patients using functional tissue-based assays.

Chapter 1 introduces BC and more specifically elaborates on *BRCA* gene defects and prediction of therapy response.

Chapter 2 provides an overview of *ex vivo* tumor culture systems for functional drug testing and therapy response prediction. This review article highlights the advantages and disadvantages of several *ex vivo* tumor culture systems such as primary cultures, spheroids, organoids and tissue slices.

The aim of the study described in **chapter 3** is to validate the REpair CAPacity (RECAP) test, a functional assay exploiting the formation of RAD51 foci in proliferating cells after *ex vivo* irradiation of fresh BC tissue, in an extensive cohort of primary BCs and provide evidence that this functional test is achievable in a pseudo-clinical setting. Additionally, thorough

molecular characterization of the HRD phenotype is performed, proving that HRD tumors encompass more than only BRCA deficiencies.

In **chapter 4** we aim to show feasibility of the RECAP test on biopsies from metastatic BC lesions to enhance the diagnostic potential and clinical applicability of this test. Next, we aim to find a molecular explanation for the observed HRD phenotype and we explore the utility of the RECAP test as a predictive tool for treatment with DSB inducing agents and PARP inhibitors in this setting. This chapter demonstrates that functional HR assessment by the RECAP test produces a unique real-time measure of the HR status.

In **chapter 5**, we investigate whether the HRD tumors, especially the non-BRCA related HRD tumors, identified by the RECAP test would also be detected by other HRD tests. To this end, a large cohort (n=71) of breast tumors with known functional HR status, measured by RECAP, is subjected to other genomic scar based HRD tests (BRCA1/2-like classifier and CHORD). For a subset (n=54) whole genome sequencing is performed to further characterize HRD tumors and especially the non-BRCA related HRD tumors. For a small subset HRD status is linked to clinical outcome data.

Chapter 6 describes the development of an *ex vivo* sensitivity assay for DSB inducing anticancer drugs (in particular cisplatin) on histological biopsies. First, we establish the optimal conditions for the *ex vivo* sensitivity assay in organotypic tissue slices from patient derived xenograft (PDX) tumors with known *in vivo* cisplatin sensitivity. The next step is to perform *ex vivo* treatment on organotypic tissue slices from primary breast tumors as well as from histological biopsies of metastatic BC lesions. We compare the results of the *ex vivo* sensitivity assay to several parameters associated with cisplatin response, such as BRCA mutation, TNBC and HR status. Finally, the *ex vivo* responses are correlated with the *in vivo* responses among those patients who were subsequently treated with a platinum containing chemotherapeutic regimen.

In **chapter 7**, we perform a comprehensive characterization of our large collection of breast and ovarian cancer cell lines to identify the functional HR status and to study the discrepancies between functional HR and BRCA mutation status. We hypothesized that the functional HRD status of cell lines would better reflect the real-time HR status of the cell line at the time of testing than BRCA mutation status. The functional HRD status is correlated to gene expression and methylation data for a panel of known HRD genes, as well as to drug sensitivity outcomes for veliparib and platinum based chemotherapies.

References

1. Siegel RL, Miller KD, Jemal A. Cancer statistics, 2019. *CA Cancer J Clin* 2019; 69: 7-34.
2. Perou CM, Sorlie T, Eisen MB et al. Molecular portraits of human breast tumours. *Nature* 2000; 406: 747-752.
3. Sorlie T, Perou CM, Tibshirani R et al. Gene expression patterns of breast carcinomas distinguish tumor subclasses with clinical implications. *Proc Natl Acad Sci U S A* 2001; 98: 10869-10874.
4. Pasche B. Recent advances in breast cancer genetics. *Cancer Treat Res* 2008; 141: 1-10.
5. Nones K, Johnson J, Newell F et al. Whole-genome sequencing reveals clinically relevant insights into the aetiology of familial breast cancers. *Ann Oncol* 2019; 30: 1071-1079.
6. Nelson HD, Fu R, Goddard K et al. 2013.
7. Hartman AR, Kaldate RR, Sailer LM et al. Prevalence of BRCA mutations in an unselected population of triple-negative breast cancer. *Cancer* 2012; 118: 2787-2795.
8. Moja L, Tagliabue L, Balduzzi S et al. Trastuzumab containing regimens for early breast cancer. *Cochrane Database Syst Rev* 2012; CD006243.
9. Veale D, Ashcroft T, Marsh C et al. Epidermal growth factor receptors in non-small cell lung cancer. *Br J Cancer* 1987; 55: 513-516.
10. Tung NM, Garber JE. BRCA1/2 testing: therapeutic implications for breast cancer management. *Br J Cancer* 2018; 119: 141-152.
11. Chang JC, Wooten EC, Tsimelzon A et al. Gene expression profiling for the prediction of therapeutic response to docetaxel in patients with breast cancer. *Lancet* 2003; 362: 362-369.
12. De Marchi T, Liu NQ, Stingl C et al. 4-protein signature predicting tamoxifen treatment outcome in recurrent breast cancer. *Mol Oncol* 2016; 10: 24-39.
13. Spentzos D, Levine DA, Kolia S et al. Unique gene expression profile based on pathologic response in epithelial ovarian cancer. *J Clin Oncol* 2005; 23: 7911-7918.
14. Angus L, Smid M, Wilting SM et al. The genomic landscape of metastatic breast cancer highlights changes in mutation and signature frequencies. *Nat Genet* 2019.
15. Davies H, Glodzik D, Morganella S et al. HRDetect is a predictor of BRCA1 and BRCA2 deficiency based on mutational signatures. *Nat Med* 2017; 23: 517-525.
16. Nik-Zainal S, Davies H, Staaf J et al. Landscape of somatic mutations in 560 breast cancer whole-genome sequences. *Nature* 2016; 534: 47-54.
17. Staaf J, Glodzik D, Bosch A et al. Whole-genome sequencing of triple-negative breast cancers in a population-based clinical study. *Nat Med* 2019.
18. Litton JK, Rugo HS, Ettl J et al. Talazoparib in Patients with Advanced Breast Cancer and a Germline BRCA Mutation. *N Engl J Med* 2018; 379: 753-763.
19. Robson M, Im SA, Senkus E et al. Olaparib for Metastatic Breast Cancer in Patients with a Germline BRCA Mutation. *N Engl J Med* 2017; 377: 523-533.

20. Tutt A, Robson M, Garber JE et al. Oral poly(ADP-ribose) polymerase inhibitor olaparib in patients with BRCA1 or BRCA2 mutations and advanced breast cancer: a proof-of-concept trial. *Lancet* 2010; 376: 235-244.
21. Hiom K. Coping with DNA double strand breaks. *DNA Repair (Amst)* 2010; 9: 1256-1263.
22. Saleh-Gohari N, Helleday T. Conservative homologous recombination preferentially repairs DNA double-strand breaks in the S phase of the cell cycle in human cells. *Nucleic Acids Res* 2004; 32: 3683-3688.
23. Li A, Geyer FC, Bleuca P et al. Homologous recombination DNA repair defects in PALB2-associated breast cancers. *NPJ Breast Cancer* 2019; 5: 23.
24. Mateo J, Lord CJ, Serra V et al. A decade of clinical development of PARP inhibitors in perspective. *Ann Oncol* 2019; 30: 1437-1447.
25. Pilié PG, Gay CM, Byers LA et al. PARP Inhibitors: Extending Benefit Beyond BRCA-Mutant Cancers. *Clin Cancer Res* 2019; 25: 3759-3771.
26. Lips EH, Mulder L, Hannemann J et al. Indicators of homologous recombination deficiency in breast cancer and association with response to neoadjuvant chemotherapy. *Ann Oncol* 2011; 22: 870-876.
27. Meijer TG, Verkaik NS, Sieuwerts AM et al. Functional *Ex vivo* Assay Reveals Homologous Recombination Deficiency in Breast Cancer Beyond BRCA Gene Defects. *Clin Cancer Res* 2018; 24: 6277-6287.
28. Vollebergh MA, Lips EH, Nederlof PM et al. An aCGH classifier derived from BRCA1-mutated breast cancer and benefit of high-dose platinum-based chemotherapy in HER2-negative breast cancer patients. *Ann Oncol* 2011; 22: 1561-1570.
29. Naipal KA, Verkaik NS, Ameziane N et al. Functional *ex vivo* assay to select homologous recombination-deficient breast tumors for PARP inhibitor treatment. *Clin Cancer Res* 2014; 20: 4816-4826.
30. Meijer TG, Verkaik NS, Deurzen van CHMv et al. Direct *Ex vivo* Observation of Homologous Recombination Defect Reversal After DNA-Damaging Chemotherapy in Patients With Metastatic Breast Cancer. *JCO Precision Oncology* 2019; 1-12.
31. Alizadeh AA, Aranda V, Bardelli A et al. Toward understanding and exploiting tumor heterogeneity. *Nat Med* 2015; 21: 846-853.
32. Marks DL, Olson RL, Fernandez-Zapico ME. Epigenetic control of the tumor microenvironment. *Epigenomics* 2016; 8: 1671-1687.
33. Kelly CM, Janjigian YY. The genomics and therapeutics of HER2-positive gastric cancer-from trastuzumab and beyond. *J Gastrointest Oncol* 2016; 7: 750-762.
34. Ceccaldi R, Rondinelli B, D'Andrea AD. Repair Pathway Choices and Consequences at the Double-Strand Break. *Trends Cell Biol* 2016; 26: 52-64.
35. Szostak JW, Orr-Weaver TL, Rothstein RJ, Stahl FW. The double-strand-break repair model for recombination. *Cell* 1983; 33: 25-35.



A large, dark, textured splash of ink or paint on a white background. The splash is irregular and has a rough, layered appearance, with various shades of gray and black. The text "Chapter 2" is centered in white, bold, sans-serif font.

Chapter 2

Ex vivo tumor culture systems for functional drug testing and therapy response prediction

Titia G. Meijer¹, Kishan A.T. Naipal¹, Agnes Jager² and Dik C. van Gent¹

¹ *Department of Molecular Genetics, Erasmus University Medical Center, Rotterdam, The Netherlands.*

² *Department of Medical Oncology, Erasmus MC Cancer Institute, Erasmus University Medical Center, Rotterdam, The Netherlands.*

Abstract

Optimal patient stratification is of utmost importance in the era of personalized medicine. Prediction of individual treatment responses by functional *ex vivo* assays require model systems derived from viable tumor samples, which should closely resemble *in vivo* tumor characteristics and microenvironment. This review discusses a broad spectrum of model systems, ranging from classic 2D monolayer culture techniques to more experimental 'cancer-on-chip' procedures. We mainly focus on organotypic tumor slices that take tumor heterogeneity and tumor-stromal interactions into account. These 3D model systems can be exploited for patient selection as well as for fundamental research. Selection of the right model system for each specific research endeavor is crucial and requires careful balancing of the pros and cons of each technology.

Lay Abstract

Selection of the right therapy for individual cancer patients is very important with the expanding number of possible treatments. How tumors respond to a therapy can be tested by treating a sample from the tumor outside the body. Various culture methods can be used to maintain this tumor sample. Each of these model systems has its own benefits and disadvantages. In this review, we discuss the advantages and drawbacks of the available model systems and how they can be used to guide personalized medicine.

Introduction

Treatment of epithelial cancers generally comprises surgical resection, radiation and/or systemic therapy. Systemic therapies traditionally consist of chemotherapeutic agents. Recently, more and more targeted therapies, such as small molecule inhibitors and monoclonal antibodies, have been developed. Targeted therapies have the potential advantage that they are directed against specific characteristics unique to the tumor cells, leaving the surrounding healthy tissue relatively unharmed. Over the last decades, cancer treatment has moved from 'one-size-fits-all' regimens towards more personalized cancer therapy. Molecular characteristics of the tumor cells are now used for therapy selection. For example, the monoclonal antibody trastuzumab, targeting the Human Epidermal growth factor Receptor 2 (HER2), dramatically improved survival for patients with breast tumors overexpressing HER2 ^[1]. These positive developments pose new challenges: proper selection of patients that are most likely to benefit from these targeted treatment regimens.

Adequate patient selection requires extensive molecular characterization of individual tumors. The search for predictive biomarkers started with specific molecular markers (e.g. *EGFR* mutation status in non-small cell lung cancer ^[2]) and developed over time into genomic, transcriptional and proteomic signatures ^[3-5]. In the future, next-generation sequencing techniques will be exploited to characterize individual patients molecularly and predict therapy response. However, validation of these biomarkers and subsequent implementation in the clinic are major bottle-necks that require extensive research.

As therapy response often cannot be predicted accurately by a single genetic marker only, alternative ways of patient stratification are needed. Beyond mutational status, many other factors influence tumor behavior and therapy response, for example epigenetic factors and the tumor microenvironment ^[6,7]. For instance, although HER2 amplification is a strong predictive marker of response to trastuzumab in breast cancer patients, its predictive value in gastric cancer is much weaker ^[8]. Therefore, the current difficulty to translate genetic information to tumor behavior necessitates development of tools to select patients for therapies based on tumor phenotype rather than genotype. *Ex vivo* assays that predict therapy response may fill this knowledge gap.

These functional assays require a viable sample from the tumor, which is then cultivated in the laboratory and exploited for drug screening or other *ex vivo* functional testing. Obviously, these tests require optimal model systems, which most closely resemble the *in vivo* tumor characteristics and microenvironment. Established tumor cell lines and genetically engineered mouse models are time consuming and do not represent the variation and heterogeneity observed in cancers from patients. Therefore, these models are usually not the optimal choice for development of assays to select patients for personalized cancer treatments ^[9]. Many alternative model systems are emerging to overcome these drawbacks and resemble *in vivo* tumors more closely. These model

systems enable execution of various *ex vivo* functional tests that aim to predict therapy response in the patient. We here discuss generation of two-dimensional (2D) and three-dimensional (3D) tumor cell culture methods, patient-derived xenografts (PDX) and organotypic tumor tissue slices (Figure 1). We here review the benefits and disadvantages of the available (preclinical) cancer model systems.

2D monolayer culture of dissociated tumor cells

To obtain a 2D monolayer of cells, the tumor is dissociated by specific proteolytic enzymes such as collagenase, dispase and/or trypsin. Depending on the tumor type, enzymatic digestion is combined with mechanical dissociation for better dispersal of the tumor mass^[10]. Not all tumors can be cultured *ex vivo* in monolayers. The need to adhere to the culture dish obviously causes a selection bias for adherent cells. Two types of 2D monolayer cultures exist: primary (tumor) cell cultures and cancer cell lines. Primary cell cultures are heterogeneous and represent the original tumor more closely but do not possess the limitless proliferative capacity that cancer cell lines have. Cancer cell lines are defined as clonal outgrowths from a primary tumor cell culture.

Once dissociated tumor cells successfully form a 2D monolayer *in vitro*, characterization of these cells can be performed in various ways. Primary (tumor) cell cultures can be exploited for diagnostic testing. Compared to cancer cell lines, primary cell cultures have less clonal selection and allow several short term functional analyses. This works well for some tumor types, such as bladder tumor cell cultures that have been used to characterize Nucleotide Excision Repair (NER) activity^[10].

Primary (tumor) cell cultures can also be established from tumor cells found in body fluids, including ascites and pulmonary effusion. For example, withdrawal of excessive ascites from ovarian cancer patients is often performed regularly for symptom relief and therefore less invasive than tumor biopsies. Generation of 2D monolayer cultures from these tumor cells has a 90% success rate, thereby providing a model system for functional testing and guiding personalized medicine for these patients^[11,12].

Human cancer cell lines have proven invaluable in both fundamental and translational research. Easy handling, homogeneous character and limitless growth make this the model system of choice for many large high-throughput experiments. High-throughput drug screenings using large panels of cancer cell lines have led to the discovery of new drug targets and gene signatures predicting therapy responses^[13,14].

Successful establishment of cancer cell lines from solid tumors is often inefficient, because of failure to adhere to the culture dish or loss of proliferative capacity after a few passages (e.g. for breast cancer the success rate is between 1 and 10%^[15]). Especially, slow growing tumors are severely underrepresented, as they do not often give rise to tumor cell lines. The optimal result is a clonal outgrowth and therefore cell lines do not represent the heterogeneity of the primary tumor. Indeed, cell lines and the *in vivo* tumors from which they originate, show many genetic, epigenetic and gene expression differences^[16].

Another limitation of cell lines is the extended time required for clonal outgrowth, minimizing the applicability of this model as a patient selection tool for personalized medicine. Genetic drift and cross-contamination are other issues often encountered when working with cell lines. This is not a problem when using primary (tumor) cell cultures in low passages for diagnostic testing, but is a major concern for extended culturing of cell lines in a laboratory setting. The latter problem can be minimized by freezing representative low passage stocks^[17].

In conclusion, 2D culture systems do not capture the subtleties of the original tumor microenvironment. However, primary tumor cell cultures may represent a valid approach to guide personalized medicine decision making. Cancer cell lines are valuable tools for high-throughput drug screening, although translation of these screens to the clinic can be difficult.

3D tumor cell models

The limited cell-cell interactions in 2D monolayer cultures introduce major changes in cellular physiology. Therefore, 3D cultures of the same cells may represent the original organ or tumor more faithfully than traditional cell cultures. 3D cancer cell line-based models have been reviewed elsewhere^[18]. Although they capture some features of tumor cell biology better than 2D culture systems, they fail to mimic tumor heterogeneity. For this reason, it would be preferred to start 3D cultures from primary tumor cells and/or tumor stem cells instead of cancer cell lines.

Some decades ago, collagen gels floating in the culture medium were shown to allow epithelial cells from different origins to form alveolus-like structures and maintain tissue function and differentiation^[19]. This was the beginning of *ex vivo* culturing of normal epithelial cells, such as mammary acini and colonic crypts, as functional units.

More recently, these 3D culture systems have been adapted such that they can grow for many passages. Such organoids can be established through isolation of adult stem cells and subsequent embedding of the cells in a three-dimensional matrix. The undifferentiated stem cells (e.g. Lgr5+ cells) are stimulated by supplements of tissue specific exogenous growth factors, in addition to growth factors endogenously produced by the stem cell microenvironment and surrounding mesenchyme^[20]. They self-organize into epithelia of the respective organ of origin, such as intestinal stem cells giving rise to formation of mini-guts, representing the epithelial architecture of the small intestine and colon^[21].

Similar technology allows 3D culture of tumor cells in spheroid structures; often referred to as tumor organoids. This technique can achieve long-term *ex vivo* expansion of tumor cells that still represent the heterogeneity of the original tumor^[22]. Tumor organoid growth can have a high success rate, even when starting material is limited^[23]. Up to date, successful human tumor derived organoids have been created from many different tumor types, including colorectal, stomach, liver and pancreas cancers^[22,24-26]. Recently, tumor

organoids have also been grown from frozen material, greatly extending the applicability of this technique ^[27]. However, it remains to be demonstrated whether tumor organoids can be grown with similar efficiencies from other tumor types.

The introduction of organoid cultures has created novel opportunities for high-throughput drug screens aiding personalized cancer treatment, biomarker discovery and studies on drug resistance mechanisms. A living organoid biobank for colorectal cancer patients is currently being collected, allowing gene expression analysis to detect gene-drug associations. Ideally, drug screens on these tumor organoids point towards effective personalized treatment strategies ^[28].

However, some drawbacks of the technique have surfaced, as well. The requirement of a collagen gel for 3D culturing was the initial break-through, yet seems to complicate potential drug screening and makes culturing more labor intensive.

Moreover, tumor organoids derived from a homogenous population of stem cells do not harbor the microenvironment of *in vivo* tumors, which also include non-transformed cells such as stromal fibroblasts and infiltrating immune cells. However, this technique can be developed further by introducing additional heterogeneity through patient-matched co-cultures with organoids grown from normal tissue adjacent to the tumor. Hybrid organoids consisting of tumor cells and stromal cells show promising potential for unraveling metastatic processes and tumor-stroma characteristics ^[29]. These co-cultures can also be adapted for other 3D culturing techniques to mimic the tumor microenvironment. For example, the development of 3D tumor co-cultures from cancer cell lines grown in combination with fibroblasts, endothelial cells, immune cells or bone cells enable crosstalk between tumor cells and the stromal cells of the microenvironment ^[30-33].

Organoid culture systems are suboptimal as a diagnostic tool, since their generation takes several weeks and clinical diagnostic testing for individual therapy selection should be conclusive within a much shorter timeframe ^[28]. On the other hand, one could envision organoid generation from primary tumor or metastasis material of patients treated with chemotherapy. Simultaneous treatment of the tumor organoid with various therapeutics could guide further therapy selection for these patients. The correlation between organoid and *in vivo* tumor therapy response would require extensive validation in this case.

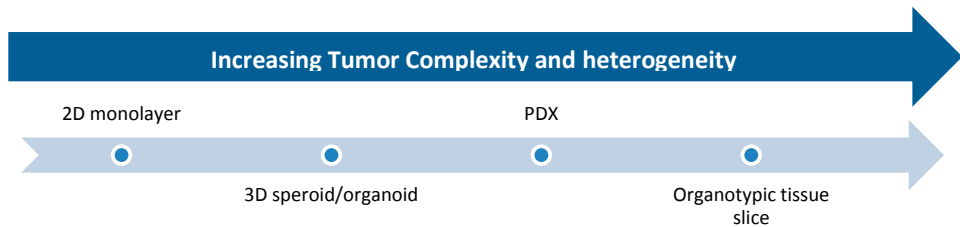
In conclusion, 3D organoid cultures are valuable tools for drug screens, biomarker discovery and studies on drug resistance mechanisms. Nevertheless, this model lacks the complexity of the tumor microenvironment and is less suited to guide personalized medicine.

Patient-derived Xenografts (PDX)

Dissociation of the tumor tissue is a prerequisite for 2D monolayer cultures and tumor organoids. This leads to loss of tumor heterogeneity and outgrowth of a specific subset of tumor cells. Another method to expand and preserve individual tumors from cancer patients is implantation of fresh pieces of the tumor in immune-deficient mice,

subcutaneously or in a place that more closely resembles the original tumor location ^[34,35]. These so-called patient-derived xenograft (PDX) tumor models retain intra-tumor heterogeneity ^[36]. The first PDX models were generated in the 1980s and they are still important and widely used in cancer research ^[37]. PDX models have been exploited for drug screening, biomarker discovery, identification of resistance mechanisms and pre-clinical evaluation of (personalized) treatment strategies ^[34]. PDX models maintain several characteristics of the *in vivo* tumor, including histopathological features, gene expression profiles, copy number variation and metastatic behavior ^[38-41].

Systematic analysis of PDX models enables biobanking of genomically well-defined tumors ^[34]. These biobanks are valuable resources for developing new predictive or prognostic biomarkers and individualized treatment strategies, thereby potentially guiding personalized medicine ^[42]. Also, co-clinical trials have been designed, in which PDX models are treated with anti-cancer therapies in parallel with the same treatment of patients in clinical trials ^[43,44]. The co-clinical trial concept allows integration of preclinical and clinical data, facilitating personalized treatment selection for patients, discovery of predictive biomarkers and identification of resistance mechanisms. Whether responses to chemotherapy observed in PDX models resemble the response rates of patients in clinical trials still remains to be elucidated ^[45,46].



	2D monolayer		3D spheroids		PDX	Organotypic tissue slice
	Primary cultures	Cell lines	3D Cell line cultures	3D Organoids		
Ease of maintenance	+/-	+	-	-	-	+/-
Preservation of tumor morphology	-	-	-	-	+/-	+
Extended <i>ex vivo</i> cell viability	+/-	+	+	+	+	-
Non-selective cell/tumor outgrowth	+/-	-	-	-	-	+
Preservation of micro-environment/heterogeneity	-	-	-	-	+/-	+
High-throughput drug screens	+/-	+	+/-	+/-	-	-
Success rate of model system generation	+/-	-	+/-	+/-	-	+
Short generation time	+	-	-	-	-	+
Similarity to original tumor	-	-	-/+	+/-	+/-	+
Costs	+	+	+/-	+/-	-	+

+ indicates advantages of the method, - indicates disadvantages of the method

Figure 1: Comparison of *ex vivo* tumor culture techniques. Fresh viable tumor tissue can be preserved and cultured *ex vivo* in several ways, each having its own advantages and disadvantages. A tumor sample can be dissociated using enzymatic and/or mechanical methods and subsequently cultured either as a 2D monolayer or in a 3D tumor spheroid culture. To mimic the *in vivo* situation as much as possible dissected tumor samples can be implanted in immunodeficient mice to generate patient-derived xenograft models. Organotypic tumor tissue slices can be generated by precision slicing of a tumor specimen, keeping general tumor/tissue architecture intact.

More recently, a pilot study with a similar concept was carried out. Treatments for patients with advanced cancer were selected on the basis of activity against a personalized tumorigraft derived from the *in vivo* tumor [47]. These personalized tumor graft models led to selection of a treatment regimen for 12 out of 14 patients. The treatments selected for each individual patient were not obvious and would not have been the first choice for a conventional second or third line treatment. In 9 out of 12 patients the selected treatment resulted in durable partial remission [47]. These results are quite striking, since the expected response rate with phase I agents, the only available option for some of these patients, is less than 10% [48]. These results need to be confirmed in larger cohorts of patients to get a better idea of the level of concordance between response in personalized tumorigraft models and the tumor of origin.

While ingenious advancements have been made in PDX applications, PDX models still harbor some important disadvantages. The first major drawback is the variable success rate of tumor engraftment [47]. Therefore, the variation observed in the cancer patient population may not be recapitulated faithfully in PDX models due to this selective engraftment rate [34]. Clinically aggressive tumors with many proliferative cancer cells, have the highest engraftment rate [49,50].

A second major drawback is the long generation time of PDX models, which limits their use in personalized medicine. The time between implantation and progressive growth of the xenograft tumor (PDX generation time or tumor graft latency) can range from 2 to 12 months [51,52]. In case of metastasized disease, patients may not even survive the PDX generation time [51]. PDX models may have limited use in diagnostics due to their low-throughput character and relatively high costs.

In addition to these practical problems for use of PDX models in personalized medicine, their use is also somewhat limited because of fundamental imperfections of the model. Although they retain intra-tumor heterogeneity, they fail to maintain the heterogeneity in the human tumor microenvironment, as the tumor stroma is slowly substituted by mouse stroma upon passaging. Therefore, the contribution of tumor-stroma interaction cannot be deduced faithfully from PDX models for drug screening.

Furthermore, PDX formation requires tumor implantation in severely immunocompromised host animals, complicating the evaluation of tumor immunology and drugs targeting the immune system [53]. This problem could be circumvented by using mice carrying a humanized immune system, although problems with graft-versus-host disease limit this approach severely [54]. Thus, when studying immunotherapies or tumor-stromal interactions there is a need for alternative model systems that allow exploration of the tumor microenvironment.

Overall, PDX models harbor more intra-tumor complexity than 2D monolayers or various 3D culturing techniques because the tumor is not dissociated. Since the generation time of PDX models is rather long, this model is less suitable for drug screening

and personalized medicine but still important for drug validation, investigation of therapy resistance mechanisms and biomarker development.

Organotypic tumor tissue slices

Various 3D culture systems have been designed to resemble *in vivo* tumors as closely as possible, taking tumor heterogeneity and tumor-stromal interactions into account. Most of these 3D culture approaches mimic tumor complexity only partially. The initial step for all techniques is dissociation of tumor tissue before the cells are stimulated to grow in 3D. Organotypic tumor slices, on the other hand, retain the complexity of tumors *in vivo* without extensive manipulation of the tissue. This leads to a model system in which the tumor cells are surrounded by their original microenvironment, rather than artificial matrices.

The first publications on organotypic tissue slices originate from the 1960s involving cardiac and brain tissue ^[55]. This technique involves precision slicing of tissue using specifically designed machines; the Krumdieck tissue slicer was considered the golden standard, until more recently the vibrating blade microtome (vibratome) was introduced ^[56]. The Krumdieck tissue slicer punches a cylindrical core from the tissue, which is then sliced by a rotating knife. The vibratome uses a vibrating knife to cut the tissue and has lower mechanical impact. Tissue slicing does not interfere with morphology and functional activity of the tissue and was soon exploited to study many different tissues including liver, retina, prostate, breast and testicular tissue ^[57-61]. Direct comparison of the Leica VT1200S vibrating blade microtome and the Krumdieck tissue slicing techniques revealed that the vibratome produces more precise and reproducible slices ^[60]. However, this may not be true for all tumor types. For example, the Krumdieck tissue slicer outperforms the vibratome when slicing the viscous texture of glioblastomas ^[62].

Table 1: Comparison of various reports on organotypic tumor slices. Many different methods for cultivation of organotypic tissue slices exist and the optimal system remains to be selected. Various reports on organotypic tumor tissue slices used different methods for slice cultivation. Moreover, assays and quality standards differ between reports, making it difficult to draw conclusions.

Report	Tissue	Slicing method	Specific culture condition	Validation tool for culture conditions/ Assay read-out	Duration of successful culture	Investigated compound	Study size
Van der Kuip et al. 2006 ⁽⁷¹⁾	Breast	Krumdieck	<ul style="list-style-type: none"> • Composite medium • Rotation (150rpm) • 200µm 	<ul style="list-style-type: none"> • TMRM/SYTO-63/Picogreen three color assay 	4 days	<ul style="list-style-type: none"> • Taxol 	22
Vaira et al. 2010 ⁽⁶⁷⁾	Colon Lung Prostate	Vibratome	<ul style="list-style-type: none"> • Culture plate inserts • No rotation • 400µm slices 	<ul style="list-style-type: none"> • Ki-67 staining • MTT assay • TUNEL assay (apoptosis) • BrdU incorporation • p-Akt and p-S6RP protein levels 	5 days	<ul style="list-style-type: none"> • LY294002 (PI3K inhibitor) 	42
Davies et al. 2015 ⁽⁶⁴⁾	Breast Prostate Lung	Vibratome	<ul style="list-style-type: none"> • Composite medium • No rotation • Culture plate inserts • 200–300µm slices • High/low oxygen 	<ul style="list-style-type: none"> • Ki-67 staining • CICK18 staining (apoptosis) • Cleaved caspase 3 staining • qPCR and IHC analysis of several other biomarkers • Morphologic examination 	4 days	NA	No cohort
Holliday et al. 2013 ⁽⁸¹⁾	Breast	Vibratome	<ul style="list-style-type: none"> • Regular medium • No rotation • 250 µm slices 	<ul style="list-style-type: none"> • MIB1 staining (proliferation) • M30 staining (apoptosis) • Morphologic examination 	7 days (no quantification)	<ul style="list-style-type: none"> • Doxorubicin • Tamoxifen 	10
Naipal et al. 2016 ⁽⁶⁸⁾	Breast	Vibratome	<ul style="list-style-type: none"> • Composite medium • Rotation (60rpm) • 300 µm slices 	<ul style="list-style-type: none"> • EduJ incorporation • TUNEL assay (apoptosis) • Morphologic examination 	7 days	<ul style="list-style-type: none"> • FAC (5-FU, Doxorubicin, Cyclophosphamide) 	15
Gerlach et al. 2014 ⁽⁶⁵⁾	Head and neck	Both vibratome and Krumdieck	<ul style="list-style-type: none"> • Composite medium • Culture plate inserts • 350 µm slices 	<ul style="list-style-type: none"> • Ki-67 staining • Cleaved caspase 3 staining • Morphologic examination 	6 days (no quantification)	<ul style="list-style-type: none"> • Cisplatin • Cetuximab • Docetaxel 	No cohort
Koerber et al. 2016 ⁽⁶⁶⁾	Gastric and Esophageal	Krumdieck	<ul style="list-style-type: none"> • Regular medium • Culture plate inserts • No rotation • 400µm slices 	<ul style="list-style-type: none"> • Cytokeratin • Ki-67 staining • Cleaved caspase 3 staining • Morphologic examination 	6 days	<ul style="list-style-type: none"> • 5-FU • cisplatin 	8
Carranza et al. 2015 ⁽⁶¹⁾	Breast	Krumdieck	<ul style="list-style-type: none"> • Composite medium • Rotation (25 rpm) • 250-300µm slices 	<ul style="list-style-type: none"> • Alamar Blue assay LDH release • Morphologic examination Ki67 staining 	3-4 days	<ul style="list-style-type: none"> • Paclitaxel • Caffeic acid • Ursolic acid • Rosmarinic acid 	9



Ex vivo drug screens and other functional tests require optimal culture conditions for these organotypic tumor tissue slices. Tumor slicing is usually achieved within hours of surgical resection of the primary tumor to minimize deterioration of the tissue and loss of cellular viability^[63]. Short term culture of tumor tissue slices can be achieved without extensive optimization of culture conditions. In some cases, short term culture of tissue slices suffices for selection of optimal treatment strategies. For example, a functional assay for homologous recombination capacity has been established. This test exploits RAD51 accumulation at DNA double strand breaks after *ex vivo* irradiation of tumor slices or biopsies to select breast cancer patients for targeted treatment with PARP inhibitors^[63].

However, preservation of tumor slices for extended periods without losing tumor viability, necessary for *ex vivo* drug screening, required extensive optimization of media composition and/or culture conditions.

Culture conditions can generally be divided in slices cultured on the bottom of the dish, freely floating in the medium or grown on membrane supports. This can be combined with rotational movement of the cultures to achieve optimal diffusion of oxygen and nutrients. Some studies report growth under low oxygen conditions^[64], but this in general leads to low tumor slice viability. Culture media that have been used are very diverse. The basis is generally one of the commercially available media for cell culture, supplemented with fetal bovine serum and antibiotics. Furthermore, various growth factors have been added to optimize conditions for specific tumor types.

Tissue slices can be cultured on Teflon membrane inserts, which have 0.4- μm pores that allow preservation of 3D tissue structure in culture and position the tissue slice at the air/liquid interface enabling efficient oxygenation. Colon, lung, head and neck, gastric, esophageal and prostate cancer slices have been reported to be preserved by incubation on Teflon membrane inserts^[65-67]. Davies et al have extensively studied the impact of various incubation methods^[64]. They found that tumor transportation and slicing had little impact on stress protein expression, whereas different cultivation methods significantly changed tissue vitality and expression of stress proteins. Vitality of tumor slices of various origins was maintained better when cultured on a membrane support compared to on the bottom of a culture dish. Although, even under these conditions, changes were observed in the slices after a few days in culture. Cultivation of the slice on the bottom of a culture dish led to significant alteration of a number of stress pathways and loss of tissue integrity, which can probably be explained by lack of oxygen and nutrient exchange. To overcome this issue, tissue slices can be incubated while floating in medium, which can be achieved via continuous movement using an orbital shaker. Breast cancer slice viability was preserved for prolonged periods of time when slices were incubated under constant rotation. Slices from the same breast tumor cultured under rotation showed more proliferating cells after 48 hours compared to slices cultured in static conditions^[68]. Breast cancer slices, obtained via vibratome slicing and cultured under constant rotation, remained vital for 7 days^[68] (Table 1).

Prolonged culture of tumor slices is an absolute requirement for investigation of cytotoxic drug responses. Improved efficiency of drug response prediction is clearly needed, since only 7.5% of the anti-cancer compounds tested in Phase I clinical trials eventually obtains approval^[69]. One of the main reasons for this disappointing percentage is the use of preclinical models that do not represent the complexity of *in vivo* tumors^[70]. Organotypic tissue slices could serve as a model to examine response of the tumor to anti-cancer compounds *ex vivo*, as it most closely resembles the heterogeneity and microenvironment of *in vivo* tumors. Indeed, cytotoxic responses to targeted therapies as well as classic chemotherapeutic agents have been predicted in organotypic tissue slices^[61,65-68,71]. Also in this case, concordance between *ex vivo* sensitivity and *in vivo* treatment response rates still remains to be validated. For this purpose, pre-treatment biopsies should be obtained for *ex vivo* sensitivity assays, subsequently comparing these results to *in vivo* post-treatment response evaluations. Therefore, the tissue slicing technique and incubation should be optimized for biopsy specimens, taking the first steps towards clinical validation and subsequent diagnostic application of this model system.

A major disadvantage of tumor tissue slices as a method for drug testing is its relatively low-throughput. The technique is rather laborious and requires specialized analysis tools that may not be easily implemented outside research settings. Markers that are generally used for determining response are analyzed by immunofluorescent microscopy and quantification of these markers is still challenging. Therefore, it is to be expected that this culture system will only be used in a laboratory setting and connected to clinical studies in the near future. Depending on the concordance between *ex vivo* outcomes and tumor response in patients, these methods could be adapted for a more routine clinical setting. However, automation of the processing and read-out is not easily possible and will require technical adaptations such as a cancer-on-chip approach described below.

Hypoxia is another potential problem of organotypic tissue slice cultures as a model system^[72]. Because intact vascularity is absent in tissue slices, the amount of oxygen available is limited to gas diffusion. Several parameters influence this oxygen diffusion, such as slice thickness, matrix stiffness, cellularity and metabolic and proliferative activity of the tumor and stromal cells^[68,72]. Especially long term cultures with extensive proliferation of tumor cells may cause hypoxia in the center of these growing tumor slices. On the other hand, organotypic tissue slices may allow detailed investigation of gradients of oxygen tension observed in patient tumors in a controlled setting *in vitro*^[72].

A drawback of many model systems, including organotypic tissue slices, is the lack of systemic features such as an immune system. The engineering of personalized tumor ecosystems, which conserve the microenvironment through cultivation of tissue slices in defined tumor grade-matched matrix support and in the presence of autologous serum, may be a next step in organotypic tissue slice cultivation^[73]. In these personalized tumor ecosystems, patient serum derived immune cells could infiltrate the tissue slice, extending the possible applications of this model system.

To conclude, organotypic tissue slices represent a solid model system for functional assays and drug sensitivity testing for personalized medicine, due to its fast generation time and reflection of intra-tumor heterogeneity and tumor-stromal interactions. However, many different methods for cultivation of organotypic tissue slices exist and the optimal system remains to be selected.

Although many publications on tumor slice cultures lack careful comparison of culture conditions and are not easily comparable to each other, a common denominator begins to emerge from the literature. Tissue slices from various tumor types, including lung, prostate, colon, gastric and head and neck cancer have been cultured for several days [65-68]. Glioblastoma tissue slices remained vital and still harbored histological characteristics of the original tumor even after 16 days of culture [62]. Different tumors require different culture conditions. Highly proliferative tumors, for instance, require more oxygen exchange, whereas very fragile tissue slices benefit from incubation on supportive material. Furthermore, each tumor type has its own nutrient and growth factor requirements. For example, several reports on breast cancer tissue slices used addition of insulin [61,68,71].

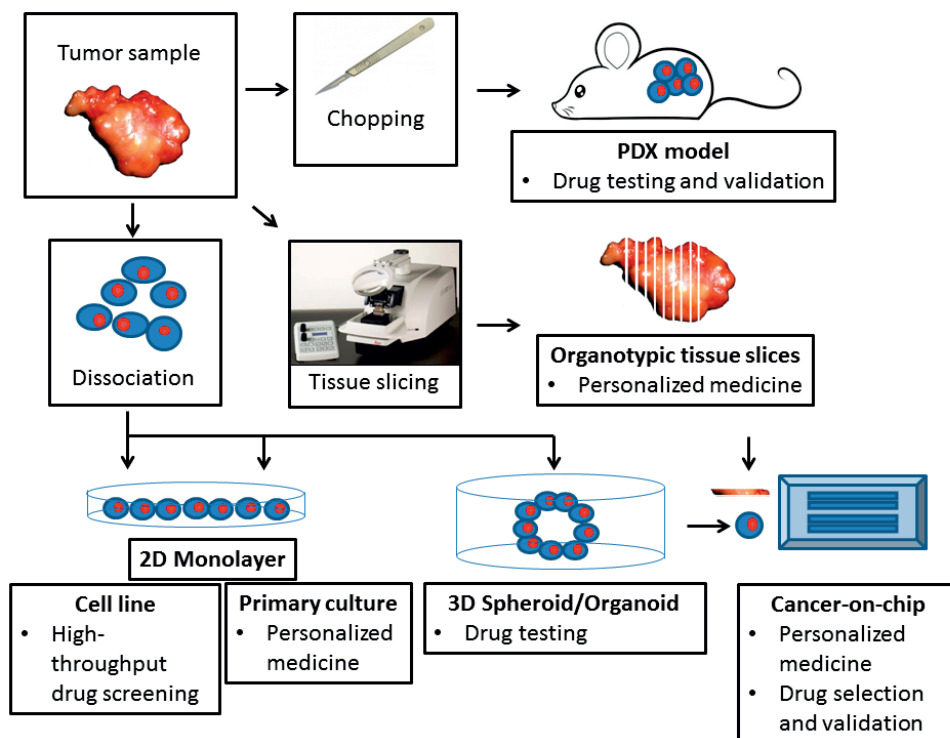


Figure 2: Main applications of different *ex vivo* model systems. An *ex vivo* model system should be chosen according to the purpose of the specific research. Each *ex vivo* model system has its own benefits and disadvantages, making one more applicable for a specific research endeavor than the others.

It is not easy to evaluate the merits of each tumor tissue slice culture system, as different assays and quality standards have been used to characterize tissue quality at various time points (table 1). Most investigators report on tissue morphology and cell death, although careful quantification is sometimes lacking. However, proliferation is not always monitored over time or different methods were used to assess proliferation. Often proliferation rate is estimated using Ki67 staining and several tissue slicing publications use this same marker. However, this may not faithfully reflect the proliferative state at the time of assay, as Ki-67 is expressed in all phases of the cell cycle, except G0^[74]. Therefore, proliferation should be evaluated with markers for S/G2 phase cells (geminin or cyclin A) or DNA synthesis (EdU incorporation), which measure active proliferation directly.

We propose a minimal standard, which should be performed for each tissue slice culture method, to enhance transparency and improve comparison between experiments and research groups. This standard should at least include morphology, proliferation and apoptosis of the tumor cells assessed up to 7 days of incubation. Moreover, it is of utmost importance to report all culture conditions used, instead of only those achieving optimal results. This should allow selection of the optimal culture system for organotypic tissue slices which can subsequently be adopted as the standard in the field of personalized medicine and drug testing.

Cancer-on-chip

New 3D culture systems incorporate advances in biomaterials, microfluidics, and tissue engineering to improve culture quality and reproducibility. Cancer-on-chip is a general term to describe various 3D microculture systems to maintain tumor cells in a controllable microenvironment. For example, cultivation of difficult-to-preserve primary patient-derived multiple myeloma cells has been achieved in a device consisting of a 3D tissue scaffold constructed in a perfused microfluidic environment^[75]. Recent progress in the cancer-on-chip field, specifically in hydrogel-incorporated microfluidics for long-term cell maintenance and exploitation of these culture devices for automated bioassay applications was reviewed by Lee et al^[76]. Specific microfluidics devices have been designed to study metastasis formation as well as personalized immunotherapy^[77,78].

Up to date, most cancer-on-chip systems facilitate cultivation of tumor cells. Yet, organotypic tissue slices can be inserted into these microfluidic devices as well, enabling long-term culturing with decreased handling of tissue slices. The conditions in these devices can be very similar to *in vivo* conditions, with constant supply of nutrients, waste removal and controlled access to oxygen. Moreover, endothelial barriers and interstitial pressure can also be mimicked in the more elaborate versions of these cancer-on-chip set-ups^[79]. Thereby, the maximum time that slices remain vital in culture could be expanded and cultivation will be more high-throughput compared to original organotypic tissue slice cultures^[80]. Optimization of the exact geometry and growth conditions of these microfluidics set ups hold great promise for tumor slice culturing and development of

predictive diagnostic assays. Although 3D microculture systems have been developed, this technique requires extensive optimization to achieve systems facilitating tissue slice cultivation.

Conclusions and future prospects

Patient stratification is of utmost importance in the era of personalized medicine. Selection of patients for precision therapies should ideally be based on the tumor phenotype. Functional *ex vivo* assays may be the ultimate selection method when unique molecular markers have not been identified for particular drugs.

Approaches for patient stratification should be fast, simple and widely applicable to many tumor types or subtypes without being biased for cell selection and tumor heterogeneity. As generation time of organotypic tissue slices is very fast and results can be obtained within days, this model is in principle suitable for drug selection in the personalized medicine era, whereas 2D monolayers, 3D organoids and PDX models require longer generation times. On the other hand, organoids and 2D monolayers can be exploited for high-throughput drug screenings, yet tissue slices remain a low-throughput technique. This indicates that selecting the right model system for the right purpose is at least as important as developing new and improved culture systems (Figure 2). Therefore, a thorough understanding of the advantages and drawbacks of each culture method is important.

In the future, developments in the field of cancer-on-chip might integrate the best of both worlds, incorporating tumor heterogeneity and tumor-stroma interactions represented in organotypic tissue slices in a more high-throughput fashion.

References

1. Moja L, Tagliabue L, Balduzzi S *et al.* Trastuzumab containing regimens for early breast cancer. *Cochrane Database Syst Rev*, (4), CD006243 (2012).
2. Veale D, Ashcroft T, Marsh C, Gibson GJ, Harris AL. Epidermal growth factor receptors in non-small cell lung cancer. *Br J Cancer*, 55(5), 513-516 (1987).
3. Chang JC, Wooten EC, Tsimelzon A *et al.* Gene expression profiling for the prediction of therapeutic response to docetaxel in patients with breast cancer. *Lancet*, 362(9381), 362-369 (2003).
4. De Marchi T, Liu NQ, Stingl C *et al.* 4-protein signature predicting tamoxifen treatment outcome in recurrent breast cancer. *Mol Oncol*, 10(1), 24-39 (2016).
5. Spentzos D, Levine DA, Kolia S *et al.* Unique gene expression profile based on pathologic response in epithelial ovarian cancer. *J Clin Oncol*, 23(31), 7911-7918 (2005).
6. Alizadeh AA, Aranda V, Bardelli A *et al.* Toward understanding and exploiting tumor heterogeneity. *Nat Med*, 21(8), 846-853 (2015).
7. Marks DL, Olson RL, Fernandez-Zapico ME. Epigenetic control of the tumor microenvironment. *Epigenomics*, 8(12), 1671-1687 (2016).
8. Kelly CM, Janjigian YY. The genomics and therapeutics of HER2-positive gastric cancer-from trastuzumab and beyond. *J Gastrointest Oncol*, 7(5), 750-762 (2016).
9. Burdall SE, Hanby AM, Lansdown MR, Speirs V. Breast cancer cell lines: friend or foe? *Breast Cancer Res*, 5(2), 89-95 (2003).
10. Naipal KA, Raams A, Bruens ST *et al.* Attenuated XPC expression is not associated with impaired DNA repair in bladder cancer. *PLoS One*, 10(4), e0126029 (2015).
11. Mukhopadhyay A, Elattar A, Cerbinskaite A *et al.* Development of a functional assay for homologous recombination status in primary cultures of epithelial ovarian tumor and correlation with sensitivity to poly(ADP-ribose) polymerase inhibitors. *Clin Cancer Res*, 16(8), 2344-2351 (2010).
12. Mukhopadhyay A, Plummer ER, Elattar A *et al.* Clinicopathological features of homologous recombination-deficient epithelial ovarian cancers: sensitivity to PARP inhibitors, platinum, and survival. *Cancer Res*, 72(22), 5675-5682 (2012).
- * 2D monolayer cultures can be generated by isolation of tumor cells derived from ascites of ovarian cancer patients, who undergo ascites withdrawal regularly for symptom relief. These 2D monolayer cultures represent a model system for functional testing and guiding personalized medicine for these patients.
13. Greshock J, Bachman KE, Degenhardt YY *et al.* Molecular target class is predictive of in vitro response profile. *Cancer Res*, 70(9), 3677-3686 (2010).
14. Sos ML, Michel K, Zander T *et al.* Predicting drug susceptibility of non-small cell lung cancers based on genetic lesions. *J Clin Invest*, 119(6), 1727-1740 (2009).
15. Lacroix M, Leclercq G. Relevance of breast cancer cell lines as models for breast tumours: an update. *Breast Cancer Res Treat*, 83(3), 249-289 (2004).

16. van Staveren WC, Solis DY, Hebrant A, Detours V, Dumont JE, Maenhaut C. Human cancer cell lines: Experimental models for cancer cells in situ? For cancer stem cells? *Biochim Biophys Acta*, 1795(2), 92-103 (2009).
17. Masters JR. Human cancer cell lines: fact and fantasy. *Nat Rev Mol Cell Biol*, 1(3), 233-236 (2000).
18. Fong EL, Harrington DA, Farach-Carson MC, Yu H. Heralding a new paradigm in 3D tumor modeling. *Biomaterials*, 108, 197-213 (2016).
19. Emerman JT, Pitelka DR. Maintenance and induction of morphological differentiation in dissociated mammary epithelium on floating collagen membranes. *In Vitro*, 13(5), 316-328 (1977).
20. Yin X, Mead BE, Safaee H, Langer R, Karp JM, Levy O. Engineering Stem Cell Organoids. *Cell Stem Cell*, 18(1), 25-38 (2016).
21. Jung P, Sato T, Merlos-Suarez A *et al.* Isolation and in vitro expansion of human colonic stem cells. *Nat Med*, 17(10), 1225-1227 (2011).
22. Sato T, Stange DE, Ferrante M *et al.* Long-term expansion of epithelial organoids from human colon, adenoma, adenocarcinoma, and Barrett's epithelium. *Gastroenterology*, 141(5), 1762-1772 (2011).
23. Weeber F, van de Wetering M, Hoogstraat M *et al.* Preserved genetic diversity in organoids cultured from biopsies of human colorectal cancer metastases. *Proc Natl Acad Sci U S A*, 112(43), 13308-13311 (2015).
24. Bartfeld S, Bayram T, van de Wetering M *et al.* In vitro expansion of human gastric epithelial stem cells and their responses to bacterial infection. *Gastroenterology*, 148(1), 126-136 e126 (2015).
25. Boj SF, Hwang CI, Baker LA *et al.* Organoid models of human and mouse ductal pancreatic cancer. *Cell*, 160(1-2), 324-338 (2015).
26. Broutier L, Andersson-Rolf A, Hindley CJ *et al.* Culture and establishment of self-renewing human and mouse adult liver and pancreas 3D organoids and their genetic manipulation. *Nat Protoc*, 11(9), 1724-1743 (2016).
27. Walsh AJ, Cook RS, Sanders ME, Arteaga CL, Skala MC. Drug response in organoids generated from frozen primary tumor tissues. *Sci Rep*, 6, 18889 (2016).
28. van de Wetering M, Francies HE, Francis JM *et al.* Prospective derivation of a living organoid biobank of colorectal cancer patients. *Cell*, 161(4), 933-945 (2015).
- * The establishment of 'living biobanks' containing well-characterized organoids of colorectal carcinomas, allows drug screening and detection of gene-drug associations.
29. Skardal A, Devarasetty M, Rodman C, Atala A, Soker S. Liver-Tumor Hybrid Organoids for Modeling Tumor Growth and Drug Response In Vitro. *Ann Biomed Eng*, 43(10), 2361-2373 (2015).

30. Alonso-Nocelo M, Abuin C, Lopez-Lopez R, de la Fuente M. Development and characterization of a three-dimensional co-culture model of tumor T cell infiltration. *Biofabrication*, 8(2), 025002 (2016).
31. Bray LJ, Binner M, Holzheu A *et al.* Multi-parametric hydrogels support 3D in vitro bioengineered microenvironment models of tumour angiogenesis. *Biomaterials*, 53, 609-620 (2015).
32. Majety M, Pradel LP, Gies M, Ries CH. Fibroblasts Influence Survival and Therapeutic Response in a 3D Co-Culture Model. *PLoS One*, 10(6), e0127948 (2015).
33. Subia B, Dey T, Sharma S, Kundu SC. Target specific delivery of anticancer drug in silk fibroin based 3D distribution model of bone-breast cancer cells. *ACS Appl Mater Interfaces*, 7(4), 2269-2279 (2015).
34. Hidalgo M, Amant F, Biankin AV *et al.* Patient-derived xenograft models: an emerging platform for translational cancer research. *Cancer Discov*, 4(9), 998-1013 (2014).
35. Williams SA, Anderson WC, Santaguida MT, Dylla SJ. Patient-derived xenografts, the cancer stem cell paradigm, and cancer pathobiology in the 21st century. *Lab Invest*, 93(9), 970-982 (2013).
36. Kopetz S, Lemos R, Powis G. The promise of patient-derived xenografts: the best laid plans of mice and men. *Clin Cancer Res*, 18(19), 5160-5162 (2012).
37. Kameya T, Shimosato Y, Tumoraya M, Ohsawa N, Nomura T. Human gastric choriocarcinoma serially transplanted in nude mice. *J Natl Cancer Inst*, 56(2), 325-332 (1976).
38. Bertotti A, Migliardi G, Galimi F *et al.* A molecularly annotated platform of patient-derived xenografts ("xenopatients") identifies HER2 as an effective therapeutic target in cetuximab-resistant colorectal cancer. *Cancer Discov*, 1(6), 508-523 (2011).
39. Daniel VC, Marchionni L, Hierman JS *et al.* A primary xenograft model of small-cell lung cancer reveals irreversible changes in gene expression imposed by culture in vitro. *Cancer Res*, 69(8), 3364-3373 (2009).
40. DeRose YS, Wang G, Lin YC *et al.* Tumor grafts derived from women with breast cancer authentically reflect tumor pathology, growth, metastasis and disease outcomes. *Nat Med*, 17(11), 1514-1520 (2011).
41. Zhao X, Liu Z, Yu L *et al.* Global gene expression profiling confirms the molecular fidelity of primary tumor-based orthotopic xenograft mouse models of medulloblastoma. *Neuro Oncol*, 14(5), 574-583 (2012).
42. Dowst H, Pew B, Watkins C *et al.* Acquire: an open-source comprehensive cancer biobanking system. *Bioinformatics*, 31(10), 1655-1662 (2015).
43. Nardella C, Lunardi A, Patnaik A, Cantley LC, Pandolfi PP. The APL paradigm and the "co-clinical trial" project. *Cancer Discov*, 1(2), 108-116 (2011).
44. Chen Z, Cheng K, Walton Z *et al.* A murine lung cancer co-clinical trial identifies genetic modifiers of therapeutic response. *Nature*, 483(7391), 613-617 (2012).

- * The co-clinical trial concept exploiting PDX models allows integration of preclinical and clinical data, thereby facilitating personalized treatment selection for patients and discovery of predictive biomarkers and resistance mechanisms. Predictive value of these co-clinical trials remains to be elucidated.
45. Rubio-Viqueira B, Hidalgo M. Direct in vivo xenograft tumor model for predicting chemotherapeutic drug response in cancer patients. *Clin Pharmacol Ther*, 85(2), 217-221 (2009).
 46. Pompili L, Porru M, Caruso C, Biroccio A, Leonetti C. Patient-derived xenografts: a relevant preclinical model for drug development. *J Exp Clin Cancer Res*, 35(1), 189 (2016).
 47. Hidalgo M, Bruckheimer E, Rajeshkumar NV *et al*. A pilot clinical study of treatment guided by personalized tumorgrafts in patients with advanced cancer. *Mol Cancer Ther*, 10(8), 1311-1316 (2011).
 48. Horstmann E, McCabe MS, Grochow L *et al*. Risks and benefits of phase 1 oncology trials, 1991 through 2002. *N Engl J Med*, 352(9), 895-904 (2005).
 49. Lawrence MG, Pook DW, Wang H *et al*. Establishment of primary patient-derived xenografts of palliative TURP specimens to study castrate-resistant prostate cancer. *Prostate*, 75(13), 1475-1483 (2015).
 50. Moon HG, Oh K, Lee J *et al*. Prognostic and functional importance of the engraftment-associated genes in the patient-derived xenograft models of triple-negative breast cancers. *Breast Cancer Res Treat*, 154(1), 13-22 (2015).
 51. Bergamaschi A, Hjortland GO, Triulzi T *et al*. Molecular profiling and characterization of luminal-like and basal-like in vivo breast cancer xenograft models. *Mol Oncol*, 3(5-6), 469-482 (2009).
 52. Dangles-Marie V, Pocard M, Richon S *et al*. Establishment of human colon cancer cell lines from fresh tumors versus xenografts: comparison of success rate and cell line features. *Cancer Res*, 67(1), 398-407 (2007).
 53. Cassidy JW, Caldas C, Bruna A. Maintaining Tumor Heterogeneity in Patient-Derived Tumor Xenografts. *Cancer Res*, 75(15), 2963-2968 (2015).
 54. Shultz LD, Brehm MA, Garcia-Martinez JV, Greiner DL. Humanized mice for immune system investigation: progress, promise and challenges. *Nat Rev Immunol*, 12(11), 786-798 (2012).
 55. Bousquet J, Meunier JM. [Organotypic culture, on natural and artificial media, of fragments of the adult rat hypophysis]. *C R Seances Soc Biol Fil*, 156, 65-67 (1962).
 56. Krumdieck CL. Development of a live tissue microtome: reflections of an amateur machinist. *Xenobiotica*, 43(1), 2-7 (2013).
 57. Arman AC, Sampath AP. Patch clamp recordings from mouse retinal neurons in a dark-adapted slice preparation. *J Vis Exp*, (43) (2010).
 58. Blauer M, Tammela TL, Ylikomi T. A novel tissue-slice culture model for non-malignant human prostate. *Cell Tissue Res*, 332(3), 489-498 (2008).

59. Laughlin AM, Welsh TH, Jr, Love CC *et al.* In vitro culture of precision-cut testicular tissue as a novel tool for the study of responses to LH. *In Vitro Cell Dev Biol Anim*, 46(1), 45-53 (2010).
60. Zimmermann M, Lampe J, Lange S *et al.* Improved reproducibility in preparing precision-cut liver tissue slices. *Cytotechnology*, 61(3), 145-152 (2009).
61. Carranza-Torres IE, Guzman-Delgado NE, Coronado-Martinez C *et al.* Organotypic culture of breast tumor explants as a multicellular system for the screening of natural compounds with antineoplastic potential. *Biomed Res Int*, 2015, 618021 (2015).
62. Merz F, Gaunitz F, Dehghani F *et al.* Organotypic slice cultures of human glioblastoma reveal different susceptibilities to treatments. *Neuro Oncol*, 15(6), 670-681 (2013).
63. Naipal KA, Verkaik NS, Ameziane N *et al.* Functional ex vivo assay to select homologous recombination-deficient breast tumors for PARP inhibitor treatment. *Clin Cancer Res*, 20(18), 4816-4826 (2014).
64. Davies EJ, Dong M, Gutekunst M *et al.* Capturing complex tumour biology in vitro: histological and molecular characterisation of precision cut slices. *Sci Rep*, 5, 17187 (2015).
65. Gerlach MM, Merz F, Wichmann G *et al.* Slice cultures from head and neck squamous cell carcinoma: a novel test system for drug susceptibility and mechanisms of resistance. *Br J Cancer*, 110(2), 479-488 (2014).
66. Koerfer J, Kallendrusch S, Merz F *et al.* Organotypic slice cultures of human gastric and esophagogastric junction cancer. *Cancer Med*, 5(7), 1444-1453 (2016).
67. Vaira V, Fedele G, Pyne S *et al.* Preclinical model of organotypic culture for pharmacodynamic profiling of human tumors. *Proc Natl Acad Sci U S A*, 107(18), 8352-8356 (2010).
68. Naipal KA, Verkaik NS, Sanchez H *et al.* Tumor slice culture system to assess drug response of primary breast cancer. *BMC Cancer*, 16, 78 (2016).
- * To our knowledge, within the organotypic tissue slice cultivation field, this paper describes the most successful method for culturing breast cancer tissue slices for up to 1 week.
69. Toniatti C, Jones P, Graham H, Pagliara B, Draetta G. Oncology drug discovery: planning a turnaround. *Cancer Discov*, 4(4), 397-404 (2014).
70. Rubin EH, Gilliland DG. Drug development and clinical trials--the path to an approved cancer drug. *Nat Rev Clin Oncol*, 9(4), 215-222 (2012).
71. van der Kuip H, Murdter TE, Sonnenberg M *et al.* Short term culture of breast cancer tissues to study the activity of the anticancer drug taxol in an intact tumor environment. *BMC Cancer*, 6, 86 (2006).
72. Hammond EM, Asselin MC, Forster D, O'Connor JP, Senra JM, Williams KJ. The meaning, measurement and modification of hypoxia in the laboratory and the clinic. *Clin Oncol (R Coll Radiol)*, 26(5), 277-288 (2014).

73. Majumder B, Baraneedharan U, Thiyagarajan S *et al.* Predicting clinical response to anticancer drugs using an ex vivo platform that captures tumour heterogeneity. *Nat Commun*, 6, 6169 (2015).
74. Gerdes J, Lemke H, Baisch H, Wacker HH, Schwab U, Stein H. Cell cycle analysis of a cell proliferation-associated human nuclear antigen defined by the monoclonal antibody Ki-67. *J Immunol*, 133(4), 1710-1715 (1984).
75. Zhang W, Lee WY, Zilberberg J. Tissue Engineering Platforms to Replicate the Tumor Microenvironment of Multiple Myeloma. *Methods Mol Biol*, 1513, 171-191 (2017).
76. Lee DH, Bae CY, Kwon S, Park JK. User-friendly 3D bioassays with cell-containing hydrogel modules: narrowing the gap between microfluidic bioassays and clinical end-users' needs. *Lab Chip*, 15(11), 2379-2387 (2015).
77. Bersini S, Jeon JS, Dubini G *et al.* A microfluidic 3D in vitro model for specificity of breast cancer metastasis to bone. *Biomaterials*, 35(8), 2454-2461 (2014).
78. Lu YT, Pendharkar GP, Lu CH, Chang CM, Liu CH. A microfluidic approach towards hybridoma generation for cancer immunotherapy. *Oncotarget*, 6(36), 38764-38776 (2015).
79. Han B, Qu C, Park K, Konieczny SF, Korc M. Recapitulation of complex transport and action of drugs at the tumor microenvironment using tumor-microenvironment-on-chip. *Cancer Lett*, 380(1), 319-329 (2016).
80. Bakmand T, Troels-Smith AR, Dimaki M *et al.* Fluidic system for long-term in vitro culturing and monitoring of organotypic brain slices. *Biomed Microdevices*, 17(4), 71 (2015).
81. Holliday DL, Moss MA, Pollock S *et al.* The practicalities of using tissue slices as preclinical organotypic breast cancer models. *J Clin Pathol*, 66(3), 253-255 (2013).

A large, dark, textured splash of ink or paint on a white background. The splash is irregular and has a rough, splattered appearance. The text "Chapter 3" is centered in white, bold, sans-serif font.

Chapter 3

Functional *ex vivo* assay reveals homologous recombination deficiency in breast cancer beyond BRCA gene defects

Titia G. Meijer¹, Nicole S. Verkaik¹, Anieta M. Sieuwerts², Job van Riet^{3,4}, Kishan A.T. Naipal¹, Carolien H.M. van Deurzen⁵, Michael A. den Bakker⁶, Hein F.B.M. Sleddens⁵, Hendrikus-Jan Dubbink⁵, T. Dorine den Toom⁵, Winand N.M. Dinjens⁵, Esther Lips⁷, Petra M. Nederlof⁷, Marcel Smid², Harmen J. G. van de Werken^{3,4}, Roland Kanaar¹, John W. M. Martens², Agnes Jager² and Dik C. van Gent¹

¹ Erasmus MC University Medical Center Rotterdam, Department of Molecular Genetics and Oncode Institute, The Netherlands

² Erasmus MC Cancer Institute, Erasmus MC University Medical Center, Department of Medical Oncology

³ Erasmus MC University Medical Center Rotterdam, Cancer Computational Biology Center

⁴ Erasmus MC University Medical Center Rotterdam, Department of Urology

⁵ Erasmus MC University Medical Center Rotterdam, Department of Pathology

⁶ Maastad ziekenhuis, Rotterdam, The Netherlands

⁷ Department of Pathology, Netherlands Cancer Institute, Amsterdam, The Netherlands

Abstract

Introduction Tumors of germline *BRCA1/2* mutated carriers show homologous recombination (HR) deficiency (HRD), resulting in impaired DNA double strand break (DSB) repair and high sensitivity to Poly-(ADP-Ribose)-Polymerase (PARP) inhibitors. Although this therapy is expected to be effective beyond germline *BRCA1/2* mutated carriers, a robust validated test to detect HRD tumors is lacking. In the present study we therefore evaluated a functional HR assay exploiting the formation of RAD51 foci in proliferating cells after *ex vivo* irradiation of fresh breast cancer (BrC) tissue: the REpair CAPacity (RECAP) test.

Methods Fresh samples of 170 primary BrCs were analyzed using the RECAP test. The molecular explanation for the HRD phenotype was investigated by exploring *BRCA* deficiencies, mutational signatures, tumor infiltrating lymphocytes (TILs) and microsatellite instability (MSI).

Results RECAP was completed successfully in 125 out of 170 samples (74%). Twenty-four tumors showed HRD (19%), whereas six tumors were HR intermediate (HRi) (5%). HRD was explained by *BRCA* deficiencies (mutations, promoter hypermethylation, deletions) in 16 cases, whereas seven HRD tumors were non-*BRCA* related. HRD tumors showed an increased incidence of high TIL counts ($p=0.023$) compared to HR proficient (HRP) tumors and MSI was more frequently observed in the HRD group (2/20, 10%) than expected in BrC (1%) ($p=0.017$).

Conclusion RECAP is a robust functional HR assay detecting both *BRCA1/2* deficient and *BRCA1/2* proficient HRD tumors. Functional assessment of HR in a pseudo-diagnostic setting is achievable and produces robust and interpretable results.

Introduction

Breast cancer (BrC) is the most common malignancy in women with the second highest cancer related mortality rate ^[1]. Approximately 3% of all BrC cases are due to germline mutations in *BRCA1/2* ^[2], and in triple negative BrCs (TNBCs) this percentage is even 10-20% ^[3]. The BRCA proteins play an important role in the homologous recombination (HR) pathway, the error-free DNA double strand break (DSB) repair pathway that operates during the S- and G2-phase of the cell cycle. HR deficiency (HRD) leading to impaired DNA DSB repair is frequently caused by, but not limited to, defects in *BRCA1/2* ^[4].

Therapies specifically targeting tumor cells with impaired HR capacity are Poly ADP-Ribose Polymerase (PARP)-inhibitors (PARPi), as well as classical chemotherapies such as platinum-derivates and alkylating agents ^[5]. PARPi causes persistence of single strand DNA breaks (SSBs) by trapping PARP1 on DNA, while platinum-derivates cause DNA interstrand crosslinks. Both types of lesions result in replication fork stalling and/or collapse, frequently leading to DSBs that need HR for their repair ^[5]. The targeted approach of PARPi kills tumor cells lacking HR, whereas normal cells remain unharmed, due to their normal DSB repair capacity, a phenomenon often referred to as synthetic lethality. Recently FDA approval was granted for the use of Olaparib in germline *BRCA* mutated BrC based on the results of the Olympiad trial ^[6].

Although evidence is emerging that the use of PARPi could be extended beyond germline *BRCA1/2* mutated cancers to sporadic cancers with BRCA-like features, a gold standard test for predicting response to treatments targeting HR is not yet available ^[7]. Several different HRD tests exist, mostly based on genomic patterns or transcriptional predictors of BRCAness ^[8-12].

These genomic tests measure the accumulation of mutations and chromosomal aberrations over time, but not necessarily reflect the real-time HR status. Beyond mutational status, several other factors influence tumor behavior and therapy response, such as epigenetic changes and the microenvironment of the tumor cells. Independent of the underlying cause, the downstream effect of HR impairment (phenotype) can be assessed functionally. A functional diagnostic assay therefore has the potential for more precisely detecting patients who may benefit from PARPi than genomic assays.

A functional HRD assay was first described by Graeser et al, assessing RAD51 focus formation, a marker of HR competence, in tumor biopsies obtained 24 hours after *in vivo* anthracycline treatment ^[13]. This provided the first evidence that RAD51 focus formation can serve as a predictive biomarker. To enhance clinical utility of this biomarker, test outcomes should be available before start of treatment. Therefore, we developed the homologous REpair CAPacity (RECAP) test exploiting the formation of RAD51 foci in proliferating cells after *ex vivo* irradiation of fresh BrC tissue, providing a real-time HR status of the tumor ^[14]. The aim of the current study was to validate the RECAP test in an extensive cohort of primary BrCs and provide evidence that this functional test is achievable in a pseudo-

clinical setting. Additionally, thorough molecular characterization of the HRD phenotype is performed, proving that HRD tumors encompass more than only BRCA deficiencies.

Methods

Primary breast cancer specimens

Residual fresh BrC tissue was prospectively collected from lumpectomy of the breast or mastectomy specimens in the Erasmus MC Cancer Institute, Haven hospital and Maastad hospital in Rotterdam, The Netherlands between 1 October 2011 and 1 September 2016. The first 41 patients were also included in our previous cohort ^[14]. After macroscopic evaluation of the surgical specimen by trained pathologists, residual tumor tissue was collected for our research purposes according to the “Code of proper secondary use of human tissue in the Netherlands” established by the Dutch Federation of Medical Scientific Societies and approved by the local Medical Ethical committees (MEC-11-098). Patients who had objected to secondary use of residual tumor material for research purposes were not included in this study. Patients with ductal carcinoma *in situ* (DCIS) only or patients receiving neo-adjuvant chemotherapy were excluded.

RECAP test

Obtained tissue samples were immediately transferred into customized breast tissue culture medium, as described in Naipal et al ^[14]. Processing of samples was performed within 4 hours after the tissue was resected. Microscopic analysis of Hematoxylin and Eosin (HE) stained sections was performed to determine presence of invasive carcinoma. The RECAP test, a functional assay exploiting the formation of RAD51 foci in proliferating cells after *ex vivo* irradiation of fresh BrC tissue, was performed and results were analyzed as described previously ^[14]. In brief, presence of RAD51 foci was determined in S/G2 cells only, which stain positive for Geminin. At least 30 Geminin expressing cells were counted per tumor sample. A cell was considered RAD51 positive when at least 5 RAD51 foci could be detected. Based on previous experiments with patient derived xenograft (PDX) models with known BRCA status, tumors were classified as HR proficient (HRP), HR deficient (HRD) or intermediate (HRi) when more than 50%, less than 20% or between 20-50% of geminin positive cells showed ≥ 5 RAD51 foci, respectively.

Workflow of molecular characterization of the HRD phenotype

To unravel the possible molecular mechanism underlying the HRD phenotype, several molecular tests were performed retrospectively (Figure 2 and Figure S1). As no DNA could be obtained for 1 HRD sample, we conducted the analyses for 23 HRD and 6 HRi samples. First, *BRCA* sequencing and *BRCA1* promoter methylation analysis was performed in HRD and HRi samples, as well as in all TNBC (n=5), ER/PR- HER2+ (n=2) and 21 ER/PR+ HRP tumors (total n=28) (Figure S1). The HRD and HRi tumors without molecular explanation

for their phenotype were subjected to *BRCA1* and *BRCA2* MLPA analysis to identify large genomic rearrangements (LGRs), as LGRs are not usually identified by targeted sequencing. In addition to this targeted approach, morphological examination of TILs as well as Whole Exome Sequencing (WES) was performed on a selection of tumors to further explore molecular aspects connected to the HRD phenotype.

DNA isolation

Isolation of DNA from 30 μm fresh frozen tissue section samples was performed using the NucleoSpin Tissue Kit (Macherey-Nagel, Düren, Germany) according to the manufacturer's instructions. Quantity and quality checks of isolated DNA were performed using the MultiNA microchip electrophoresis system (Shimadzu, 's Hertogenbosch, The Netherlands), Nanodrop 2000-v.1 (Thermo Fisher Scientific) and Qubit (Thermo Fisher Scientific).

BRCA1/2 analyses

Ion semiconductor sequencing on the Ion Torrent Personal S5XL was performed according to manufacturer's instructions (Thermo Fisher Scientific). Adapter-ligated libraries were constructed using the AmpliSeq Library kit 2.0 with amplicons designed targeting *BRCA1/2* and TP53. Generation of sequence reads, trimming adapter sequences, filtering, and removal of poor signal-profile reads was performed via the Ion Torrent platform-specific pipeline software Torrent Suite v5.2.2. Initial variant calling was performed by comparison to the reference genome hg19 (build 37) using the "Torrent Variant Caller v5.2.0.34" plug-in from the Torrent Suite Software. All *BRCA2* variants were validated by Sanger sequencing and pathogenicity was evaluated using interactive Biosoftware Alamut Visual v.2.7.2. *BRCA1* promoter methylation was analyzed as previously described ^[15]. Multiplex ligation-dependent probe amplification (MLPA) analysis of *BRCA1* and *BRCA2* was undertaken to identify large rearrangements using the SALSA MLPA kit P002B, and for confirmation of observed abnormalities, the SALSA MLPA kit P087 was used (MRC Holland, Amsterdam, The Netherlands). Analyses were performed according to the manufacturer's instruction; products were run on an ABI automated sequencer (ABI 3730XL), and the data were analyzed by Genemarker version 2.7.0 (Softgenetics, State College, PA).

In situ detection of BRCA1 RNA

In situ detection of *BRCA1* mRNA was performed using RNAScope (Advanced Cell Diagnostics, Newark, USA) on the automated Ventana Discovery Ultra system (Ventana Medical Systems, Roche, Tucson, USA). *BRCA1* and positive control peptidylprolyl isomerase B (*PPIB*) probes (product codes: 485479 and 313909) were purchased from the same company. RNAScope analysis was performed according to manufacturer's instructions using the reagent kit (VS Reagent Kit 320600; Advanced Cell Diagnostics) on proteinase K (0.1 %, 5 min at 37 °C)-treated paraffin sections (4 μm).

Exome sequencing

DNA libraries for Illumina sequencing were generated using standard protocols (Illumina, San Diego, CA, USA) and subsequently sequenced in an Illumina HiSeq 2500 system by GATC-biotech (Konstanz, Germany). Exome-targeting was performed using the Sureselect v5 (v6 for tumors M077, M209, M211) methods using standard protocols (Agilent Technologies, Santa Clara, CA). DNA libraries were whole-exome sequenced (2x125bp) using the HiSeq v4 paired-end sequencing protocol to a minimum depth base coverage of 90x for tumor samples and 60x for matched normal. Sequence reads were mapped against human reference genome GRCh37 using Burrows–Wheeler Aligner (v0.7.12) with default settings [16]. Sequence reads originating from multiple lanes were merged after alignment using Samtools (v1.5) prior to further analysis [17]. Sequence duplicates were marked using PicardTools (v1.129) [18]. Somatic variant calling was performed by Mutect2 (v3.7) using a matched-normal design whilst utilizing the dbSNP (v149, hg19) and COSMIC (v80, hg19) databases and using default settings [19-21]. Variant annotation was performed by ANNOVAR [22]. Heuristic filtering removed variants not passing all standard Mutect2 post-calling filters. Sequence data has been deposited at the European Genome-phenome Archive (EGA, <http://www.ebi.ac.uk/ega/>), which is hosted by the EBI, under accession number EGAD00001003929.

Mutational signatures

For each somatic variant, its trinucleotide context was derived from the human reference genome GRCh37 and enumerated into a mutational spectrum matrix M_{ij} ($i = 96$; number of trinucleotide contexts; $j =$ number of samples) using the MutationalPatterns R package (v1.4.0) in the R statistical platform [23]. Multi-allelic and InDel variants were not included in this analysis. The thirty consensus mutational signatures, as established by Alexandrov et al., (matrix S_{ij} ; $i = 96$; number of trinucleotide motifs; $j =$ number of signatures) were downloaded from COSMIC (as visited on 8-11-2017) [24]. Per sample, a constrained linear combination of the 30 validated mutational signatures was constructed, which reconstructs the sample-specific mutational spectrum, using non-negative least squares regression implemented in the R package pracma (v1.9.3). Signatures with lower relative contribution than 3% were summarized into a “Filtered” category.

MSI analysis, MMR protein IHC and MLH1 promotor methylation assay

These analyses were performed as previously described [25].

Tumor infiltrating lymphocytes

Tumor infiltrating lymphocytes (TILs) were scored on HE stained sections, according to the consensus by the International TILs Working Group 2014 [26].

Statistical analysis

Statistical analyses were all 2-sided and performed using IBM SPSS statistics v21. Significance was calculated by Fisher's exact test for categorical data, by Mann-Whitney test for continuous data and by exact binomial test for the incidence of MSI. P-values of <0.05 were considered significant.

Results

Ex vivo functional RECAP test

A total of 170 samples were subjected to the RECAP test (Figure S1) ^[14]. In 125 out of 170 (74%) primary BrC tissues RECAP was completed successfully (Figure 1). In all cases, the reason for failure (n= 45) was lack of proliferating tumor cells. No differences in clinicopathologic characteristics between tumors that yielded successful versus non-successful tests were observed (Table S1). The first 41 patients were also included in our previous cohort. Here, we show that execution of a functional assay in a pseudo-diagnostic setting is achievable and validate the findings from the earlier cohort (11% HRD in cohort 1 versus 19% HRD in cohort 2, $p=0.339$). In total, we identified 95 (76%) HRP, 24 (19%) HRD and 6 (5%) HRi samples (Figure 1). Both HRi and HRD tumors were more frequently TN ($p < 0.001$) and Bloom and Richardson (B&R) grade 3 ($p < 0.001$) than HRP tumors. Also, HRD tumors had a larger size ($p = 0.050$) and were never B&R grade 1 (Table S2).

Identification of BRCA defects in HRD breast cancers

Pathogenic *BRCA2* mutations were found in six (6/23=26%) HRD samples, but not in the tested HRP samples (Table 1). In six tumors (2 HRD, 1 HRi and 3 HRP) *BRCA2* variants were detected that were classified as benign. We did not identify any *BRCA1* point mutations. Next, *BRCA1* promoter hypermethylation was detected in 6 (6/23=26%) HRD tumors and in 1 HRi tumor, but not in tested HRP samples (Table 1). Interestingly, all 6 HRD tumors displaying *BRCA1* promoter hypermethylation were TNBCs (Table 1 and Table S3). *Vice versa*, of the 6 HRD tumors harboring a pathogenic *BRCA2* mutation, 5 showed hormone receptor positivity.

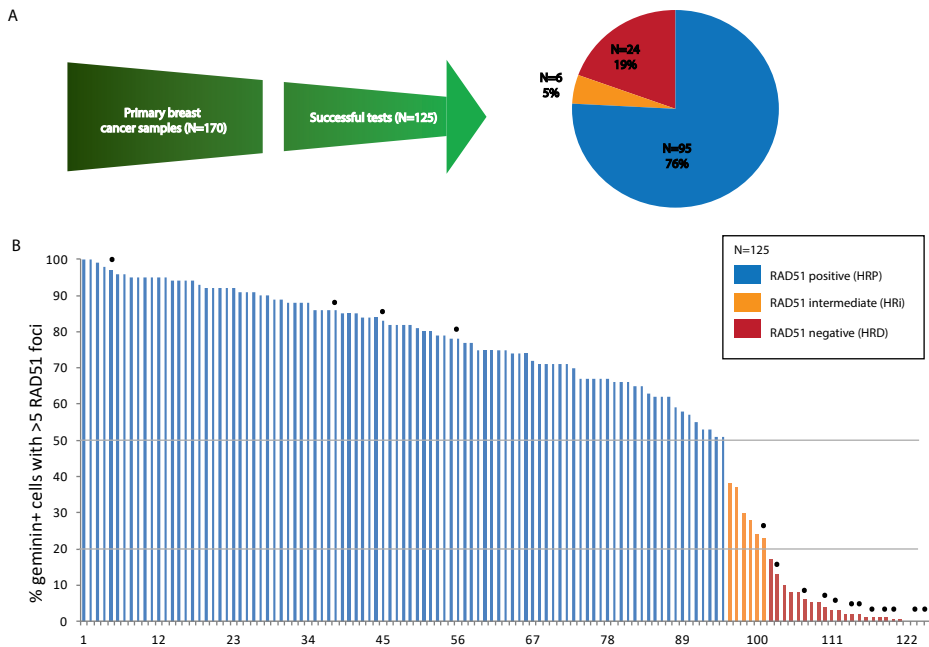


Figure 1: RECAP test results: 19% of primary breast cancers showed HRD. A) Schematic representation of the primary BrCs obtained for RECAP testing. B) Percentage of RAD51 foci positive tumor cells among geminin-expressing nuclei in the 125 successful tests. 95 BrC samples were HRP (>50% Geminin positive cells with RAD51 foci), 24 were HRD (<20% Geminin positive cells with RAD51 foci) and 6 samples were HRi (>20%/<50% Geminin positive cells with RAD51 foci). Black dots indicate TNBCs.

Thus, 12/23 HRD and 1/6 HRi samples were explained by a *BRCA2* mutation or *BRCA1* promoter hypermethylation. Subsequently, we proceeded with an MLPA analysis for *BRCA1* and *BRCA2* on the sixteen HRD and HRi samples that remained unexplained to identify possible LGRs. Large *BRCA1* deletions were found in four samples and *BRCA2* deletions in two samples (Table 1), of which one tumor harbored both a *BRCA1* and *BRCA2* deletion. Two tumors (M248 (HRD) and M112 (HRi)) showed extensive chromosomal instability as they contained a mosaic *BRCA1* deletion (meaning the deletion was present in a subclone of the tumor) as well as a *BRCA2* duplication (Table 1). In total, *BRCA* defects have thus been identified in 16/23 HRD and 2/6 HRi samples.

Silencing of *BRCA1* was validated in tumors with *BRCA1* promoter hypermethylation (n=7) and *BRCA1* LGRs (n=4) by RNAscope *in situ* RNA hybridization (Figure S2 and Table 1). All tumors displaying *BRCA1* promoter hypermethylation showed absence of *BRCA1* RNA, except for two heterogeneous samples which contained *BRCA1* positive as well as negative areas (Figure S2). As expected, the *BRCA1* deletion in tumor M094 led to a total absence of *BRCA1* mRNA (Figure S2). The mosaic *BRCA1* deletions did not result in complete *BRCA1* silencing (Figure S2). Neither did the *BRCA1* deletion in M232, however this tumor also harbored a *BRCA2* deletion that can explain the HRD phenotype.

Table 1: Overview of samples with BRCA defects

Sample	BRCA2 mutation		Pathogenicity	BRCA1 promoter hypermethylation (score)	BRCA1 mRNA RNAscope	BRCA LGRs	Tumor %	RECAP status
	Mutation	Mutation						
M057	c.517G>C p.G173R		Pathogenic \$				>50%	Negative (HRD)
P002	c.7617+1G>T		Pathogenic				60%	Negative (HRD)
M096	c.7285G>T p.E2429X		Pathogenic \$				50-70%	Negative (HRD)
M188	c.3846_3847del p.T1282fs		Pathogenic				Macrodissected (FPPE)	Negative (HRD)
M231	c.755_758del p.D252fs		Pathogenic				65%	Negative (HRD)
M275	c.3269delT p.M1090fs		Pathogenic				33%	Negative (HRD)
M213	c.1708A>C p.N570H		Benign				>50%	Positive (HRP)
M114	c.6829T>C p.L2277L		Benign				40%	Positive (HRP)
P9	c.3445A>G p.M1149V		Benign				50%	Positive (HRP)
M211	c.5054C>T p.S1685L		Benign	- (0.02)	Positive		>50	Negative (HRD)
M106	c.6347A>G p.H2116R		Benign	- (0.01)	Positive		50-70	Negative (HRD)
P001				+ (NA)	Negative		-	Negative (HRD)
M028				+ (NA)	Negative		-	Negative (HRD)
M119				+ (0.56)	Negative		50-70	Negative (HRD)
M131				+ (0.82)	Heterogeneous		>70	Negative (HRD)
M182				+ (0.45)	Negative		>50	Negative (HRD)
M277				+ (0.24)	Heterogeneous		20	Negative (HRD)
M141				+ (0.29)	Negative		50	Intermediate (HRI)
M094				- (0.01)	Negative	BRCA1 deletion	50-70	Negative (HRD)
M232				- (0.02)	Positive	BRCA 1 + 2 deletion	>70	Negative (HRD)
M248				- (0.01)	Positive	Mosaic BRCA1 deletion, BRCA2 duplication	50-70	Negative (HRD)
M112	c.6935A>T p.D2312V		Benign	- (0.01)	Positive	Mosaic BRCA1 deletion, BRCA2 duplication	50	Intermediate (HRI)

M156	- (0.01)	Positive	BRCA2 deletion	>70	Negative (HRD)
M093	- (0.01)	Positive	WT	>70	Negative (HRD)
M260	- (0.01)	Positive	WT	30	Negative (HRD)
M270	- (0.01)	Positive	WT	50-70	Negative (HRD)
M271	- (0.01)	Positive	WT	30	Negative (HRD)
M077	- (0.01)	Positive	WT	>50	Negative (HRD)
M253	- (0.01)	Positive	WT	50	Intermediate (HRI)
M209	- (0.01)	Positive	WT	50	Intermediate (HRI)
M055	- (0.01)	Positive	WT	50-70	Intermediate (HRI)
M278	- (0.01)			10	Intermediate (HRI)

Methylation score between 0.0 and 1.0, cut-off for presence of promotor hypermethylation is >0.2. \$ Mutations were somatic.

After thorough analysis of the *BRCA* genes using several techniques, 13/23 HRD and 1/6 HRi samples could be explained by deficiencies in *BRCA*. Moreover, 3/23 HRD (M131, M277 and M248) and 1/6 HRi (M112) tumors also harbored *BRCA* deficiencies (*BRCA1* promoter methylation or mosaic *BRCA1* deletions), which explain the HRi and partially the HRD phenotype, as these tumors showed heterogeneous *BRCA1* mRNA expression. Finally, 7/23 HRD and 4/6 HRi tumors did not show any *BRCA* defects and therefore remained unexplained (Figure 2). To further characterize these HRD tumors, functional features correlating with the HRD phenotype were determined.

HRD tumors show more tumor infiltrating lymphocytes than HRP tumors

Recently, a subgroup of TNBC patients was identified who showed good response to immune checkpoint inhibition through Programmed Death-ligand 1 (PD-L1) blockade^[27,28]. This subgroup was characterized by having >10% tumor infiltrating lymphocytes (TILs) and high CD8 lymphocyte counts in the tumor centers^[28]. Since 11/17 TNBCs in our study showed HRD, we hypothesized that the RECAP test might select for a specific subgroup of TNBC patients who might benefit from PD-L1 therapy. We found that significantly more HRD tumors (6/22) had >10% TILs than HRP tumors (0/28) ($p=0.004$) (Figure 3). Also, tumors with *BRCA* defects showed more frequently >10% TILs compared to non-*BRCA* tumors ($p=0.001$), which was also true for TNBCs compared to ER/PR+ tumors ($p=0.026$).

HRD tumors show mutational signatures related to *BRCA* deficiencies and microsatellite instability

Next, Whole Exome Sequencing (WES) was performed to determine the molecular landscape of HRD tumors. A selection of HRD ($n=8$) and HRi ($n=3$) tumors with *BRCA1/2* mutations/deletions, *BRCA1* promoter hypermethylation and *BRCA* WT tumors as well as 1 HRP tumor were subjected to WES. First, mutational load was determined in these tumors and high mutational load did not correlate with high numbers of TILs. Second, we did not identify commonly mutated genes other than *BRCA1/2*, that might explain the functional HR defect. Third, WES data were used to identify mutational signatures which are specific combinations of mutations that arise due to a certain underlying mutational or DNA repair processes^[29].

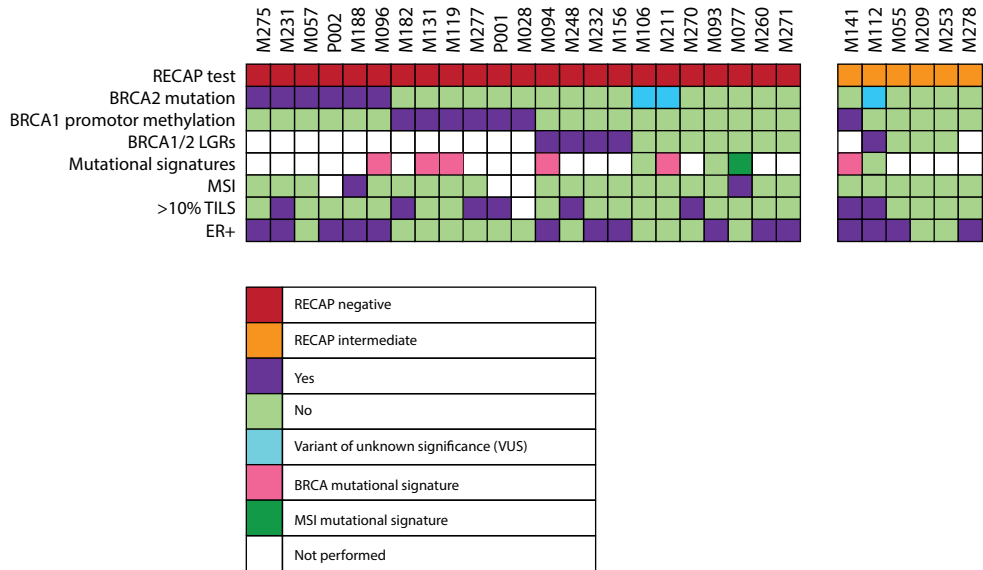


Figure 2: Characteristics of HRD and HRi tumors. Overview of molecular alterations and TIL counts in each HRD or HRi tumor (NB, data for one HRD tumor is absent, because DNA was unavailable). LGR = large genomic rearrangements, MSI = microsatellite instability, TILs = tumor infiltrating lymphocytes in tumor stroma, ER = estrogen receptor. High TILs were defined as >10% TILs.

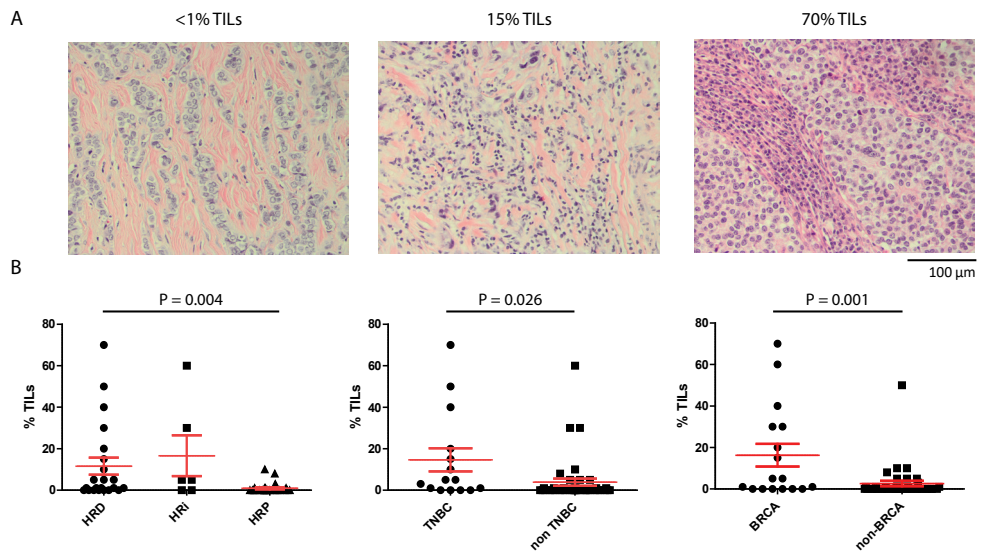


Figure 3: HRD tumors more frequently showed >10% tumor infiltrating lymphocytes than HRP tumors.

A) HE sections were scored for stromal tumor infiltrating lymphocytes (TILs). Examples of samples with <1%, 15% and 70% TILs are shown respectively. B) More HRD tumors (6/22) had >10% TILs than HRP tumors (0/28) (P=0.004). Also, tumors with BRCA defects showed more frequently >10% TILs compared to non-BRCA tumors (p=0.001), which was also true for TNBCs compared to ER/PR+ tumors (p=0.026). Significance was calculated by Fisher's exact test.

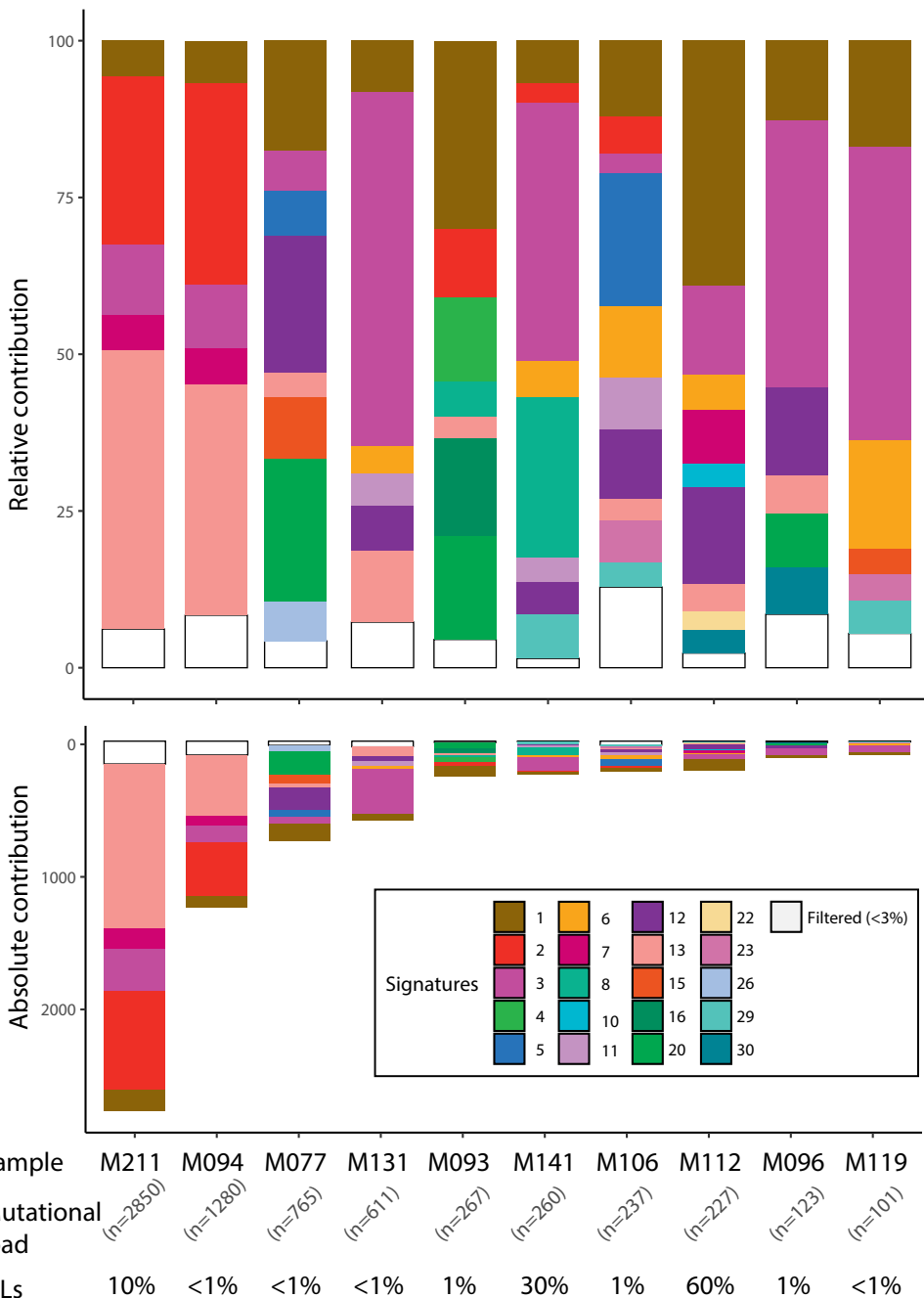


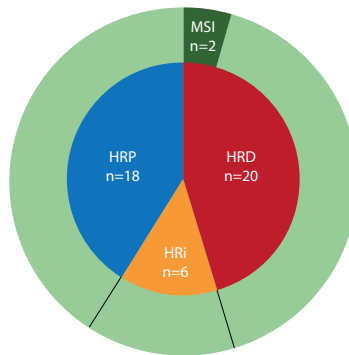
Figure 4: HRD and HRi tumors showed mutational signatures related to BRCA as well as microsatellite instability. Relative and absolute contribution of the mutational signatures in WES datasets is depicted, as well as total numbers of single-nucleotide mutations and percentage of TILs in the sample.



Mutational signatures were derived from the WES data from HRD/HRi tumors of which matching normal DNA was available to filter out germline variants (n=10) to explore novel mechanisms related to or underlying the HRD phenotype. Since discussion in the field exists that mutational signatures can only be faithfully obtained from whole genome sequencing (WGS) instead of WES data, we first carried out a pilot experiment comparing mutational signature analysis using all somatic mutations in 5 BrC WGS datasets^[30] and filtered these WGS datasets to only contain somatic mutations on exonic regions. Both methods resulted in similar distributions of the mutational signatures (Figure S3).

Mutational signature 3 is related to failure of DSB repair by HR and associated with germline and somatic *BRCA1/2* defects in breast, pancreatic, and ovarian cancers^[31]. Signature 3 was present in 6/10 analyzed samples (M94, M95, M119, M131, M141, and M221) (Figure 4). APOBEC related mutagenesis (predominantly C>G or C>T substitutions in TCA or TCT motifs) is captured in signatures 2 and 13, which arise through activity of the AID/APOBEC family. BRCA related signatures could also be identified to a lesser extent in samples (M211 and M094) having a high mutational burden of signatures 2 and 13.

A



B

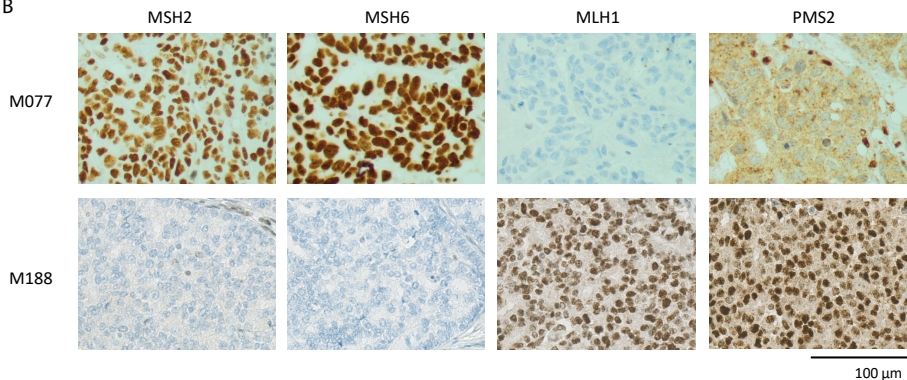


Figure 5: Two HRD breast tumors showed microsatellite instability. A) MSI was found in two HRD tumors, but not in any HRP or HRi tumors. B) Immunohistochemical staining of MLH1, PMS2, MSH2 and MSH6.

Microsatellite instability in HRD breast cancers

One tumor (M077) showed a high mutational load as well as high contributions of signatures 15, 20 and 26, which are related to microsatellite instability (MSI) and mismatch repair (MMR) deficiency (<http://cancer.sanger.ac.uk/cosmic/signatures>). MSI is a common feature in endometrial and gastro-intestinal cancers, caused by either germline (Lynch syndrome) or somatic mutations in one of the MMR genes and/or promoter hypermethylation [32,33]. Presence of MSI in tumor M077 was confirmed using pentaplex PCR and immunohistochemistry for the MMR proteins, which showed absence of MLH1 and PMS2, caused by *MLH1* promoter methylation (Figure S4).

A set of 44 tumors (20 HRD, 6 HRI, 18 HRP) was subjected to MSI analysis by pentaplex PCR and immunohistochemistry for the MMR proteins. One HRD tumor (M188) of which mutational signatures were not available, also showed MSI. MSI was never detected in any HRP tumors (Figure 5). Tumor M188 showed absence of MSH2 and MSH6, caused by a homozygous deletion of *MSH2* (Figure S4). The two MSI BrCs (M077 and M188) were TN and *BRCA* WT and ER positive and *BRCA2* mutated, respectively (Figure 2). The incidence of MSI within the HRD group (2/20, 10%) is significantly higher than the incidence of MSI in the unselected BrC population (1%) ($p=0.017$) [34,35].

Discussion

Here, a unique series of fresh primary BrC tissues ($n=125$) has been analyzed for HRD using the functional RECAP test. This first large validation study, describes that functional assessment of HR in a pseudo-diagnostic setting is achievable and produces robust and interpretable results for most patients (74%). We found that the percentage of HRD tumors detected by the RECAP test is similar in this larger cohort, as compared with our previous report. Therefore, both cohorts were combined to achieve more power to thoroughly investigate the molecular mechanism underlying the HRD phenotype. Sixteen HRD samples showed deficiencies in *BRCA1/2* (*BRCA* mutations, deletions or promoter hypermethylation), whereas seven HRD tumors were non-*BRCA* related, demonstrating that HRD tumors encompass more than only *BRCA* deficient tumors.

Several different HRD tests have been designed to identify HRD tumors in addition to the *BRCA* mutated or promoter methylated tumors to enlarge the population of BrC patients that could benefit from treatments targeting the HR pathway. For example, the BRCAness classifier, which is based on specific genomic patterns derived from copy number data of *BRCA1/2* mutated BrCs that also occur in sporadic cancers [10,11] and the Myriad MyChoice HRD test, which is a combined score of three different structural chromosomal aberrations (telomeric allelic imbalance (TAI), large-scale transition (LST) and loss of heterozygosity (LOH)) [36]. Both the BRCAness classifier and MyChoice are robust, easily applicable in the clinic and have also been validated to predict *in vivo* response to high dose chemotherapy and neo-adjuvant platinum based therapy, respectively, in TNBC patients [37,38]. As opposed

to the neo-adjuvant setting, the MyChoice HRD test did not predict response to PARPi therapy in platinum-sensitive recurrent ovarian cancer ^[39]. These genomic HRD tests have the drawback that they do not determine the real-time HR status, also it remains unclear whether all HRD cases are identified. In theory, the functional RECAP test can also detect reversion of the HRD phenotype in BRCA deficient tumors, that have been treated with various DNA damaging chemotherapies that may have induced resistance. Moreover, the BRCAness classifier focusses on TNBC only, whereas the RECAP test identifies HRD independent of hormonal status. More recently, a HRD test based on several genomic signatures has been published, HRDetect ^[40]. This test has recently been shown to predict *in vivo* response to platinum-based therapies in advanced breast cancer ^[41]. HRDetect relies on whole genome sequencing and is therefore more expensive and has a longer turnaround time for biopsy results, hampering its clinical implementation. Furthermore, the tumor cell percentage needs to be above 50% for reliable results, which is not a prerequisite for the RECAP test. On the other hand, HRDetect has the advantage that it can be performed on frozen material, whereas the RECAP test requires fresh material. The percentage of non-BRCA HRD tumors (approximately 33%) detected by the HRDetect and the RECAP test are quite comparable, although it remains elusive whether these tests identify the same tumors, therefore comparison of several HRD tests within the same patient cohort is required.

The major strength of the current study is that functional diagnostics have been applied to a unprecedented large collection of tumors. The advantage of the RECAP test over genetic tests, is its functional character for exploring the HR phenotype rather than the static nature of genomic tests. Also, the RECAP test is feasible in samples with low tumor percentage, since the microscopic read-out allows differentiation between tumor and stromal cells. The RECAP test has a high success rate and results are available within one week after the biopsy procedure. In this study, reproducibility and robustness of the RECAP test is validated in an independent set of 129 tumors. For the molecular analyses to unravel the mechanisms underlying the HRD phenotype, the 41 samples included in our previous publication were also included, to achieve more power. The main limitation of this study is that although prospective trials evaluating the predictive value of RECAP for *in vivo* patient response to PARPi have been initiated, results are not yet available. However, previously a functional RAD51 test performed on biopsies obtained from patients 24 hours after start of therapy correlated with response to anthracycline based therapies, indicating that functional assessment of HR can have predictive value for therapy response ^[13].

Among the spectrum of BRCA defects, we have not identified any *BRCA1* mutations. This is somewhat remarkable but could be due to a selection bias, as the Erasmus Medical Center is specialized in hereditary BrC and all patients with TNBC are tested, therefore most families with hereditary *BRCA1* mutations have been identified and carriers are offered strict screening programs or undergo prophylactic surgery in The Netherlands ^[42]. Also, in

this study there is a selection bias for tumor size, as the tumor should be large enough to provide residual material without compromising standard diagnostic procedures. Since *BRCA* mutation carriers are offered strict screening programs, tumors are often identified at an early stage and residual material is not available for the RECAP test. Also, many *BRCA1* mutation carriers with TNBC are treated with neoadjuvant chemotherapy, which was an exclusion criterion for this study.

Clinical consequences of *BRCA1* promoter methylation are unclear^[43]. In the current study, *BRCA1* promoter methylation resulted in absence of *BRCA1* RNA in four samples, but in two tumors there was still heterogeneous expression of *BRCA1* RNA (Figure S2). In these tumors, the percentage of cells with RAD51 foci was 1% and 2%, respectively. The discrepancy between the very low HRD score and heterogeneous *BRCA1* RNA could be explained by sampling from different areas of the tumor, since the tumor sample for the RECAP test was irradiated and an unirradiated tumor sample was used for molecular analyses. This sampling error is not limited to this study, but also occurs in regular diagnostics when biopsies are obtained from a certain region of a heterogeneous tumor. Tumor heterogeneity in *BRCA1* promoter methylated tumors is very important for clinical decisions on PARPi use. If subsequent studies reveal that this phenomenon is observed in a large fraction of these tumors, PARPi may not be very effective in tumors with *BRCA1* promoter methylation.

We identified 6 HRi BrCs in the current cohort. Only in one of the HRi tumors, distinct areas of RAD51 negative and RAD51 positive tumor cells were observed, suggesting clonal heterogeneity. The other HRi tumors all showed interspersed RAD51 negative as well as RAD51 positive tumor cells. As a *BRCA* defect was found in 2/6 HRi tumors, they biologically resemble HRD tumors. However, whether HRi tumors benefit from PARPi treatment remains to be elucidated.

Mutational signature analyses were performed to explore novel mechanisms related to or underlying the HRD phenotype. One HRD tumor that showed a large contribution of three signatures related to MSI and MMR deficiency, proved to be truly MSI. Using pentaplex PCR and immunohistochemistry, MSI was discovered in two HRD (2/20, 10%) but not in HRP or HRi tumors. This incidence is much higher than in the unselected BrC population (1%)^[34,35], suggesting that the RECAP test may also identify MSI tumors. The relation between MSI and HRD as well as the order in which tumors develop these deficiencies remains unclear and future research is required. We hypothesize that either MSI tumors acquire HRD over time due to accumulation of mutations in genes involved in HR^[44], or HRD tumors acquire MSI at a later stage of tumor development as a compensatory mechanism, to lower replication fork instability by not repairing mismatches but rather continuing DNA replication. As MSI tumors have many neo-antigens, PD-L1 blockade therapy showed anti-tumor activity in phase I trials^[45]. Recently, a first report of a patient with MSI BrC showing a profound response to PD-L1 blockade was published^[46]. Moreover, tumors with high numbers of TILs are generally more sensitive to immunotherapy^[47].

Interestingly, in our cohort, the two MSI tumors comprise a different subset of HRD tumors than the ones with high TILs. Thus, the RECAP test identifies not only tumors with *BRCA* defects (n=16), but also a subgroup of BrCs that might respond well to immunotherapy due to either MSI (n=2) or high TIL counts (n=6).

The RECAP test is a robust functional HR assay detecting both *BRCA1/2* deficient and *BRCA1/2* proficient HRD tumors. Functional assessment of HR in a pseudo-diagnostic setting is achievable and produces robust and interpretable results. Clinical trials evaluating the predictive value of the RECAP test for *in vivo* response to PARPi have been initiated.

Acknowledgements

The authors thank many colleagues from the departments of Molecular Genetics, Medical Oncology and Pathology at Erasmus MC as well as from the Maastad hospital, who contributed to the collection of patient material. We thank Lindsey Oudijk for her assistance with the TILs scoring. We thank Ronald van Marion for expert technical assistance. D.C. van Gent, A. Jager and R. Kanaar have received funding from the Dutch Cancer Society (Alpe d'Huzes grant number EMCR 2014-7048 and grant number EMCR 2008-4045). This work is part of the Oncode Institute which is partly financed by the Dutch Cancer Society and was funded by the gravitation program CancerGenomiCs.nl from the Netherlands Organisation for Scientific Research (NWO).

References

1. Siegel RL, Miller KD, Jemal A. Cancer Statistics, 2017. *CA Cancer J Clin*, 67(1), 7-30 (2017).
2. Nelson HD, Fu R, Goddard K *et al.*, (2013).
3. Hartman AR, Kaldate RR, Sailer LM *et al.* Prevalence of BRCA mutations in an unselected population of triple-negative breast cancer. *Cancer*, 118(11), 2787-2795 (2012).
4. Konecny GE, Kristeleit RS. PARP inhibitors for BRCA1/2-mutated and sporadic ovarian cancer: current practice and future directions. *Br J Cancer*, 115(10), 1157-1173 (2016).
5. Lord CJ, Ashworth A. The DNA damage response and cancer therapy. *Nature*, 481(7381), 287-294 (2012).
6. Robson M, Im SA, Senkus E *et al.* Olaparib for Metastatic Breast Cancer in Patients with a Germline BRCA Mutation. *N Engl J Med*, 377(6), 523-533 (2017).
7. Wendie DdB, Kasmintan AS, Sophie S *et al.* Homologous Recombination Deficiency in Breast Cancer: A Clinical Review. *JCO Precision Oncology*, -(1), 1-13 (2017).
8. Abkevich V, Timms KM, Hennessy BT *et al.* Patterns of genomic loss of heterozygosity predict homologous recombination repair defects in epithelial ovarian cancer. *Br J Cancer*, 107(10), 1776-1782 (2012).
9. Birkbak NJ, Wang ZC, Kim JY *et al.* Telomeric allelic imbalance indicates defective DNA repair and sensitivity to DNA-damaging agents. *Cancer Discov*, 2(4), 366-375 (2012).
10. Jooose SA, Brandwijk KI, Devilee P *et al.* Prediction of BRCA2-association in hereditary breast carcinomas using array-CGH. *Breast Cancer Res Treat*, 132(2), 379-389 (2012).
11. Jooose SA, van Beers EH, Tielen IH *et al.* Prediction of BRCA1-association in hereditary non-BRCA1/2 breast carcinomas with array-CGH. *Breast Cancer Res Treat*, 116(3), 479-489 (2009).
12. Konstantinopoulos PA, Spentzos D, Karlan BY *et al.* Gene expression profile of BRCAness that correlates with responsiveness to chemotherapy and with outcome in patients with epithelial ovarian cancer. *J Clin Oncol*, 28(22), 3555-3561 (2010).
13. Graeser M, McCarthy A, Lord CJ *et al.* A marker of homologous recombination predicts pathologic complete response to neoadjuvant chemotherapy in primary breast cancer. *Clin Cancer Res*, 16(24), 6159-6168 (2010).
14. Naipal KA, Verkaik NS, Ameziane N *et al.* Functional ex vivo assay to select homologous recombination-deficient breast tumors for PARP inhibitor treatment. *Clin Cancer Res*, 20(18), 4816-4826 (2014).
15. Gross E, van Tinteren H, Li Z *et al.* Identification of BRCA1-like triple-negative breast cancers by quantitative multiplex-ligation-dependent probe amplification (MLPA) analysis of BRCA1-associated chromosomal regions: a validation study. *BMC Cancer*, 16(1), 811 (2016).
16. Li H, Durbin R. Fast and accurate short read alignment with Burrows-Wheeler transform. *Bioinformatics*, 25(14), 1754-1760 (2009).

17. Li H, Handsaker B, Wysoker A *et al.* The Sequence Alignment/Map format and SAMtools. *Bioinformatics*, 25(16), 2078-2079 (2009).
18. <https://broadinstitute.github.io/picard/><http://broadinstitute.github.io/picard/BIPthbgipAa.>
19. Forbes SA, Beare D, Boutselakis H *et al.* COSMIC: somatic cancer genetics at high-resolution. *Nucleic Acids Res*, 45(D1), D777-D783 (2017).
20. McKenna A, Hanna M, Banks E *et al.* The Genome Analysis Toolkit: a MapReduce framework for analyzing next-generation DNA sequencing data. *Genome Res*, 20(9), 1297-1303 (2010).
21. Sherry ST, Ward MH, Kholodov M *et al.* dbSNP: the NCBI database of genetic variation. *Nucleic Acids Res*, 29(1), 308-311 (2001).
22. Wang K, Li M, Hakonarson H. ANNOVAR: functional annotation of genetic variants from high-throughput sequencing data. *Nucleic Acids Res*, 38(16), e164 (2010).
23. Blokzijl F, Janssen, R., van Boxtel, R. & Cuppen, E. MutationalPatterns: an integrative R package for studying patterns in base substitution catalogues Francis. bioRxiv Prepr. 0–0 (2017). doi:10.1093/bioinformatics/xxxxx.
24. Alexandrov LB, Nik-Zainal S, Wedge DC, Campbell PJ, Stratton MR. Deciphering signatures of mutational processes operative in human cancer. *Cell Rep*, 3(1), 246-259 (2013).
25. van Lier MG, Wagner A, van Leerdam ME *et al.* A review on the molecular diagnostics of Lynch syndrome: a central role for the pathology laboratory. *J Cell Mol Med*, 14(1-2), 181-197 (2010).
26. Salgado R, Denkert C, Demaria S *et al.* The evaluation of tumor-infiltrating lymphocytes (TILs) in breast cancer: recommendations by an International TILs Working Group 2014. *Ann Oncol*, 26(2), 259-271 (2015).
27. Kurozumi S, Fujii T, Matsumoto H *et al.* Significance of evaluating tumor-infiltrating lymphocytes (TILs) and programmed cell death-ligand 1 (PD-L1) expression in breast cancer. *Med Mol Morphol*, 50(4), 185-194 (2017).
28. Peter Schmid CC, Fadi S. Braithe *et al.* Atezolizumab in metastatic TNBC (mTNBC): Long-term clinical outcomes and biomarker analyses. Abstract #2986, AACR 2017.
29. Nik-Zainal S, Alexandrov LB, Wedge DC *et al.* Mutational processes molding the genomes of 21 breast cancers. *Cell*, 149(5), 979-993 (2012).
30. Nik-Zainal S, Davies H, Staaf J *et al.* Landscape of somatic mutations in 560 breast cancer whole-genome sequences. *Nature*, 534(7605), 47-54 (2016).
31. Alexandrov LB, Nik-Zainal S, Wedge DC *et al.* Signatures of mutational processes in human cancer. *Nature*, 500(7463), 415-421 (2013).
32. Geurts-Giele WR, Leenen CH, Dubbink HJ *et al.* Somatic aberrations of mismatch repair genes as a cause of microsatellite-unstable cancers. *J Pathol*, 234(4), 548-559 (2014).
33. Lynch HT, Snyder CL, Shaw TG, Heinen CD, Hitchins MP. Milestones of Lynch syndrome: 1895-2015. *Nat Rev Cancer*, 15(3), 181-194 (2015).

34. Dudley JC, Lin MT, Le DT, Eshleman JR. Microsatellite Instability as a Biomarker for PD-1 Blockade. *Clin Cancer Res*, 22(4), 813-820 (2016).
35. Le DT, Durham JN, Smith KN *et al.* Mismatch repair deficiency predicts response of solid tumors to PD-1 blockade. *Science*, 357(6349), 409-413 (2017).
36. Timms KM, Abkevich V, Hughes E *et al.* Association of BRCA1/2 defects with genomic scores predictive of DNA damage repair deficiency among breast cancer subtypes. *Breast Cancer Res*, 16(6), 475 (2014).
37. Vollebergh MA, Lips EH, Nederlof PM *et al.* An aCGH classifier derived from BRCA1-mutated breast cancer and benefit of high-dose platinum-based chemotherapy in HER2-negative breast cancer patients. *Ann Oncol*, 22(7), 1561-1570 (2011).
38. Telli ML, Timms KM, Reid J *et al.* Homologous Recombination Deficiency (HRD) Score Predicts Response to Platinum-Containing Neoadjuvant Chemotherapy in Patients with Triple-Negative Breast Cancer. *Clin Cancer Res*, 22(15), 3764-3773 (2016).
39. Mirza MR, Monk BJ, Herrstedt J *et al.* Niraparib Maintenance Therapy in Platinum-Sensitive, Recurrent Ovarian Cancer. *N Engl J Med*, 375(22), 2154-2164 (2016).
40. Davies H, Glodzik D, Morganella S *et al.* HRDetect is a predictor of BRCA1 and BRCA2 deficiency based on mutational signatures. *Nat Med*, 23(4), 517-525 (2017).
41. Zhao EY, Shen Y, Pleasance E *et al.* Homologous Recombination Deficiency and Platinum-Based Therapy Outcomes in Advanced Breast Cancer. *Clin Cancer Res*, 23(24), 7521-7530 (2017).
42. Drooger JC, Hoening MJ, Seynaeve CM *et al.* Diagnostic and therapeutic ionizing radiation and the risk of a first and second primary breast cancer, with special attention for BRCA1 and BRCA2 mutation carriers: a critical review of the literature. *Cancer Treat Rev*, 41(2), 187-196 (2015).
43. Sun T, Ruscito I, Dimitrova D *et al.* Genetic Versus Epigenetic BRCA1 Silencing Pathways: Clinical Effects in Primary Ovarian Cancer Patients: A Study of the Tumor Bank Ovarian Cancer Consortium. *Int J Gynecol Cancer*, (2017).
44. Zhao H, Thienpont B, Yesilyurt BT *et al.* Mismatch repair deficiency endows tumors with a unique mutation signature and sensitivity to DNA double-strand breaks. *Elife*, 3, e02725 (2014).
45. Westdorp H, Fennemann FL, Weren RD *et al.* Opportunities for immunotherapy in microsatellite instable colorectal cancer. *Cancer Immunol Immunother*, 65(10), 1249-1259 (2016).
46. Marleen K, Hugo MH, Petur S *et al.* Profound Immunotherapy Response in Mismatch Repair-Deficient Breast Cancer. *JCO Precision Oncology*, (1), 1-3 (2017).
47. Gibney GT, Weiner LM, Atkins MB. Predictive biomarkers for checkpoint inhibitor-based immunotherapy. *Lancet Oncol*, 17(12), e542-e551 (2016).

Supplementary data

Supplementary Table 1: Comparison of clinicopathologic characteristics between successful tests and not successful tests.

	Successful test	Not successful test	P-value
Tumor size (median, cm)	2.8	2.5	P = 0.181
Histological subtype			
Ductal carcinoma	99 (79.2%)	39 (86.7%)	P = 0.597
Lobular carcinoma	22 (17.6%)	5 (11.1%)	
Other	4 (3.2%)	1 (2.2%)	
Histological grade			
1	13 (10.4%)	6 (13.3%)	P = 0.069
2	49 (39.2%)	25 (55.6%)	
3	63 (50.4%)	14 (31.1%)	
Receptor Status			
ER/PR +, HER2-	91 (72.8%)	39 (86.7%)	P = 0.160
HER2+*	18 (14.4%)	4 (8.9%)	
TNBC	16 (12.8%)	2 (4.4%)	
Total	125	45	

***independent of ER/PR status.** Significance was calculated by Fisher's exact test for categorical data and by Mann-Whitney test for continuous data (tumor size).

Supplementary Table 2: Comparison of clinicopathologic characteristics RECAP positive/negative/intermediate tumors.

	HRP	HRi	HRD	P-value HRP vs HRi	P-value HRP vs HR
Tumor size (median, cm)	2.7	3.2	3.1	P = 0.459	P = 0.118
Histological subtype					
Ductal carcinoma	75 (78.9%)	6 (100%)	18 (75%)	P = 0.616	P = 0.038
Lobular carcinoma	19 (20%)	0	3 (12.5%)		
Other	1 (1.1%)	0	3 (12.5%)		
Histological grade					
1	13 (13.7%)	0	0	P = 0.010	P < 0.001
2	44 (46.3%)	0	5 (21%)		
3	38 (40%)	6 (100%)	19 (79%)		
Receptor Status					
ER/PR +, HER2-	79 (83.2%)	2 (33%)	10 (41.7%)	P = 0.014	P < 0.001
HER2+*	12 (12.6%)	3 (50%)	3 (12.5%)		
TNBC	4 (4.2%)	1 (17%)	11 (45.8%)		
Total	95	6	24		

***independent of ER/PR status.** Significance was calculated by Fisher's exact test for categorical data and by Mann-Whitney test for continuous data (tumor size).

Supplementary table 3: All characteristics and RECAP test outcomes per tumor.

Sample ID	Histological subtype	ER	PR	HER2	B&R grade	Tumor size (cm)	RECAP outcome	RAD51 FOCI %
P001*	metaplastic	neg	neg	neg	3	5.5	negative	1
P002*	ductal/lobular	pos	pos	neg	3	4.8	negative	1
P003*	ductal	pos	pos	neg	3	3	positive	88
P005*	ductal	pos	neg	neg	2	2.5	NA	
P008*	ductal	pos	neg	neg	3	2.2	NA	
P009*	ductal	pos	pos	neg	1	1.5	positive	75
P012*	ductal	neg	neg	pos	3	5.1	NA	
M002*	ductal	pos	neg	pos	2	3.2	NA	
M003*	lobular	pos	neg	neg	2	2.8	NA	
M005*	ductal	pos	neg	neg	1	5.5	NA	
M007*	ductal	pos	pos	neg	3	2.6	NA	
M009*	lobular	pos	pos	neg	2	2.8	positive	71
M018*	ductal	pos	pos	neg	3	12.5	positive	71
M019*	lobular	pos	pos	neg	3	8.2	positive	77
M021*	ductal	neg	neg	pos	3	2.4	positive	67
M022*	ductal	pos	pos	neg	1	1.6	positive	81
M023*	ductal	pos	pos	neg	3	3.4	positive	89
M025*	ductal	pos	pos	neg	2	1.7	positive	67
M026*	ductal	pos	pos	neg	2	4.5	NA	
M028*	ductal	neg	neg	neg	3	4.8	negative	3
M029*	ductal	pos	pos	pos	3	3.5	positive	62
M030*	ductal	pos	pos	neg	2	10	positive	67
M031*	ductal	pos	pos	neg	2	2.1	NA	
M043*	ductal	pos	neg	neg	3	4.3	positive	75
M046*	ductal	neg	neg	pos	3	2.3	positive	70
M047*	ductal	pos	pos	neg	3	2.5	NA	
M048*	lobular	pos	neg	neg	3	5.8	positive	86
M051*	ductal	pos	pos	neg	3	2.7	positive	75
M052*	ductal	pos	pos	neg	3	7.5	positive	71
M055*	ductal	pos	pos	neg	3	5.4	intermediate	38
M056*	ductal	pos	neg	neg	3	2.9	positive	74
M057*	ductal	neg	neg	neg	3	2.2	negative	13
M058*	ductal	pos	pos	neg	3	2.6	positive	79
M059*	ductal	pos	neg	neg	2	3.4	positive	84
M060*	ductal	pos	pos	neg	2	2.2	positive	84
M061*	ductal	pos	pos	neg	2	1.4	NA	

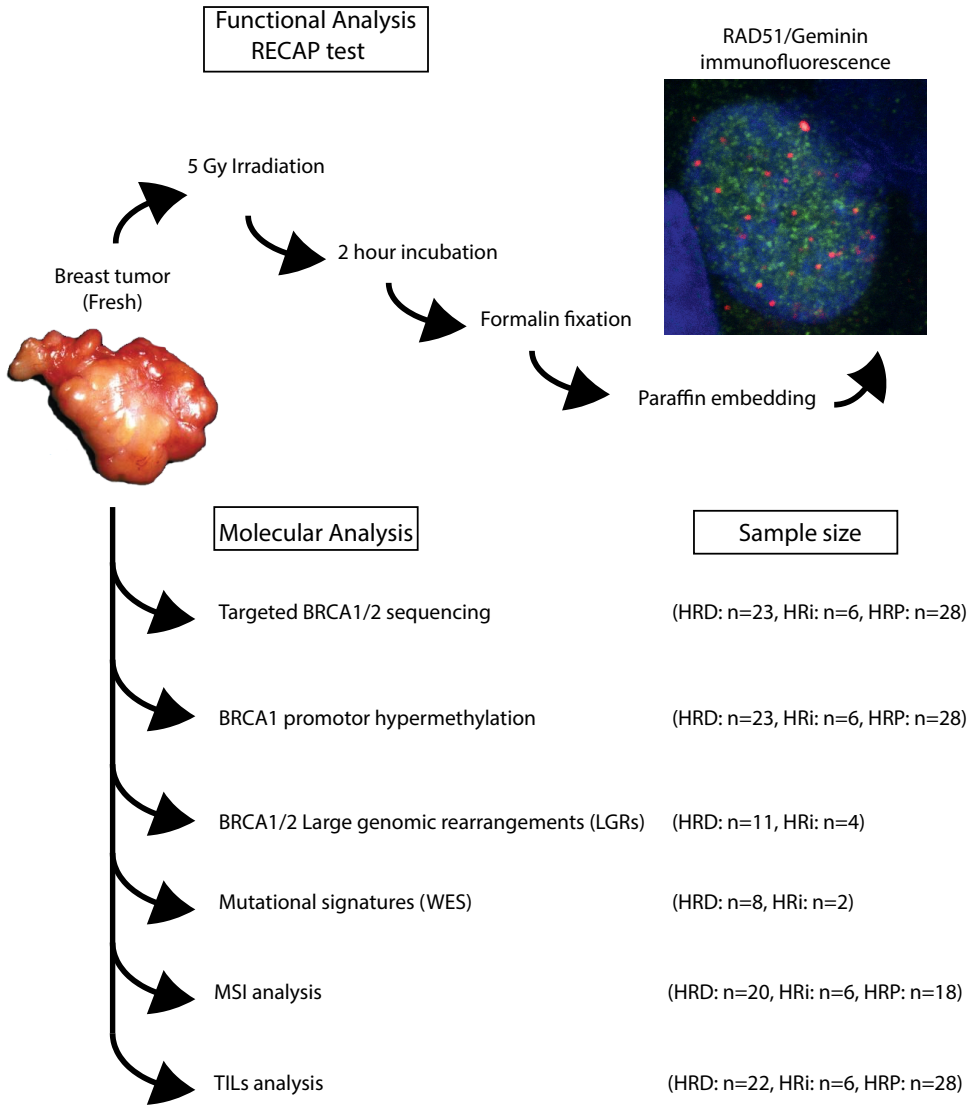
M062*	ductal	neg	neg	neg	3	3.4	positive	83
M063*	ductal	pos	pos	neg	2	1.4	positive	71
M064*	ductal	pos	pos	neg	2	3.4	NA	
M065*	ductal	pos	pos	pos	3	2.1	positive	57
M066*	ductal	pos	neg	neg	1	1.8	NA	
M067*	lobular	pos	pos	neg	2	1.3	positive	74
M068*	ductal	pos	pos	neg	1	1.5	NA	
M069*	ductal	pos	pos	neg	3	1.9	NA	
M070*	lobular	pos	pos	neg	2	4	NA	
M071*	lobular	pos	pos	neg	2	5.5	positive	75
M072*	ductal	pos	pos	neg	2.00	11.00	positive	74
M073*	lobular	pos	pos	neg	2.00	1.80	NA	
M074*	ductal	pos	pos	neg	2.00	10.50	positive	77
M075*	ductal	pos	pos	neg	3	10.00	NA	
M077	ductal	neg	neg	neg	3	2.30	low/negative	0.5
M078	ductal	pos	pos	neg	3	2.50	positive	53
M079	ductal	pos	pos	neg	2	1.50	NA	
M080	ductal	pos	pos	neg	3	2.10	positive	85
M082	micro papillary	pos	pos	neg	2	6.50	NA	
M083	ductal	pos	pos	neg	2	6.50	positive	62
M084	lobular	pos	pos	neg	2	2.50	positive	65
M086	ductal	pos	pos	neg	1	1.40	NA	
M088	ductal	pos	neg	neg	2	3.8	NA	
M089	ductal	pos	pos	neg	3	3.8	positive	82
M090	ductal	pos	neg	neg	3	3.4	positive	85
M092	ductal	pos	neg	neg	2	9	NA	
M093	lobular	pos	pos	neg	2	2.5	low/negative	8
M094	ductal	pos	neg	pos	2	1.7	low/negative	8
M096	ductal	pos	pos	neg	3	2.8	low/negative	4
M097	ductal	pos	pos	neg	3	2.6	NA	
M098	ductal	pos	pos	neg	1	1.9	NA	
M099	ductal	pos	pos	neg	1	1	NA	
M100	ductal	neg	neg	neg	3	2.5	positive	97
M101	ductal	neg	neg	neg	3	1.6	NA	
M102	lobular	pos	pos	neg	3	7	NA	
M104	ductal	pos	pos	neg	3	1.3	positive	90
M106	ductal	neg	neg	pos	3	2.6	low/negative	6
M107	ductal	pos	pos	neg	2	1.4	NA	
M108	ductal	pos	pos	neg	2	2.6	positive	80

M109	ductal	pos	pos	neg	1	2.5	positive	94
M110	lobular	pos	pos	neg	1	2.9	positive	94
M111	ductal	pos	pos	pos	1	3.5	positive	90
M112	ductal	pos	pos	pos	3	3.5	different	30
M113	ductal	pos	neg	neg	2	1.2	positive	55
M114	lobular	pos	neg	neg	2	3	positive	78
M115	ductal	pos	pos	neg	2	1.8	positive	51
M116	ductal	pos	pos	neg	2	3.8	NA	
M117	ductal	pos	pos	neg	3	1.8	positive	67
M118	ductal	pos	pos	neg	3	1.7	NA	
M119	ductal	neg	neg	neg	3	7	low/negative	0.5
M120	ductal	pos	pos	neg	2	3	positive	59
M121	lobular	pos	neg	neg	2	9.7	positive	86
M125	ductal	pos	pos	neg	3	2.6	positive	66
M128	ductal	pos	neg	pos	3	1.4	positive	67
M129	ductal	pos	pos	neg	1	1.6	positive	91
M130	ductal	pos	pos	neg	3	2.5	NA	
M131	ductal	neg	neg	neg	3	5.5	low/negative	1
M133	ductal	pos	pos	neg	2	5.5	positive	84
M135	ductal	pos	pos	neg	3	5.5	positive	95
M136	ductal	neg	neg	neg	3	2.3	low/negative	5
M141	ductal	pos	neg	neg	3	2.5	intermediate	28
M142	ductal	pos	neg	pos	2	3.2	positive	80
M143	ductal	pos	pos	neg	3	2.7	positive	96
M144	ductal	neg	neg	neg	3	2.2	NA	
M146	ductal	pos	pos	neg	2	1.9	positive	58
M147	ductal	pos	pos	neg	2	2.2	NA	
M148	ductal	pos	pos	neg	3	2.5	NA	
M149	ductal	pos	pos	pos	3	2.6	positive	53
M150	ductal	pos	pos	neg	2	1.3	positive	92
M152	ductal	pos	pos	neg	2	5.5	NA	
M153	ductal	pos	pos	neg	3	4	positive	95
M155	lobular	pos	neg	neg	2	1.8	positive	65
M156	ductal	pos	pos	neg	2	2.5	negative	5
M157	ductal	pos	pos	neg	1	1.4	positive	88
M159	ductal	pos	pos	neg	2	3	positive	95
M162	ductal	pos	pos	neg	1	1.5	positive	93
M163	ductal	pos	pos	neg	2	2.2	NA	
M164	ductal	pos	pos	neg	2	2.5	positive	88

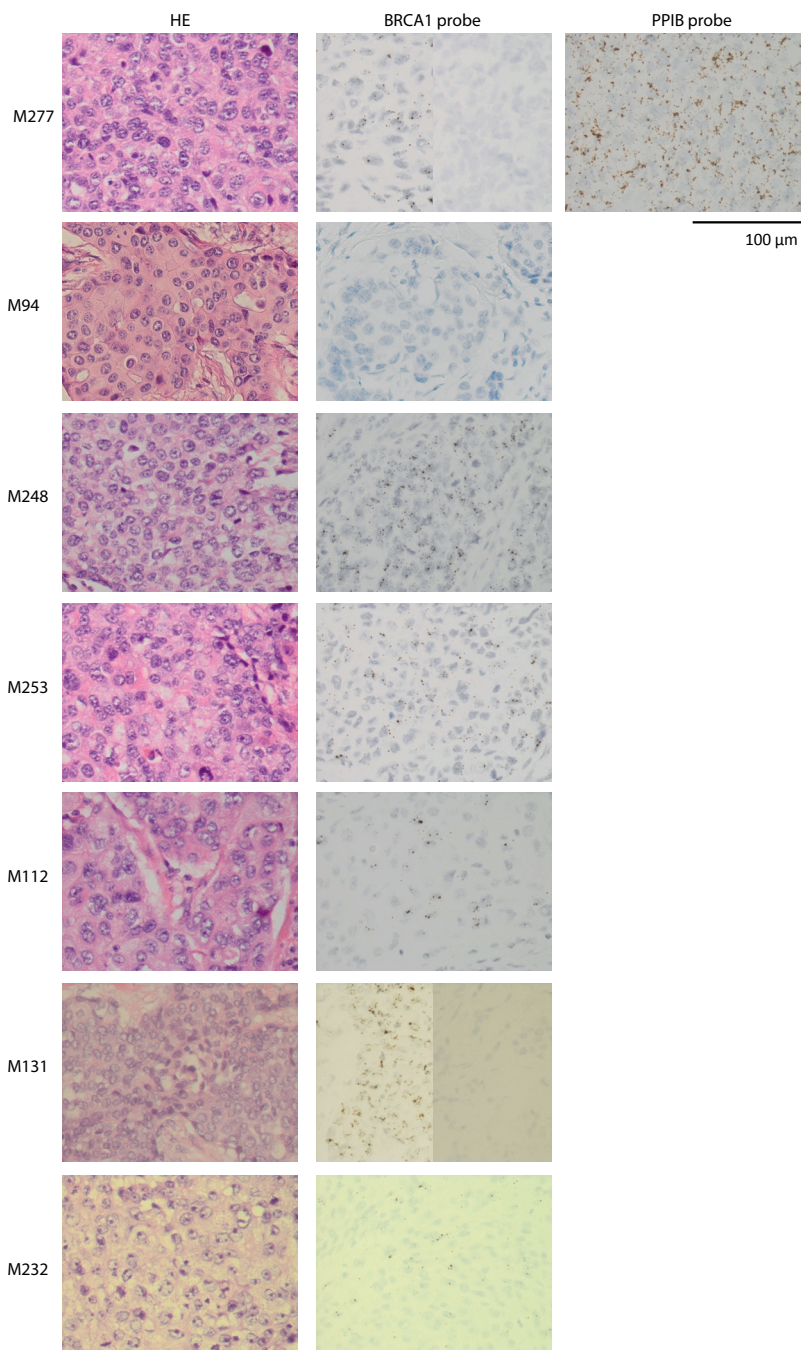
M166	ductal	pos	pos	neg	3	3	positive	92
M169	ductal	pos	pos	neg	3	4	positive	66
M170	ductal	pos	pos	neg	3	4.5	positive	51
M171	ductal	pos	pos	pos	3	7.5	positive	63
M175	ductal	pos	pos	neg	2	1.1	NA	
M176	ductal	pos	pos	neg	2	4.4	NA	
M178	ductal	pos	pos	pos	2	1.7	NA	
M179	ductal	pos	pos	neg	1	2.2	positive	75
M180	ductal	pos	neg	neg	2	2.2	positive	71
M181	ductal	neg	neg	neg	3	5.5	positive	78
M182	ductal	neg	neg	neg	3	1.9	negative	2
M183	ductal	pos	pos	neg	2	1.3	positive	66
M187	ductal	pos	pos	neg	2	3.2	positive	96
M188	ductal	pos	pos	neg	3	12.1	negative	1
M191	lobular	pos	pos	neg	2	3	NA	
M193	ductal	pos	pos	neg	3	1.2	positive	82
M195	lobular	pos	neg	neg	2	2.4	positive	82
M197	mucineus	pos	pos	neg	2	2	positive	91
M198	ductal	pos	neg	neg	2	2.8	NA	
M199	ductal	pos	neg	pos	1	7	positive	72
M200	ductal	pos	pos	neg	3	3.5	positive	89
M201	lobular	pos	pos	neg	2	4.5	positive	94
M204	ductal	pos	pos	neg	2	2.6	NA	
M205	lobular	pos	pos	neg	2	5.1	positive	88
M208	ductal	pos	neg	pos	2	2.2	positive	79
M209	ductal	neg	neg	pos	3	2.8	intermediate	25
M210	lobular	pos	neg	neg	3	1.2	positive	86
M211	ductal	neg	neg	pos	3	4	negative	0
M213	ductal	neg	neg	neg	2	2.9	positive	86
M217	ductal	pos	neg	neg	3	7	positive	91
M218	ductal	pos	pos	neg	2	1.2	positive	95
M225	ductal	pos	pos	neg	2	2.8	positive	95
M229	ductal	pos	pos	neg	1	4.5	positive	100
M231	ductal	pos	neg	neg	3	2.2	negative	2
M232	ductal	pos	neg	neg	3	3.2	negative	0
M233	lobular	pos	pos	neg	2	1.1	positive	94
M237	lobular	pos	pos	pos	3	3.5	positive	95
M239	ductal	pos	pos	neg	1	1	positive	85
M244	lobular	pos	pos	neg	2	2.5	positive	82

M247	ductal	pos	pos	neg	2	4.5	positive	90
M248	ductal	neg	neg	neg	3	3.5	negative	0
M253	ductal	neg	neg	neg	3	4	intermediate	26
m255	ductal	neg	neg	pos	3	6.5	NA	
M258	ductal	pos	pos	neg	2	4.1	positive	100
M259	ductal	pos	pos	neg	2	2.6	positive	92
M260	ductal	pos	pos	neg	3	8.5	negative	10
M262	lobular	pos	pos	neg	2	1.4	positive	99
M263	ductal	neg	pos	neg	2	1.4	NA	
M264	ductal	pos	neg	neg	1	1.2	positive	92
M266	ductal	pos	pos	neg	2	2.4	positive	98
M269	lobular	pos	pos	neg	2	3.8	positive	92
M270	ductal	neg	neg	neg	3	3	negative	0
M271	lobular	pos	neg	neg	2	7.5	negative	17
M275	lobular	pos	neg	neg	2	2.7	negative	3
M277	pappilair	neg	neg	neg	3	3.8	negative	2
M278	ductal	pos	pos	pos	3	2.4	intermediate	37

*patients were also included in our previous cohort

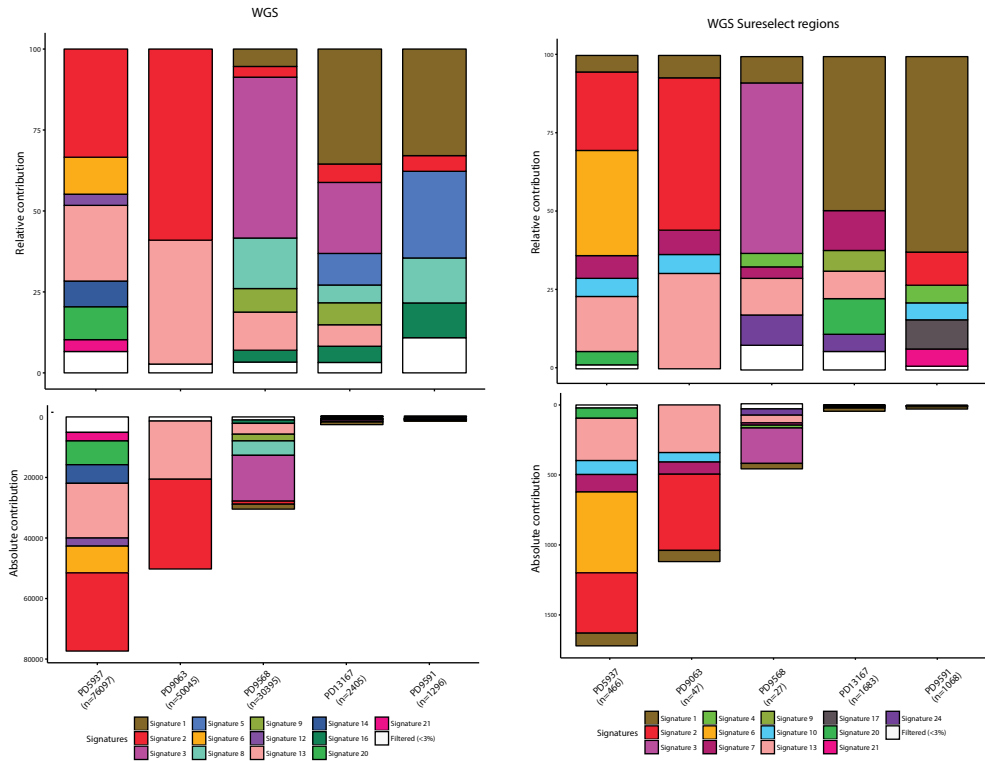


Supplemental Figure 1: Workflow of functional RECAP test and molecular analyses. Fresh primary breast tumor specimens were collected and irradiated with 5 Gy, incubated for 2 hours before formalin fixation and paraffin embedding. Immunofluorescence with RAD51 and Geminin antibodies was carried out on paraffin sections. Molecular analyses were all performed on an unirradiated sample from the same tumor.



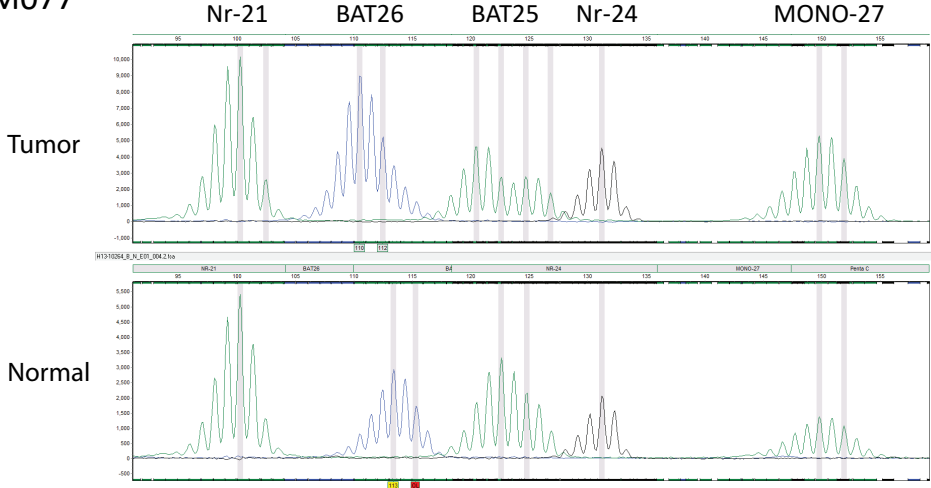
Supplemental Figure 2: *BRCA1* promoter hypermethylation and RNA in situ hybridization by RNAscope. M248, M253, M112 and M232 clearly showed presence of *BRCA1* RNA, whereas in M94 (*BRCA1* deletion) no *BRCA1* RNA was present. M131 and M277 showed heterogeneous presence of *BRCA1* RNA. PPIB probe = positive control.

3

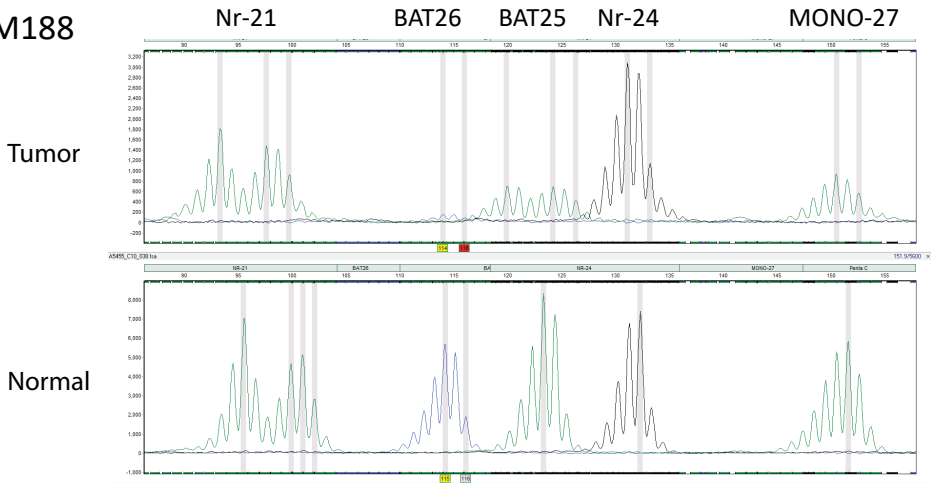


Supplemental Figure 3: Comparison of mutational signature analysis using all WGS-derived somatic mutations versus using somatic mutations present on SureSelect v5 target regions only.

M077



M188



Supplemental Figure 4: Microsatellite instability. Pentaplex PCR showed presence of MSI in M77 and M188.

A large, dark, textured splash of ink or paint on a white background. The splash is irregular and has a rough, layered appearance, with various shades of gray and black. The text "Chapter 4" is centered in white, bold, sans-serif font.

Chapter 4

Direct *ex vivo* observation of homologous recombination defect reversal after DNA damaging chemotherapy in metastatic breast cancer patients

Titia G. Meijer¹, Nicole S. Verkaik¹, Carolien H.M. van Deurzen², Hendrikus-Jan Dubbink², T. Dorine den Toom², Hein F.B.M. Sleddens², Esther Oomen-De Hoop³, Winand N.M. Dinjens², Roland Kanaar¹, Dik C. van Gent¹ and Agnes Jager^{3*}

¹ *Department of Molecular Genetics, Erasmus MC, University Medical Center Rotterdam and Oncode Institute, The Netherlands.*

² *Department of Pathology, Erasmus MC Cancer Institute, Rotterdam, The Netherlands.*

³ *Department of Medical Oncology, Erasmus MC Cancer Institute, Rotterdam, The Netherlands.*

Abstract

Background Biomarkers predicting response to Poly-[ADP-Ribose]-Polymerase inhibitors (PARPi) are required to detect PARPi sensitivity beyond germline *BRCA* mutated (gBRCAm) cancers and PARPi resistance among reverted gBRCAm cancers. Therefore, we previously developed the REpair CAPacity (RECAP) test, a functional homologous recombination (HR) assay exploiting the formation of RAD51 foci in proliferating cells after *ex vivo* irradiation of fresh primary breast cancer (BrC) tissue. The aim of the current study was to validate feasibility of this test on histological biopsies from metastatic BrC and to explore the utility of the RECAP test as a predictive tool for treatment with DNA damaging agents, such as PARPi.

Methods Fresh tissue biopsies from easily accessible metastatic lesions from patients with locally advanced or metastatic BrC were irradiated with 5 Gy and cultured for 2 hours, followed by detection of RAD51 foci presence (HR proficient) or absence (HR deficient). HR deficient (HRD) biopsies as well as platinum/PARP resistant biopsies were subjected to *BRCA1/2* sequencing.

Results RECAP has a success rate of 93% on biopsies from metastatic BrC lesions (n=44). While HRD was detected in 13 out of 41 biopsies (32%), only five showed a gBRCAm. In three gBRCAm patients, post-treatment RECAP tests showed HR phenotype reversion after *in vivo* progressive disease on platinum/PARPi treatment, which was explained in one patient by a secondary *BRCA1* mutation.

Conclusion The RECAP test, which reflects real-time HR status regardless of *BRCA* mutations, is feasible in metastatic BrC biopsies. Compared with gBRCA analysis, it may identify twice as many candidates for PARPi treatment.

Introduction

Tumors developed among germline *BRCA1/2* mutation (gBRCAm) carriers have a defect in homologous recombination (HR) and are therefore highly sensitive to Poly-[ADP-Ribose]-Polymerase inhibitors (PARPi) and DNA double strand break (DSB) inducing chemotherapies [1-4]. Recently, FDA approval was obtained for the use of Olaparib in advanced gBRCAm breast cancer (BrC) [3].

Until now, gBRCAm status is the only predictive biomarker for response to PARPi therapy. However, evidence is emerging that PARPi are also effective in cancers with HR deficiency (HRD) caused by other mechanisms than gBRCAm, such as somatic *BRCA1/2* mutations or mutations of other HR genes [5]. Several different HRD tests have been designed to identify HRD tumors in addition to gBRCAm tumors to enlarge the population of BrC patients that could benefit from treatments targeting the HR pathway [6-10]. However, a gold standard test for predicting response to PARPi therapy is not yet available. Most HRD tests are based on specific genomic or transcriptomic patterns derived from gBRCAm tumors, which also occur in sporadic cancers (BRCAness) [6-10]. These tests measure the accumulation of mutations and chromosomal aberrations over time, thus they do not necessarily reflect the real-time HR status of the tumor. This poses a problem for the metastatic setting, as the HR status can change over time, e.g. as a result of selective pressure from chemotherapy [11]. Therefore, a functional diagnostic assay on tumor material has the potential of more precisely detecting patients who may benefit from PARPi treatment than germline mutation analysis only.

The REpair CAPacity (RECAP) test, a functional HR assay exploiting the formation of RAD51 foci in proliferating cells after *ex vivo* irradiation of fresh BrC tissue, was previously developed for primary BrC (n=148) [12,13]. In the current study, we aimed to show feasibility of this test on biopsies from metastatic BrC lesions to enhance the diagnostic potential and clinical applicability of the RECAP test. Next, we aimed to find a molecular explanation for the observed HRD phenotype and we explored the utility of the RECAP test as a predictive tool for treatment with DSB inducing agents, such as PARPi, in this setting.

Materials and Methods

Biopsies

Patients with locally advanced or metastatic BrC, with metastatic lesions amenable for biopsies, who were planned to start systemic treatment were eligible. Therefore, patients with pulmonary and/or bone metastasis only were excluded due to risk of pneumothorax and technical difficulties with experimental procedures caused by calcifications (Supplemental table 3). Patients should have bilirubin <1.5 ULN and both AST and ALT <5x ULN in case of a liver biopsy. Platelets should be >100 x 10⁹/L and INR <1.5, unless platelet/INR values were not necessary according to local protocols or after

consent of the intervention radiologist for that particular site of biopsy (e.g. biopsy of the breast). After registration and written informed consent each patient was scheduled for a biopsy, performed by a (intervention) radiologist according to local protocols. For distant metastases a core needle biopsy with a minimum of 18 Gauge and maximum of 12 Gauge was performed under imaging guidance. Biopsies from superficial metastases were performed using a standard 4 mm biopsy puncher. The study (NL49306.078.14/MEC14-295) was approved by the medical ethics commission of the Erasmus Medical Center.

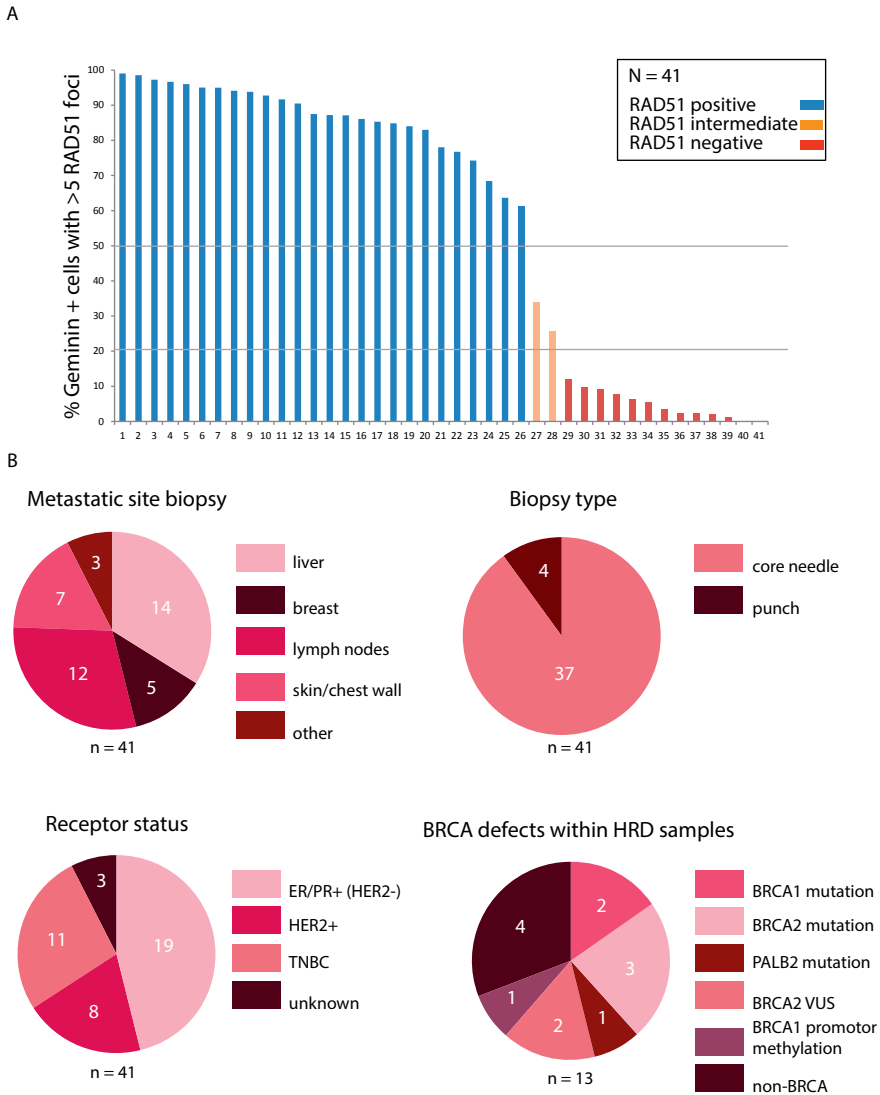


Figure 1: RECAP test has a high success rate (93%) when performed on small biopsies. A: The RECAP test could be performed successfully in 41 out of the 44 biopsies of metastatic lesions (93%). We identified 13 HRD biopsies, 2 HR intermediate (HRI) and 26 HR proficient (HRP) biopsies. B: Characteristics of RECAP biopsies.

RECAP test

Tumor samples were immediately transferred into customized breast tissue culture medium, as described previously^[13], and processed within 4 hours after tissue resection. After irradiation and 2 hours of incubation, tissue was formalin fixed and paraffin embedded. Microscopic analysis of Hematoxylin and Eosin (HE) stained sections was performed to determine presence of invasive carcinoma. The RECAP test was performed and results were analyzed as described previously (Supplemental Figure 1)^[13]. In brief, presence of RAD51 foci was determined in Geminin (GMN) positive, thus actively proliferating (S/G2), cells only. At least 30 GMN expressing cells were counted per tumor sample. A cell was considered RAD51 positive when at least 5 RAD51 foci were detected. Tumors were classified as HR proficient (HRP), HR deficient (HRD) or intermediate (HRi) when more than 50%, less than 20% or 20-50% of GMN positive cells showed ≥ 5 RAD51 foci, respectively.

BRCA1/2 analyses and RAD51 assay on cell lines

See supplementary methods.

Statistical analysis

The aim of the study was to show feasibility of the RECAP test on biopsies from metastatic BrC. The primary endpoint was the proportion of metastatic BrC patients with a successful RECAP test result. A successful test was defined as the ability to classify the tumor as HRP, HRi or HRD. A representative biopsy was defined as a biopsy upon which a pathologist is able to set the diagnosis of metastatic breast malignancy. We decided that further research is warranted if the proportion of successful tests is higher than 80% and that the test does not have clinical value if this proportion is lower than 60% (Optimal Simon 2-stage design, $\alpha=0.1$, $\beta=0.1$). According to these parameters, the required sample size was 38, with one interim analysis planned after inclusion of the 11th patient. In case ≤ 6 patients would have a successful test at the interim analysis, the study would be discontinued. Since it was expected that 10% of obtained biopsies would not be representative, a total of 43 patients were to be included. Differences between patients with successful and unsuccessful test were studied using the Chi-squared or Fisher's exact test for categorical data. Statistical analyses were all 2-sided and were performed using IBM SPSS statistics v21, where p-values of <0.05 were considered significant.

Results

The RECAP test has a high success rate

A total of 51 patients met the inclusion criteria and were enrolled between February 2015 and April 2017. In 6 patients no biopsy was obtained due to various reasons. One patient was excluded since pathological assessment of the biopsy revealed that it was a

metastasis of a neuroendocrine carcinoma (NEC) instead of BrC. Both NEC and BrC were diagnosed before in this patient. In total, 47 biopsies were obtained from 44 patients, of which 3 did not contain tumor cells, resulting in 44 representative biopsies.

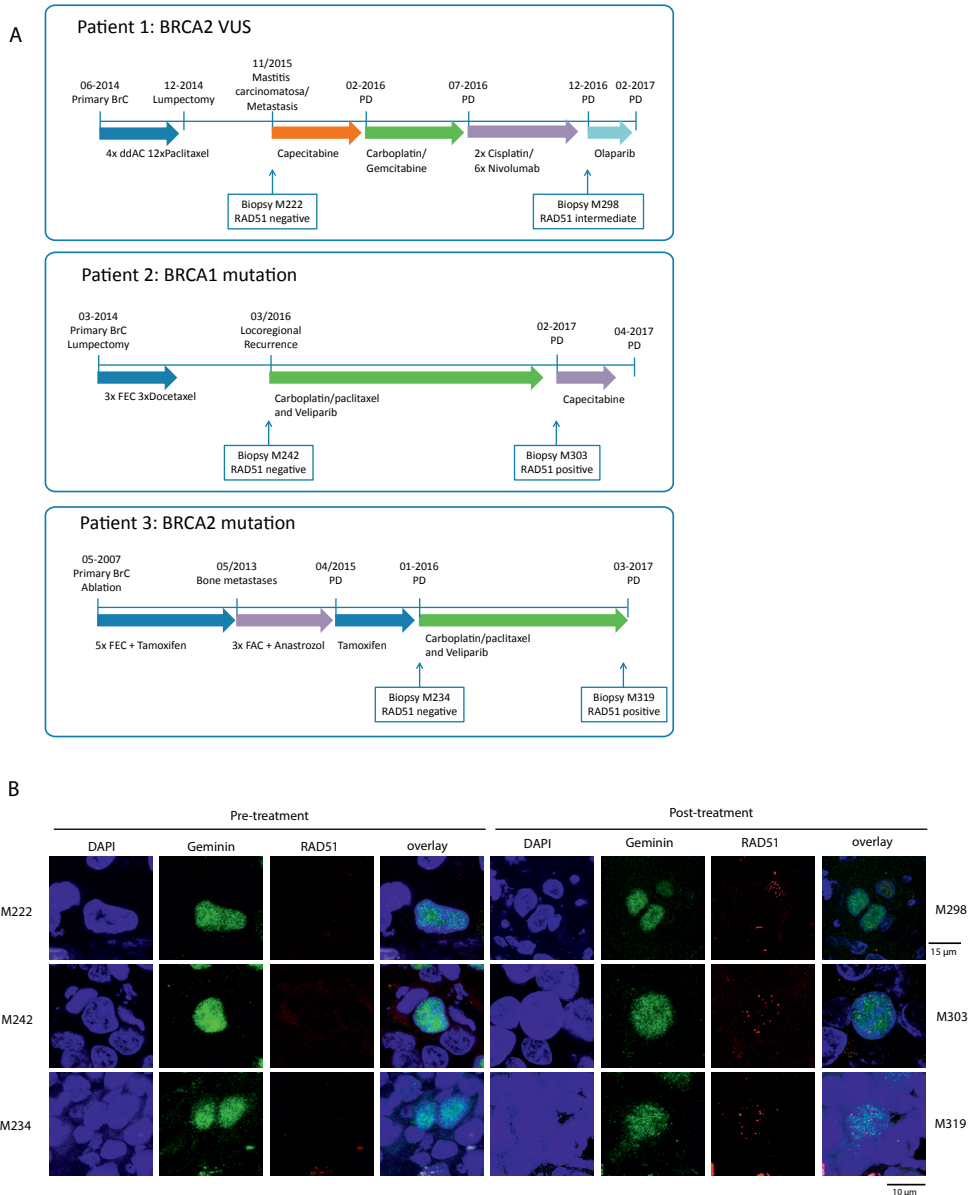


Figure 2: HRD tumor lesions became HRP after treatment with DSB inducing agents. A: Timelines of *gBRCAm* patients who developed reversal of the HR phenotype. B: Representative images of RAD51 stainings of pre- and post-treatment biopsies.

The RECAP test could be performed successfully in 41 of the 44 biopsies of metastatic lesions (93%, 95% CI: 86% - 100%, $p < 0.001$) (Figure 1A). Due to swift inclusion, slightly more patients were included than initially planned. Analysis of only the first 38 patients led to a similar conclusion. The reason for not successful testing in three biopsies was an insufficient number of proliferating (i.e. GMN positive) tumor cells (less than 30 GMN positive nuclei in M189, M250 and M332). M189, a known gBRCAm carrier, contained 10 GMN positive cells which were all RAD51 negative. M250 and M332 contained 6 and 19 GMN positive cells, respectively, which were all RAD51 positive.

Biopsies were derived from several metastatic sites (Figure 1B). No clear differences in histopathologic characteristics between biopsies that resulted in successful versus non-successful tests were observed (Supplemental Table 1). The RECAP test could be performed on core needle biopsies ($n=37$) as well as punch biopsies ($n=4$) from skin metastases. In 19 biopsies (4 triple negative BrC (TNBC), 4 HER2 positive and 11 estrogen or progesterone receptor (ER/PR) positive), we determined whether standard ER, PR and HER2 immunohistochemistry analyses could be performed on the RECAP biopsy. This yielded identical results in the RECAP biopsy and in the original pathology biopsy for 18 cases. In one case, which was originally scored as TNBC, we found 10% ER expression in the RECAP biopsy, which is just above the threshold for ER positivity (i.e. $\geq 10\%$ in The Netherlands).

Among the 41 successful RECAP test results, we identified 13 HRD, 2 HR intermediate (HRi) and 26 HR proficient (HRP) tumor samples (Figure 1). RECAP status was independent of histopathologic characteristics of the tumors, biopsy type and localization of the metastatic lesion (Supplemental table 2).

Molecular defects in HRD tumors

The 13 HRD tumors were further analyzed to find a molecular explanation for the observed HRD phenotype (Table 1). 38% (5/13) of HRD tumors harbored germline *BRCA1/2* mutations, of which one patient harbored a *BRCA2* variant of unknown significance (VUS) that was functionally validated for affecting HR^[14]. In 15% (2/13) of HRD tumors, somatic *BRCA2* VUSes were found, which are predicted to be non-pathogenic. *BRCA1* promotor hypermethylation was identified in one HRD tumor and *BRCA1* RNA was indeed absent in this tumor as assessed by RNA in situ hybridization (Supplemental figure 2). Thus, the HRD phenotype was explained by a BRCA defect in 46% (6/13), leaving 54% (7/13) of the HRD tumors to be non-BRCA related. One non-BRCA related HRD tumor harbored a germline mutation in *PALB2*.

Table 1: Molecular defects in HRD samples

Sample	RAD51 status	Gene	Mutation		Significance	Germline / Somatic	BRCA1 RNA present/ RNAscope	Large Deletion in BRCA1/2 (MLPA)	LOH BRCA	Receptor status
			Nucleotide	Protein						
M207	Negative	BRCA1	c.2197_2201del5	p.Glu733fs	Path	Germline			TN	
M242 &	Negative	BRCA1	c.4327C>T	p.Arg1443*	Path	Germline	Normal	BRCA1+2 LOH	TN	
M234 \$	Negative	BRCA2	c.5351dupA	p.Asn1784fs	Path	Germline	BRCA2 loss	BRCA2 LOH	TN	
M317	Negative	BRCA2	c.8167G>C	p.Asp2723His	Path	Germline			ER+/PR-/HER2-	
M212	Negative	BRCA2	c.1040A>G	p. Gln347Arg	VUS (class 2)	Somatic	Normal	BRCA1+2 LOH	ER+/PR-/HER2-	
M230	Negative	BRCA2	c.10095_10096delins-GAATTATATCT	p. Ser3366Asnfs	VUS (class 2/3)	Somatic	Normal (BRCA1 gain)	BRCA1+2 LOH	ER-/PR-/HER2+	
M222 @	Negative	BRCA2	c.9104A>C	p.Tyr3035Ser	VUS (pathogenic)	Germline	Normal (BRCA2 loss)	BRCA2 LOH	TN	
M256	Negative	PALB2	c.1907dupA	p.Pro637fs		Germline	Normal		ER+	
M240	Negative	Non BRCA				NA		BRCA1+2 LOH	ER-/PR+/HER2-	
M283	Negative	Non-BRCA				NA	NS	NS	ER-/PR-/HER2+	
M312	Negative	Non-BRCA				NA	Normal	BRCA1 LOH	TN	
M282	Negative	Non-BRCA				NA	Normal	Normal	ER-/PR-/HER2+	
M321	Negative	Non-BRCA				NA	Normal	BRCA2 LOH	TN	
M189	Inconclusive (negative)	BRCA2	c.8067T>A	p.Cys2689*	Path	Germline			ER+/PR-/HER2-	
M298 @	Intermediate	BRCA2	c.9104A>C	p.Tyr3035Ser	VUS (pathogenic)	Germline	Normal (BRCA2 loss)	LOH BRCA2	TN	
M313	Intermediate	Non-BRCA				NA			ER+/PR-/HER2-	
M273	Positive	BRCA2 CHECK2	c.3847_3848delGT-1100delC	p.Val1283fs p.Thr367Metfs	Path	Germline	Normal (BRCA2 gain)	NS	ER+/PR-/HER2-	
M303 &	Positive	BRCA1	c.4327C>T c.4327-4329delinsTGG	p.Arg1443* p.Arg1443_delinsTtp	Path	Germline + somatic	Normal	BRCA1+2 LOH	TN	
M319 \$	Positive	BRCA2	c.5351dupA	p.Asn1784fs	Path	Germline	BRCA2 loss	BRCA2 LOH	TN	

&, \$ and @ indicate matching biopsies pre- and post-treatment from the same patient. NA: not applicable. NS: no score.

Change of HRD phenotype in response to DSB inducing therapy

Next, we explored the added value of the RECAP test as a predictive biomarker to select patients for PARPi treatment in the metastatic setting. From three gBRCAm patients, who were treated with DSB inducing agents, pre- as well as post-treatment biopsies were subjected to the RECAP test. These tumors initially showed an HRD phenotype, corresponding to the BRCA deficient genotype (Figure 2). However, after patients had developed PD, these tumors became HRP showing reversal of the HRD phenotype.

Patient 1 (Figure 2) harbored a *BRCA2* VUS (c.9104A>C p.Tyr3035Ser) that has been shown to negatively affect HR efficiency and moderately increase risk of BrC [13]. A pre-treatment biopsy from the advanced TNBC showed HRD by the RECAP test. The patient was treated consecutively with capecitabine, carboplatin/gemcitabine and low dose cisplatin in combination with nivolumab, on which she developed PD after 6 cycles. Subsequently, olaparib (PARPi) monotherapy was started, prior to which a second biopsy was obtained for RECAP testing. The second biopsy was very heterogeneous, harboring both HRD (RAD51 negative) and HRP (RAD51 positive) cells, overall resulting in an HRI phenotype. The result of the RECAP test was concordant with in vivo patient response, as she already showed PD after the first response evaluation at 8 weeks of olaparib treatment, thus primary refractory to olaparib.

Patients 2 and 3 harbored germline mutations in *BRCA1* (c.4327C>T; p.Arg1443*) and *BRCA2* (c.5351dupA; p.Asn1784fs), respectively. The pre-treatment RECAP test reported an HRD phenotype in both patients. Interestingly, both tumors developed an HRP phenotype after they had developed resistance in response to the combination of carboplatin, paclitaxel and veliparib (PARPi) within a clinical trial. These three patients had been previously treated with anthracycline based therapy, which also induces DSB, but which did not lead to HR phenotype reversion.

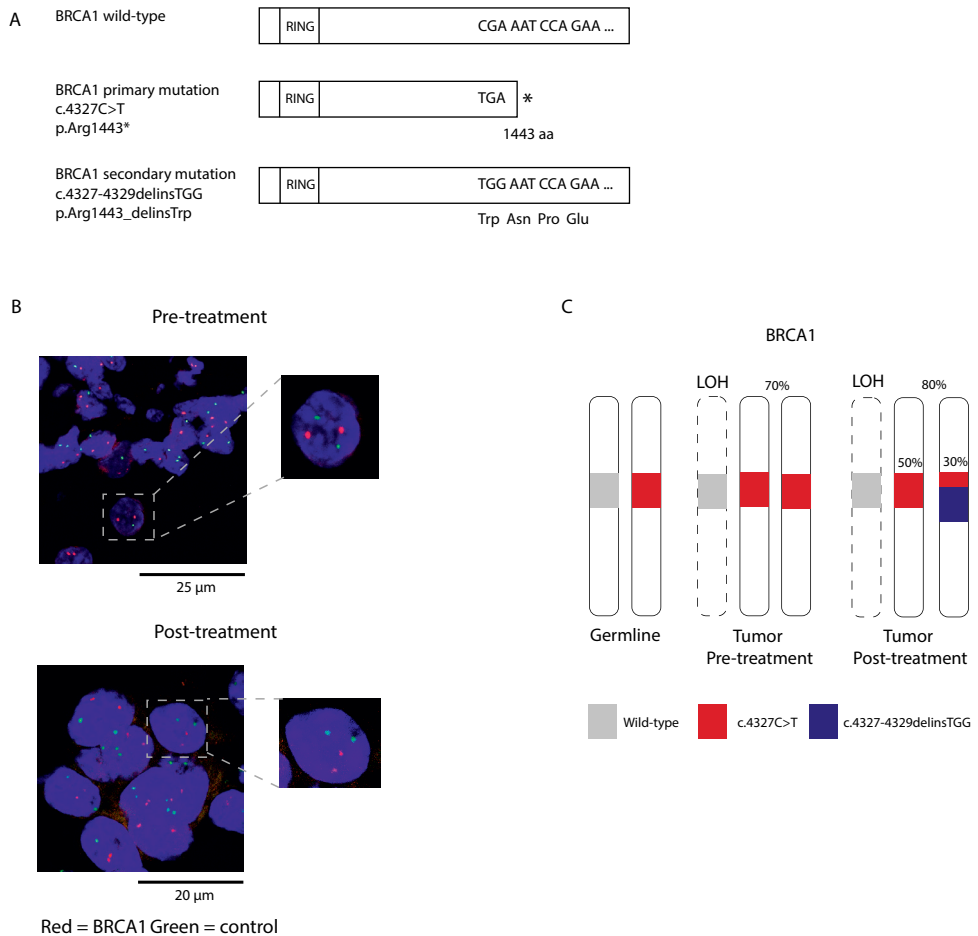


Figure 3: BRCA1 reversion mutation explains resistance in one patient. A: An additional point mutation (officially: 4327_4329delinsTGG) was acquired next to the original 4327C>T mutation, resulting in restoration of the open reading frame disrupted by the original mutation and consequently full-length BRCA1 protein production. B: FISH analysis showed that both pre- and post-treatment biopsies harbor 2 copies of *BRCA1*, indicating that the original mutated allele was duplicated. C: In both pre- and post-treatment biopsies loss of heterozygosity was observed. The tumor became HRP due to reversion of one mutant *BRCA1* copy.

To unravel the molecular mechanisms leading to resistance in these patients, we searched for secondary *BRCA1/2* mutations in the post-treatment tumor biopsies. Patient 2 acquired an additional point mutation, i.e. 4329A>G, (officially: 4327_4329delinsTGG) next to the original 4327C>T mutation, resulting in restoration of the open reading frame disrupted by the original mutation and consequently full-length BRCA1 protein production (Figure 3A). The 4327C>T mutation was observed at a MAF of 70% in the pre-treatment and 80% in the post-treatment biopsy, while the 4327_4329delinsTGG was present at MAF of 30% in the post-treatment sample. In both pre- and post-treatment biopsies loss of heterozygosity

was observed. Fluorescence in situ hybridization (FISH) analysis showed that both pre- and post- treatment biopsies harbored 2 copies of *BRCA1*, indicating that the original mutated allele was duplicated (Figure 3B). Thus, the tumor became HRP due to reversion of one mutant *BRCA1* copy.

The other two patients did not show any secondary mutations in the mutated *BRCA* gene. Other mechanisms for PARPi resistance have been proposed, such as loss of 53BP1 protein. Loss of 53BP1 was examined but not found in any resistant tumor (Supplemental Figure 3). In conclusion, the RECAP test detected reversal of the HRD phenotype, although the cause of resistance remained elusive in two out of three tumors.

CHEK2 c.1100delC mutation does not cause HRD

In addition, one tumor clearly showed an HRP phenotype, despite harboring a germline *BRCA2* mutation (c.3847_3848delGT; p.Val1283fs). The biopsy was taken when this patient showed progressive disease (PD) after 5 months of carboplatin/paclitaxel treatment, however HR status pre-treatment remains unknown as a fresh pre-treatment biopsy was not available for this patient (Figure 4). As this tumor might have developed reversal of the HRD phenotype, both pre- and post-treatment tumor material (70% tumor) was sequenced. The germline *BRCA2* mutation was present at a mutant allele fraction (MAF) of 41% and 34%, respectively, and secondary mutations were not present. The relatively low MAF of the germline *BRCA2* mutation suggested that the *BRCA2* wild-type allele was still present in the tumor, which was confirmed by FISH (Figure 4B). Additionally, this patient also carried a germline *CHEK2* mutation (c.1100delC; p.Thr367fs), present at MAF 73% and 67%, in the pre- and post-treatment biopsy, respectively. Thus, the driver mutation of this tumor was the *CHEK2* mutation instead of the *BRCA2* mutation. *CHEK2* is a known BrC susceptibility gene, but the direct effect of *CHEK2* mutations on HR status remains elusive. Therefore, the HR status of SUM102PT cells, which harbor the exact same c.1100delC mutation in *CHEK2* as found in this patient, was determined and the *CHEK2* c.1100delC mutation did not cause HRD (Figure 4D). Finally, this patient was treated with Olaparib therapy but was primary refractory despite her gBRCAm status. She showed PD after the first response evaluation after 8 weeks, corresponding to the outcome of the RECAP test (HRP) (Figure 4A).

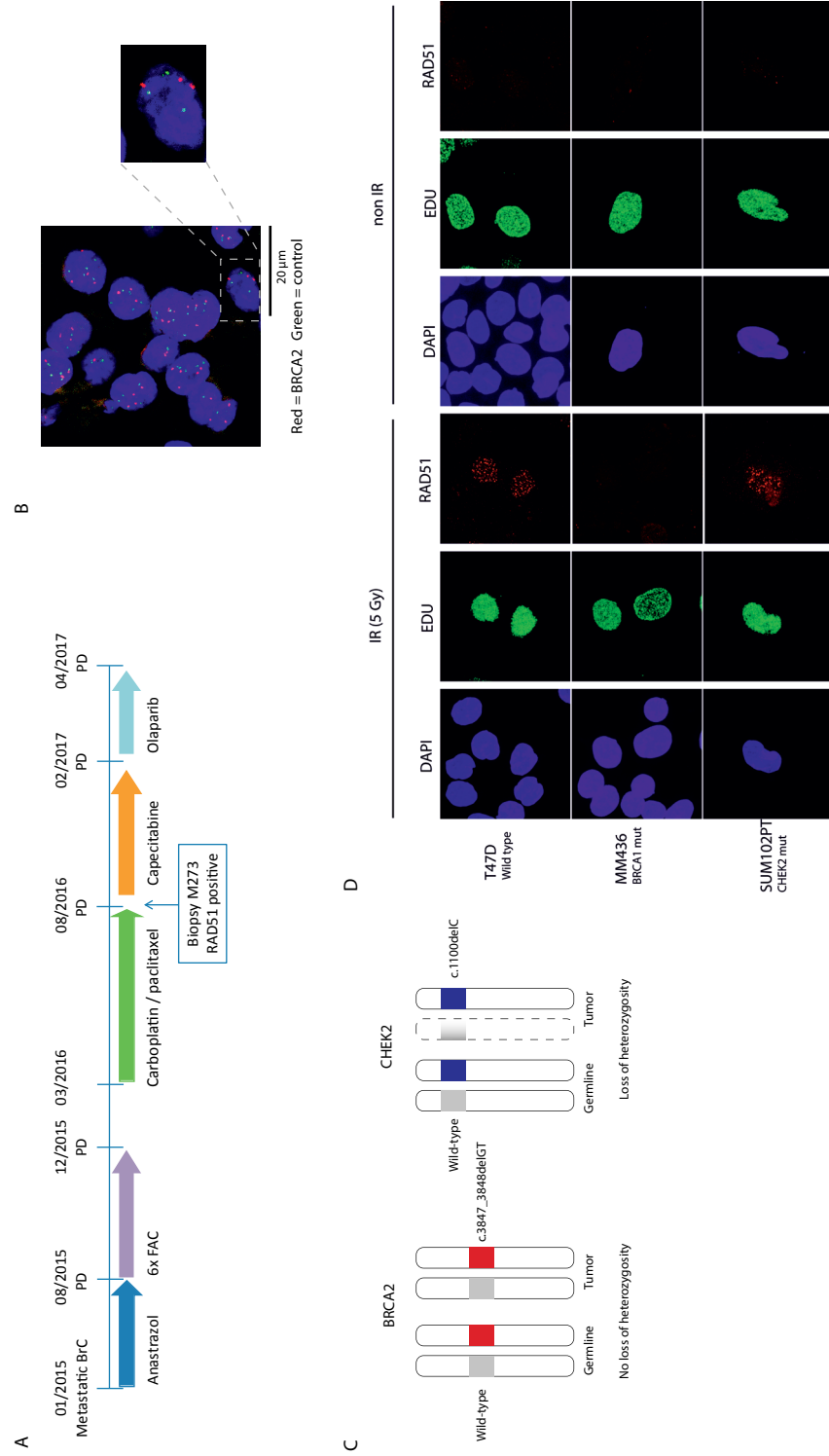


Figure 4: Coincidence of germline BRCA2 and CHEK mutations in a patient with a HRP tumor. A: Treatment timeline of a patient harboring both a germline BRCA2 and CHEK2 mutation, who was primary refractory to olaparib treatment. B: Presence of the wild-type allele for BRCA2 in the tumor was confirmed by FISH. Red = BRCA2 probe, Green = centromere control probe. C: the driver mutation of this tumor was the CHEK2 mutation instead of the BRCA2 mutation. D: SUM1102PT cells, harboring the c.1100delC mutation, were HRP. T47D wild-type controls. MM436 BRCA1 mutated negative control.

Discussion

This study shows that the RECAP test is feasible (93% successful) on metastatic BrC biopsies, greatly enhancing its diagnostic potential and clinical applicability. The functional RECAP test is robust and its applicability extends from core needle biopsies from different metastatic sites to punch biopsies from skin metastases and test results are available within one week. HRD was detected in 13 out of 41 tumors (32%). Among 13 HRD tumors only five showed a gBRCAm, indicating that the RECAP test may identify twice as many candidates for PARPi treatment compared with gBRCA analysis.

We believe this study provides the first evidence that the HR phenotype, measured by a functional HR test, changes over time in gBRCAm patients due to previous therapies. The real-time HR status measured by RECAP is consistent with therapy response of patients. Within the current cohort, reversion of the HR phenotype was detected in three patients with gBRCAm tumors after developing *in vivo* resistance to DSB inducing therapies (carbo-/cisplatin or PARPi). Another gBRCAm patient, with a BRCA proficient tumor, showed resistance to DSB inducing agents and was refractory to olaparib, which was concordant with the result of the RECAP test (HRP). These cases highlight the need for HR tests based on the phenotype such as the RECAP test, especially in the advanced setting.

The molecular mechanism leading to resistance and reversion of the HRD phenotype was explained in one of three patients by a secondary mutation in *BRCA1*. This is quite unique, as for BrC, most reversion mutations are described within *BRCA2* and a *BRCA1* reversion has only been described once before ^[15]. The incidence of *BRCA1/2* secondary mutations within resistant tumors is not clear yet, as most are described in case-reports or studies with small sample sizes. In 26 patients who had platinum-resistant recurrent ovarian cancer the incidence of *BRCA1/2* secondary mutations was 46.2% ^[16]. In two out of five (40%) gBRCAm patients with platinum/PARPi therapy resistant metastatic BrC secondary *BRCA2* mutations were detected in ctDNA ^[17]. Recent case-reports highlight that *BRCA1/2* secondary mutations are a universal resistance mechanism for different tumor types (e.g. prostate, pancreatic) with germline or somatic loss-of-function mutations ^[18-21]. However, since not all resistant patients harbor secondary mutations, detecting PARPi resistant tumors by screening for secondary *BRCA* mutations would lead to an underestimation and only identify a subgroup of resistant tumors. Yet, the RECAP test detects resistant tumors regardless of the exact underlying resistance mechanism.

Here, we show a case of coincidence of both germline *BRCA2* and *CHEK2* c.1100delC mutations in a patient with an HR proficient breast tumor. The driver mutation of this tumor was *CHEK2* instead of *BRCA2*. This highlights two important issues. First, BrC that arises in a gBRCAm patient is not necessarily BRCA associated and second, the *CHEK2* c.1100delC mutation does not cause HRD. Although the effect of the c.1100delC mutation on RAD51 focus formation has not been investigated before, it was recently reported that

mutations in *CHEK2* were not associated with mutational signature 3 (related to DNA DSB repair by HR) [22].

The major strength of this study is the functional character of the RECAP test for exploring the HR phenotype. Furthermore, the RECAP test is not dependent on high tumor percentage in a sample, since the microscopic read-out allows differentiation between tumor and stromal cells. Another advantage is its broad applicability: where many HRD tests focus specifically on TNBCs, the RECAP test detects HRD regardless of histological grade and subtype. Since RECAP procedures (irradiation and 2 hours culturing) do not influence standard hormone receptor analyses, the fresh biopsy for RECAP testing could also be used for diagnostic pathology analyses, thereby limiting the amount of tissue needed. Furthermore, its high success rate (93%) and short turnaround time make the RECAP test competitive in a clinical setting.

The current study also has some limitations. First, functional testing requires fresh (instead of paraffin embedded) tumor specimens and for the RECAP test in particular, *ex vivo* DNA damage is induced by X-ray or gamma-irradiation. Second, the RECAP test cannot be completed successfully in slow growing tumors lacking proliferating cells (in the current study 3/44). Third, whether the RECAP test predicts PARPi or DSB inducing therapy response cannot be concluded from this study, although the three highlighted cases in this article are promising.

Compared with gBRCA analysis, the RECAP test may identify twice as many candidates for PARPi treatment. Moreover, reversion of the HR phenotype is detected by RECAP, identifying patients with gBRCAm who will no longer benefit from PARPi or DSB inducing agents due to resistance. The functional RECAP test, determining the real-time HR status independent of gBRCAm status, shows great potential as a predictive biomarker for PARPi treatment of metastatic BrCs. Clinical trials evaluating the predictive value of the RECAP test for *in vivo* response to PARPi have been initiated.

Acknowledgments

The authors thank the medical oncologists of the Erasmus MC for informing patients about the trial and other activities that led to patient enrollment. We thank the (intervention-) radiologists of the Erasmus MC for obtaining the biopsies. We thank Dr. Hollestelle for kindly providing the T47D, MM463 and SUM102PT cell lines.

Supplementary Methods

BRCA1/2 sequencing and MLPA

Data on germline *BRCA1/2*, *CHEK2* and *PALB2* mutations were retrospectively obtained from medical records of patients who visited a clinical geneticist for genetic counseling and had given informed consent for sharing these data. Patients who did not visit a clinical geneticist gave informed consent to perform *BRCA1/2* and *CHEK2* sequencing of the biopsy. Also, pre- and post-treatment biopsies, from patients who received platinum or PARPi based therapies, were subjected to targeted sequencing. DNA was isolated after manual dissection of tumor tissue from hematoxylin stained paraffin sections and incubation with 5% Chelex (Bio-Rad laboratories, Hercules, CA), followed by protein kinase K (Roche, Mannheim, Germany) digestion overnight at 56°C. Ion semiconductor sequencing on the Ion Torrent Personal S5XL was performed according to manufacturer's instructions (Thermo Fisher Scientific, Waltham, USA). Adapter-ligated libraries were constructed using the AmpliSeq Library kit 2.0 with amplicons designed targeting *BRCA1/2*, *CHEK2* and *TP53*. Generation of sequence reads, trimming adapter sequences, filtering, and removal of poor signal-profile reads was performed via the Ion Torrent platform-specific pipeline software Torrent Suite v5.2.2. Initial variant calling was performed by comparison to the reference genome hg19 (build 37) using the "Torrent Variant Caller v5.2.0.34" plugin from the Torrent Suite Software. Multiplex ligation-dependent probe amplification (MLPA) analysis of *BRCA1* and *BRCA2* was undertaken to identify large rearrangements using the SALSA MLPA kit P002B, and for confirmation of observed abnormalities, the SALSA MLPA kit P087 was used (MRC Holland, Amsterdam, The Netherlands). Analyses were performed according to the manufacturer's instruction; products were run on an ABI automated sequencer (ABI 3730XL), and the data were analyzed by Genemarker version 2.7.0 (Softgenetics, State College, PA). *BRCA1* promoter methylation was assessed as previously described^[13].

BRCA1/2 FISH

To determine the *BRCA1/2* gene copy number, fluorescence in situ hybridization (FISH) was performed on 4-µm tissue sections using an in-house protocol for pretreatment and *BRCA1* or *BRCA2* and centromere control probes (Leica, Kreatech, Amsterdam, The Netherlands). Slides were mounted with DAPI containing Vectashield mounting medium.

In situ detection of BRCA1 RNA

In situ detection of *BRCA1* mRNA was performed using RNAScope (Advanced Cell Diagnostics, Newark, USA) on the automated Ventana Discovery Ultra system (Ventana Medical Systems, Roche, Tucson, USA). RNAScope analysis was performed according to manufacturer's instructions using the reagent kit (VS Reagent Kit 320600; Advanced Cell Diagnostics) on proteinase K (0.1 %, 5 min at 37 °C)-treated paraffin sections (4 µm).

ER, PR and HER2 immunohistochemistry

ER, PR and HER2 immunohistochemistry were performed using ER (ER SP1; Ventana Medical Systems, Roche, Tucson, USA), PR (PR 1E2; Ventana Medical Systems, Roche, Tucson, USA) and HER2 (HER2 4B5; Ventana Medical Systems, Roche, Tucson, USA) antibodies. ER and PR status were scored positive when $\geq 10\%$ of the tumor cells were positive, according to the Dutch Breast Cancer Guideline ^[23]. HER2 status was scored according to international guidelines ^[24].

RAD51 assay on cell lines

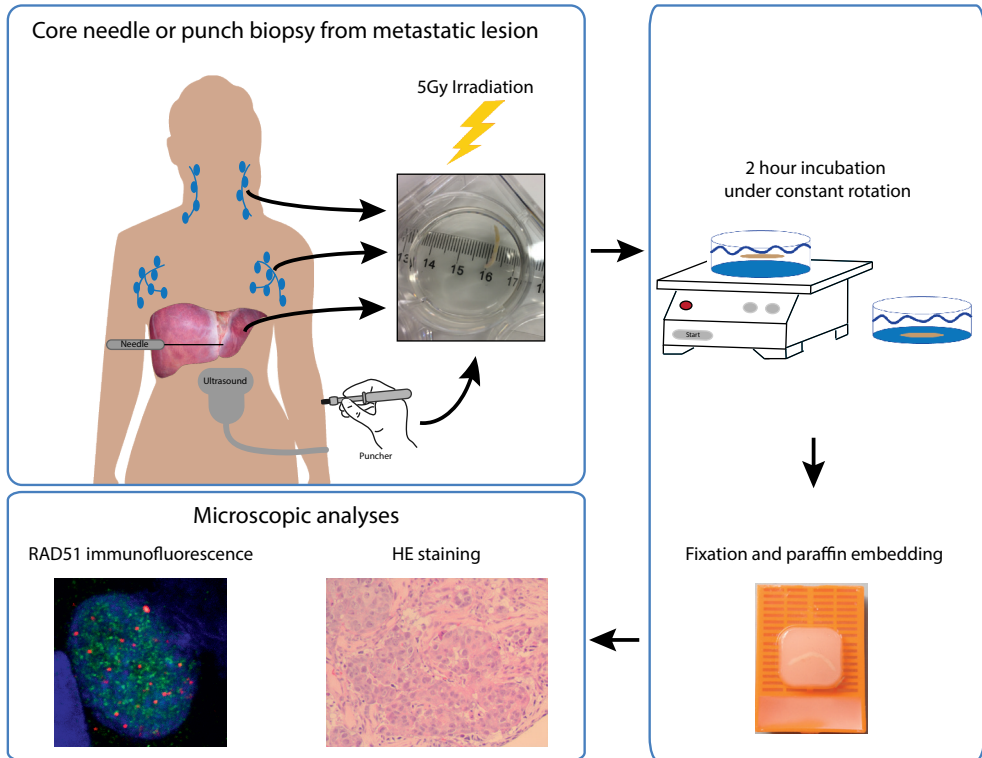
To unravel the effect of the c.1100delC mutation in *CHEK2* on HR, RAD51 focus formation was assessed in three BrC cell lines: T47D, MM463 and SUM102PT. Cell lines were grown in Roswell Park Memorial Institute (RPMI) medium with 10% Fetal Calf Serum (FCS) and antibiotics at 37°C and 5% CO₂. Cells were seeded on coverslips one day prior to irradiation with 5Gy. Proliferating cells were labeled with 3µg/ml 5-Ethynyl deoxyuridine (EdU) (Invitrogen, Thermo Fisher Scientific, Waltham, USA). After 2 hours cells were subjected to pre-extraction, fixation and immunofluorescence as previously described ^[25]. Primary antibody against RAD51 (homemade) was diluted 1:10,000 and secondary antibody (goat-anti-rabbit 594) 1:1,000. Edu incorporation was visualized using Click-it chemistry with Click-it Atto fluor 488 cocktail (Invitrogen) according to manufacturer's instructions. Samples were visualized using Leica SP5 confocal microscope.

References

1. Audeh MW, Carmichael J, Penson RT, et al: Oral poly(ADP-ribose) polymerase inhibitor olaparib in patients with BRCA1 or BRCA2 mutations and recurrent ovarian cancer: a proof-of-concept trial. *Lancet* 376:245-51, 2010
2. Ledermann J, Harter P, Gourley C, et al: Olaparib maintenance therapy in patients with platinum-sensitive relapsed serous ovarian cancer: a preplanned retrospective analysis of outcomes by BRCA status in a randomised phase 2 trial. *Lancet Oncol* 15:852-61, 2014
3. Robson M, Im SA, Senkus E, et al: Olaparib for Metastatic Breast Cancer in Patients with a Germline BRCA Mutation. *N Engl J Med* 377:523-533, 2017
4. Tutt A, Robson M, Garber JE, et al: Oral poly(ADP-ribose) polymerase inhibitor olaparib in patients with BRCA1 or BRCA2 mutations and advanced breast cancer: a proof-of-concept trial. *Lancet* 376:235-44, 2010
5. Wendie DdB, Kasmintan AS, Sophie S, et al: Homologous Recombination Deficiency in Breast Cancer: A Clinical Review. *JCO Precision Oncology*:1-13, 2017
6. Abkevich V, Timms KM, Hennessy BT, et al: Patterns of genomic loss of heterozygosity predict homologous recombination repair defects in epithelial ovarian cancer. *Br J Cancer* 107:1776-82, 2012
7. Birkbak NJ, Wang ZC, Kim JY, et al: Telomeric allelic imbalance indicates defective DNA repair and sensitivity to DNA-damaging agents. *Cancer Discov* 2:366-75, 2012
8. Davies H, Glodzik D, Morganella S, et al: HRDetect is a predictor of BRCA1 and BRCA2 deficiency based on mutational signatures. *Nat Med* 23:517-525, 2017
9. Jooisse SA, van Beers EH, Tielen IH, et al: Prediction of BRCA1-association in hereditary non-BRCA1/2 breast carcinomas with array-CGH. *Breast Cancer Res Treat* 116:479-89, 2009
10. Konstantinopoulos PA, Spentzos D, Karlan BY, et al: Gene expression profile of BRCAness that correlates with responsiveness to chemotherapy and with outcome in patients with epithelial ovarian cancer. *J Clin Oncol* 28:3555-61, 2010
11. Incorvaia L, Passiglia F, Rizzo S, et al: "Back to a false normality": new intriguing mechanisms of resistance to PARP inhibitors. *Oncotarget* 8:23891-23904, 2017
12. Meijer TG, Verkaik NS, Sieuwerts AM, et al: Functional ex vivo assay reveals homologous recombination deficiency in breast cancer beyond BRCA gene defects. *Clin Cancer Res*, 2018
13. Naipal KA, Verkaik NS, Ameziane N, et al: Functional ex vivo assay to select homologous recombination-deficient breast tumors for PARP inhibitor treatment. *Clin Cancer Res* 20:4816-26, 2014
14. Shimelis H, Mesman RLS, Von Nicolai C, et al: BRCA2 Hypomorphic Missense Variants Confer Moderate Risks of Breast Cancer. *Cancer Res* 77:2789-2799, 2017

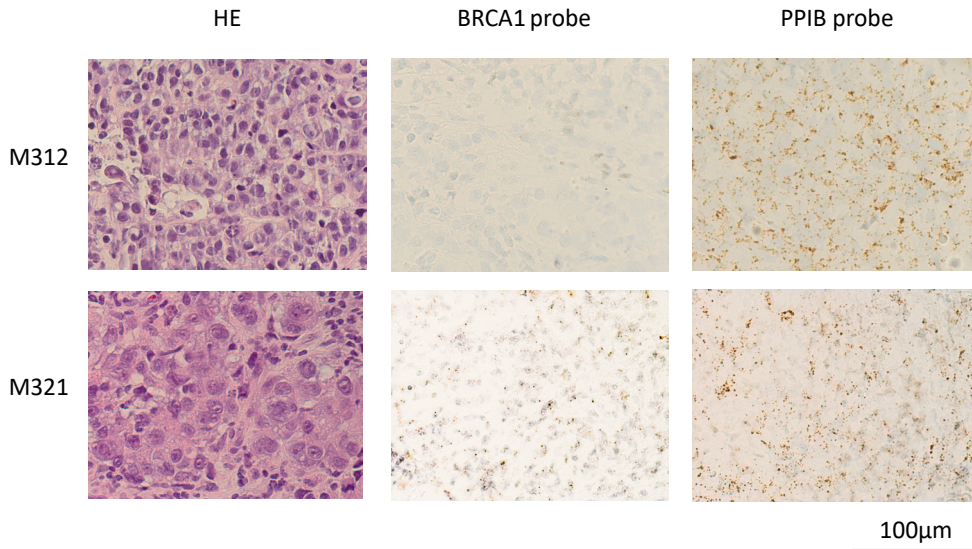
15. Afghahi A, Timms KM, Vinayak S, et al: Tumor BRCA1 Reversion Mutation Arising during Neoadjuvant Platinum-Based Chemotherapy in Triple-Negative Breast Cancer Is Associated with Therapy Resistance. *Clin Cancer Res* 23:3365-3370, 2017
16. Norquist B, Wurz KA, Pennil CC, et al: Secondary somatic mutations restoring BRCA1/2 predict chemotherapy resistance in hereditary ovarian carcinomas. *J Clin Oncol* 29:3008-15, 2011
17. Weigelt B, Comino-Mendez I, de Bruijn I, et al: Diverse BRCA1 and BRCA2 Reversion Mutations in Circulating Cell-Free DNA of Therapy-Resistant Breast or Ovarian Cancer. *Clin Cancer Res* 23:6708-6720, 2017
18. Benedito AC, Katharine Ann C, Rebecca JN, et al: Acquired Resistance to Poly (ADP-ribose) Polymerase Inhibitor Olaparib in BRCA2-Associated Prostate Cancer Resulting From Biallelic BRCA2 Reversion Mutations Restores Both Germline and Somatic Loss-of-Function Mutations. *JCO Precision Oncology*:1-8, 2018
19. Heather HC, Stephen JS, Peter SN, et al: Polyclonal BRCA2 Reversion Mutations Detected in Circulating Tumor DNA After Platinum Chemotherapy in a Patient With Metastatic Prostate Cancer. *JCO Precision Oncology*:1-5, 2018
20. Kalyan B, Elizabeth MS, David W, et al: Somatic Reversion of Germline BRCA2 Mutation Confers Resistance to Poly(ADP-ribose) Polymerase Inhibitor Therapy. *JCO Precision Oncology*:1-6, 2018
21. Pishvaian MJ, Biankin AV, Bailey P, et al: BRCA2 secondary mutation-mediated resistance to platinum and PARP inhibitor-based therapy in pancreatic cancer. *British journal of cancer* 116:1021-1026, 2017
22. Polak P, Kim J, Braunstein LZ, et al: A mutational signature reveals alterations underlying deficient homologous recombination repair in breast cancer. *Nat Genet* 49:1476-1486, 2017
23. <http://www.oncoline.nl/mammacarcinoom>. Mammacarcinoom Irv, Integraal Kankercentrum Nederland, Richtlijnen Oncologische Zorg:
24. Wolff AC, Hammond ME, Hicks DG, et al: Recommendations for human epidermal growth factor receptor 2 testing in breast cancer: American Society of Clinical Oncology/College of American Pathologists clinical practice guideline update. *Arch Pathol Lab Med* 138:241-56, 2014
25. Zhu XD, Kuster B, Mann M, et al: Cell-cycle-regulated association of RAD50/MRE11/NBS1 with TRF2 and human telomeres. *Nat Genet* 25:347-52, 2000

Supplementary Data

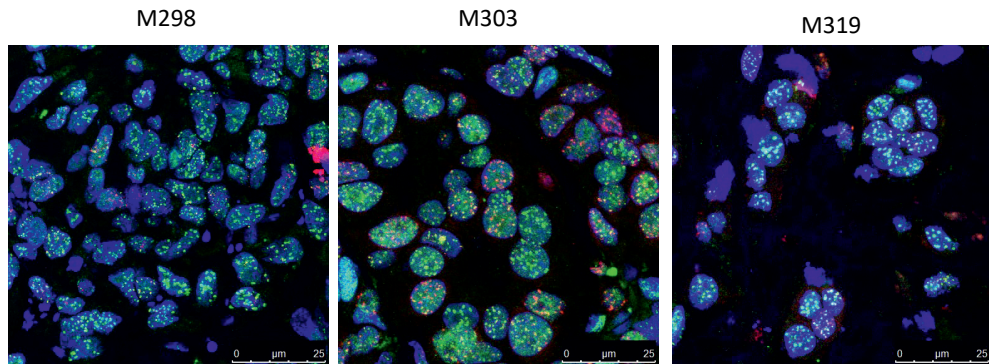


Supplemental Figure 1: Workflow of RECAP test. Fresh primary breast tumor specimens were collected and irradiated with 5 Gy, incubated for 2 hours before formalin fixation and paraffin embedding. Immunofluorescence with RAD51 and GMN antibodies was carried out on paraffin sections.

4



Supplemental Figure 2: BRCA1 RNA in situ hybridization by RNAscope. M312 clearly showed absence of BRCA1 RNA. PPIB probe = positive control.



Green = 53BP1
Red = γH2AX

Supplemental Figure 3: No loss of 53BP1 in resistant biopsies.

Supplemental table 1: Comparison of histopathologic characteristics of successful tests and non-successful tests.

	Not successful test result	Successful test result	P-value
Histological subtype			
Ductal carcinoma	3	32	
Lobular carcinoma	-	3	
Other	-	3	
Unknown	-	3	1.000
Histological grade (primary tumor)			
1	-	1	
2	1	9	
3	2	25	
Unknown	-	6	1.000
Receptor Status			
ER/PR +, HER2- HER2+*	3	19	
HER2+*	-	8	
TNBC	-	11	
Unknown	-	3	0.522
Type of biopsy			
Punch	-	4	
Core needle	3	37	0.746
Metastatic site			
Mamma	1	5	
Chestwall/skin	-	7	
Axillary/Cervical/ Pectoral LN	-	12	
Liver	2	14	
Other	-	3	0.560
Total	3	41	

***independent of ER/PR status**

Fisher's exact test

ER/PR+ was defined as >10% ER+ and/or >10% PR+. HER2+ defined as immunohistochemistry (IH) 3+ or IH 2+ and HER2 amplification detected by In situ hybridization.



Supplemental table 2: Comparison of histopathologic characteristics of RAD51 proficient, intermediate and deficient metastatic biopsies.

	RECAP +	RECAP intermediate	RECAP -	P-value
Histological subtype				
Ductal carcinoma	19	1	12	
Lobular carcinoma	3	-	-	
Other	2	-	1	
Unknown	2	1	-	0.344
Histological grade (primary tumor)				
1	1	-	-	
2	8	-	1	
3	14	1	10	
Unknown	3	1	2	0.371
Receptor Status				
ER/PR +, HER2- HER2+*	14	1	4	
HER2+*	5	-	3	
TNBC	5	-	6	
Unknown	2	1	-	0.190
Type of biopsy				
Punch	4	-	-	
Core needle	22	2	13	0.416
Metastatic site				
Mamma	3	-	2	
Chestwall/skin	5	1	1	
Axillary/Cervical/Pectoral LN	7	-	5	
Liver	8	1	5	
Other	3	-	-	0.761
Total	26	2	13	

***independent of ER/PR status**

Fisher's exact test

ER/PR+ was defined as >10% ER+ and/or >10% PR+. HER2+ defined as immunohistochemistry (IH) 3+ or IH 2+ and HER2 amplification detected by In situ hybridization.

Supplemental table 3: in-/exclusion criteria.

Inclusion criteria
<ul style="list-style-type: none"> The site of the tumor should be amendable for biopsy. NB lung metastases (high risk of hematothorax) and bone metastases (not suitable for ex vivo test because calcifications interfere with experimental procedures) are excluded. Age >18 years. WHO performance status 0 or 1. Bilirubin <1.5 ULN and both AST and ALT <5x ULN in case a liver biopsy is planned. Platelets >100 x 10e9/L st and INR <1.5, unless platelet/INR values are not necessary according to local protocols or after consent of the intervention radiologist for that particular site of biopsy (e.g. biopsy of the breast). Written informed consent.
Exclusion criteria
<ul style="list-style-type: none"> Current therapeutically use of anti-coagulant (coumarin derivates, warfarin, heparin or low molecular weight heparin [LMWH]) whereby a short interruption of drug use is not allowed. LMWH if used for prophylaxis is allowed. Any psychological condition potentially hampering compliance with the study protocol.

Supplemental Table 4: All biopsies with RAD51 counts.

Trial no	M code	Origin	Histological subtype	ER	PR	HER2	B&R grade	RECAP outcome	RAD51 FOCI %
1	M184	liver	ductal	+	-	-	2	positive	92
2	M194	ovary	lobular	-	-	+	2	positive	88
3	M196	liver	lobular	-	-	-	unknown	positive	95
4	M207	liver	ductal	-	-	-	3	negative	9
5	M212	liver	ductal	+	-	-	unknown	negative	6
6	M216	pectoralis LN	medullary	-	-	-	3	positive	83
7	M223	liver	neuro-endocrine tumor	excluded					
8	M222	axillary LN	ductal	-	-	-	3	negative	0
9	M226	liver	ductal	+	+	-	2	positive	78
10	M230	liver	ductal	-	-	+	3	negative	12
11	M186	axillary LN	ductal	+	+	-	3	positive	68
12	M189	liver	ductal/mucinous	+	-	-	3	inconclusive (<30 GMNs)	0
13	M190	mamma	ductal	?	?	?	3	positive	99
14	M228	liver	ductal	+	-	-	3	positive	64
15	M234	liver	ductal	-	-	-	2	negative	0
16	no biopsy								
17	M242	cervical LN	ductal	-	-	-	3	negative	4
18	M240	mamma	Not otherwise specified (NOS)	-	+	-	3	negative	2
19	M238	mamma	multifocal (ductal + neuro-endocrine)	+	-	-	3	positive	86
20	M252	liver	ductal	+	+	-	2	positive	93
21	M250	liver	ductal	+	-	-	2	inconclusive (<30 GMNs)	100
22	M254	axillary LN	lobular	+	-	+	unknown	positive	77
23	M256	Chest wall	ductal	+	+	-	3	negative	6
24	no biopsy								
25	no biopsy								
26	M268	axillary LN	ductal	+	+	-	1	positive	94
27	M273	skin	unknown	+	-	-	2	positive	61
28	M274	skin	lobular	-	-	-	unknown	not representative	
29	M282	axillary LN	ductal	-	-	+	3	negative	8
30	M283	axillary LN	ductal	-	-	+	unknown	negative	3
31	M290	skin	ductal	+	+	-	3	positive	74



32	M294	axillary LN	ductal	+	-	-	3	positive	99
33	no biopsy								
34	M284	liver	ductal + lobular	-	-	+	2	positive	97
35	M293	cervical LN	lobular	-	-	+	3	not representative	
36	M299	liver	ductal	+	-	-	3	positive	97
37	M298	Chest wall	ductal	?	?	?	3	intermediate	34
38	M301	cervical LN	mucinous ductal	+	+	-	unknown	positive	85
39	M303	Subcutaneous lesion	ductal	-	-	-	3	positive	85
40	M304	skin	ductal (mucinous)	-	-	+	3	positive	96
41	no biopsy								
42	M323	chest wall	ductal (sarcomatoid)	-	-	-	3	positive	87
43	M316	axillary LN	ductal	?	?	?	3	positive	95
44	M313	liver	unknown	+	-	-	unknown	intermediate	26
45	M314	presternal	ductal	+	+	-	2	positive	94
46	M312	cervical LN	ductal	-	-	-	3	negative	1
47	M315	skin	ductal	-	-	+	3	positive	90
48	no biopsy								
49	M317	liver	ductal	+	-	-	3	negative	2
50	M319	liver	unknown	-	-	-	2	positive	87
51	M321	mamma	ductal	-	-	-	3	negative	10
52	M324	mamma	ductal	+	+	-	3	positive	84
53	M330	parasternal	unknown	-	-	-	3	not representative	
54	M332	mamma	ductal	+	-	-	3	inconclusive (<30 GMNs)	100

A large, dark, textured splash of ink or paint on a white background. The splash is irregular and has a rough, splattered appearance. The text "Chapter 5" is centered in white, bold, sans-serif font.

Chapter 5

RECAP identifies homologous recombination deficiency in breast cancers undetected by DNA-based BRCAness tests

Titia G. Meijer^{1,10}, Luan Nguyen^{2,10}, Arne Van Hoeck^{2,10}, Anieta M. Sieuwerts³,
Nicole S. Verkaik^{1,10}, Marjolijn M. Ladan^{1,10}, Kirsten Ruigrok-Ritstier³,
Carolien H.M. van Deurzen⁴, Harmen J. G. van de Werken^{5,6}, Esther H. Lips⁷,
Sabine C. Linn^{7,8,9}, Roland Kanaar^{1,10}, John W. M. Martens³, Edwin Cuppen^{2,10},
Agnes Jager³ and Dik C. van Gent^{1,10}

¹ Department of Molecular Genetics, Erasmus University Medical Center, Rotterdam, The Netherlands.

² Department of Human Genetics, UMC Utrecht, Utrecht, The Netherlands.

³ Department of Medical Oncology, Erasmus MC Cancer Institute, Erasmus University Medical Center, Rotterdam, The Netherlands.

⁴ Department of Pathology, Erasmus MC Cancer Institute, Erasmus University Medical Center, Rotterdam, The Netherlands.

⁵ Cancer Computational Biology Center, Erasmus University Medical Center, Rotterdam, The Netherlands.

⁶ Department of Urology, Erasmus University Medical Center, Rotterdam, The Netherlands.

⁷ Department of Molecular Pathology, The Netherlands Cancer Institute, Amsterdam, The Netherlands.

⁸ Department of Medical Oncology, The Netherlands Cancer Institute, Amsterdam, The Netherlands.

⁹ Department of Pathology, University Medical Centre Utrecht, Utrecht, The Netherlands.

¹⁰ Onco Institute, The Netherlands.



Chapter 6

Ex vivo tissue-based cisplatin testing on metastatic breast cancer biopsies

Titia G. Meijer^{1,7}, Nicole S. Verkaik^{1,7}, Carolien H.M. van Deurzen²,
Michael A. den Bakker³, Marieke van de Ven⁴, Jos Jonkers^{5,7}, Roland Kanaar^{1,7},
Dik C. van Gent^{1,7*} and Agnes Jager^{6*}

- ¹ *Department of Molecular Genetics, Erasmus MC, University Medical Center Rotterdam, The Netherlands.*
- ² *Department of Pathology, Erasmus MC Cancer Institute, Rotterdam, The Netherlands.*
- ³ *Department of Pathology, Maastad ziekenhuis, Rotterdam, The Netherlands.*
- ⁴ *Preclinical Intervention Unit, Mouse Clinic for Cancer and Aging (MCCA), The Netherlands Cancer Institute, Amsterdam, The Netherlands.*
- ⁵ *Division of Molecular Pathology, The Netherlands Cancer Institute, Amsterdam, The Netherlands.*
- ⁶ *Department of Medical Oncology, Erasmus MC Cancer Institute, Rotterdam, The Netherlands.*
- ⁷ *Oncode Institute, The Netherlands.*



Chapter 7

Functional homologous recombination screening of breast and ovarian cancer cell lines

Titia G. Meijer^{1,4*}, Antoinette Hollestelle^{2*}, Corine Beaufort², Saskia M. Wilting²,
Teresa Robert-Finestra³, Marcel Smid², Nicole S. Verkaik^{1,4}, Roland Kanaar^{1,4},
Agnes Jager², Dik van Gent^{1,4}, John W.M. Martens²

* *These authors contributed equally*

¹ *Department of Molecular Genetics, Erasmus University Medical Center, Rotterdam, The Netherlands.*

² *Department of Medical Oncology, Erasmus MC Cancer Institute, Erasmus University Medical Center, Rotterdam, The Netherlands.*

³ *Department of Developmental Biology, Erasmus University Medical Center, Rotterdam, The Netherlands.*

⁴ *OncoCode Institute, The Netherlands.*



Chapter 8

Summary, general discussion and future perspectives

Summary

This thesis describes the improvement of biomarker development and therapy response prediction for breast cancer (BC) patients using functional tissue-based assays. Both targeted treatment strategies and classic chemotherapy require predictive biomarkers to guide clinical decision making. Targeted therapy with PARP inhibitors is available for breast and ovarian cancer patients with germline *BRCA1/2* mutation status, which is currently the only predictive biomarker for PARP inhibitor treatment. However, through patient selection based on the homologous recombination (HR) status of the tumor, instead of germline *BRCA* mutation status, the population of BC patients that could benefit from PARP inhibitor treatment can be enlarged. Chemotherapy remains the cornerstone of BC treatment and currently no standard biomarkers exist for response prediction, despite decades of biomarker driven research. Traditional biomarker assessment is executed on fixed tissue specimens or through genetic testing, but the difficulty to translate this information to tumor behavior necessitates development of tools to select patients for therapies based on tumor phenotype rather than genotype. Prediction of individual treatment responses by functional *ex vivo* assays may fill this knowledge gap. Functional assays are generally performed in primary cell cultures or animal models (patient derived xenografts). In this thesis, a novel approach to biomarker discovery is described: the measurement of the actual response of an individual BC tissue specimen to *ex vivo* chemotherapy or radiation.

First, an overview of *ex vivo* tumor culture systems for functional drug testing and therapy response prediction is provided in **chapter 2**. In this review we discuss the advantages and disadvantages of several *ex vivo* tumor culture systems such as primary cultures, spheroids, organoids and tissue slices. A key message in this chapter is that organotypic tissue slices are the best model of maintaining intratumoral heterogeneity and tumor-stromal interactions. Organotypic tissue slices are widely applicable in both translational research and personalized medicine, as almost any relevant treatment could be tested in this system. In the future, these tissue based *ex vivo* sensitivity assays could individualize therapy response prediction for patients in clinical practice.

In **chapter 3**, we provide evidence that the REpair CAPacity (RECAP) test, a functional assay exploiting the formation of RAD51 foci in proliferating cells after *ex vivo* irradiation of fresh BC tissue, identifies homologous recombination deficient (HRD) tumors and we demonstrate its reproducibility in an extensive cohort of primary BCs. The RECAP test is successfully completed in the great majority of the cases (74%) in what is by far the largest set (n=125) of functional HR capacity assays performed on fresh BC specimens. Approximately two-third of the HRD cases can be explained by *BRCA* gene defects, while several of the non-*BRCA* HRD tumors also showed mutational 'BRCAness' signatures, suggesting that these are also *bona fide* HRD cases. The large cohort size allowed us to link HRD to increased incidence of high tumor infiltrating lymphocyte (TIL) counts and microsatellite instability (MSI). The main clinical implications of this study are that

the RECAP test identified 50% more patients eligible for PARP inhibitor treatment than germline *BRCA* analysis alone and that this group of tumors may also contain tumors that may benefit from immunotherapy.

Functional HR assessment by the RECAP test produces a unique real-time measure of the HR status, as can be read in **chapter 4**. HRD was detected in 13 out of 41 biopsies (32%) analyzed metastatic BC lesions. Among 13 HRD tumors only five showed a germline *BRCA* mutation, indicating that the RECAP test identifies approximately 60% more patients who may benefit from PARP inhibitor treatment than germline *BRCA* analysis only. From three patients with germline *BRCA* mutated tumors, paired-biopsies were available before and at disease progression after treatment with double strand break (DSB) inducing chemotherapy. Reversion of the HR phenotype (from HR deficient to HR proficient/intermediate) was discovered, highlighting the clinical need for phenotype based HRD tests such as the RECAP test to guide treatment choice. *BRCA* reversal in one of three DSB inducing therapy resistant patients was caused by a secondary mutation in *BRCA1*. For the other two patients, the mechanism of resistance remains to be elucidated. The RECAP test is thus capable of detecting resistance among reverted germline *BRCA* mutated tumors, regardless of the knowledge of the exact underlying resistance mechanism. Therefore, the RECAP test shows great potential for prediction of sensitivity to DSB inducing therapy in metastatic BC patients, who have been treated with multiple lines of previous therapies that could have caused *BRCA*/HRD status reversal.

In **chapter 5**, a large cohort (n=71) of breast tumors with known functional HR status, measured by RAD51 focus formation after irradiation, was subjected to other genomic scar based HRD tests (*BRCA1/2*-like classifier and CHORD). For a subset (n=54) whole genome sequencing was performed to further characterize HRD tumors and especially the non-*BRCA* related HRD tumors. We demonstrate that only half of the non-*BRCA* related RECAP-HRD tumors were also classified as HRD by other HRD tests. *In vivo* therapy response of some HRD tumors were available. The main implication of this chapter is that different HRD tests (including the RAD51 based functional assay and HRD-genomic scars) do not identify exactly the same population of BC patients (60-70% concordance between tests). In the future, multiple HRD tests should be included in a clinical trial to determine how well these tests predict *in vivo* response, as it is not yet possible to choose one ultimate HRD test.

Chapter 6 describes the development of a sensitivity assay for cisplatin chemotherapy by performing *ex vivo* treatment on organotypic tissue slices from histological biopsies of metastatic BC lesions. The novel scientific value of this is two-fold and has both technical and clinical implications. First, this chapter describes that *ex vivo* drug screening on organotypic tissue slices is feasible using limited histological biopsy material as input instead of larger pieces of tissue from resections. Second, the *ex vivo* drug sensitivity of organotypic tumor slices was compared with the *in vivo* responses of patients. The *ex vivo* sensitivity assay described in this chapter measures the actual response of the tumor

of an individual patient to a certain therapy, which might be a more accurate method for predicting chemotherapy response than using predictive biomarkers that generally correspond to a better outcome.

The results of a functional homologous recombination screen in 54 breast and 38 ovarian cell lines are shown in **chapter 7**. HRD was found among 19% (10/54) of the BC and in 8% (3/38) of the OC cell lines. Of these HRD cell lines 77% (10/13) were not explained by a BRCA defect. One non-BRCA related cell line harbored an *EXO1* mutation that could explain its HRi phenotype. Among the *BRCA* mutated cell lines, HRD was absent in 56% of the BC (5/9) and 38% of the OC (3/8) cell lines. In four of these cases, a putative cause for the discrepancy was found, such as loss of *SHLD2*. Further research is ongoing to unravel the discrepancies between BRCA mutation and functional HR status. HRD cell lines comprise a heterogeneous group in which not all cell lines represent *BRCA* deficient or HRD tumor specimens. Since cell lines are so broadly applied as model systems for a wide range of experiments across all fields of cancer research, it is of utmost importance to realize that the specific cell line used influences the conclusions that are drawn from these experiments tremendously.

In conclusion, the studies described in this thesis use functional assays on tumor tissue to improve the selection of BC patients for double strand break inducing chemotherapy and PARP inhibitor therapy. This represents a novel approach to biomarker discovery: the measurement of the actual response of an individual BC tissue specimen to *ex vivo* chemotherapy or radiation. In the future, these tissue based *ex vivo* assays could individualize therapy response prediction for patients in clinical practice.

General discussion and future perspectives

Since breast cancer (BC) is the most common malignancy in women with the second highest cancer related mortality rate, more research is needed to improve patient outcomes. New knowledge is generated in the laboratory through fundamental research, but what do these findings mean for patients? The gap between a laboratory bench and a hospital bed is not only physically but also figuratively large. Translational research is required to channel the data that is being generated at that laboratory bench into the direction of the hospital beds. By collaborations among fundamental researchers, translational researchers and medical doctors, research findings can be translated in knowledge that has clinical utility and applicability.

The development of new anticancer therapies only contributes to improvement of patient outcomes when the right therapy is administered to the right patient. Over the last decades, cancer treatment has moved from 'one-size-fits-all' regimens towards more personalized cancer therapy. Therefore, the need for better predictive biomarkers is imperative. Biomarker-driven research has yielded strong predictive biomarkers that correlate with patient response to a certain drug. For example, the monoclonal antibody trastuzumab, targeting HER2, dramatically improved survival for patients with BC overexpressing HER2. However, for many other therapies, predictive biomarkers do not yet exist.

Besides specific molecular markers (such as *BRCA* mutation status in BC) the field of biomarker discovery has moved to genomic, transcriptional and proteomic predictive signatures. As next-generation sequencing techniques are becoming more and more common and affordable, whole genome sequencing is exploited to characterize individual patients and predict therapy response. However, validation of these biomarkers and subsequent integration in the diagnostic process are major bottle-necks that require extensive research. For example, there are concerns regarding turn-around time of the generation of these biomarkers, what to do with variants of unknown significance, whether the tests detect historic events or reflects real-time tumor characteristics and how to cope with complex data analyses. It is a long road from biomarker discovery and assay development to implementation in the clinic.

As therapy response often cannot be predicted accurately by a single genetic marker only, alternative ways of patient stratification are needed. Beyond mutational status, many other factors influence tumor behavior and therapy response, for example epigenetic factors and the tumor microenvironment. Therefore, the current difficulty to translate genetic information to tumor behavior necessitates development of tools to select patients for therapies based on tumor phenotype rather than genotype. Ex vivo assays that predict therapy response may fill this knowledge gap.

The general aim of this thesis was to improve biomarker development and therapy response prediction for BC patients using functional tissue-based assays. This thesis

demonstrates that selection of patients for precision therapies should ideally be based on the tumor phenotype, since the tumor (HR) phenotype changes over time due to previous therapies. This is exemplified in chapter 4, where reversion of the HR phenotype was detected in three patients with germline *BRCA* mutated tumors after developing *in vivo* resistance to DSB inducing therapies. The real-time HR status measured by the RECAP test was consistent with therapy response of patients. These cases highlight the need for HR tests based on the phenotype such as the RECAP test, especially in the advanced setting. Chapter 3 reflects the power of functional phenotype based testing: more patients who are eligible for PARP inhibitor or DSB inducing chemotherapy treatment are identified than by analysis of a single genetic marker only (germline *BRCA* analysis). Chapter 7 demonstrates that this is also true in a well characterized selection of cell lines. Chapter 5 shows that functional phenotype based testing and genomic based assays result in a partially different HR classification of tumors. To elucidate the consequences of this different classification, clinical trials should include multiple HRD tests to determine how well these tests are able to predict *in vivo* response to PARP inhibitor therapy. Next, therapy response prediction based on the tumor phenotype has broad applicability beyond the scope of this thesis. Organotypic tissue slices are widely applicable in both translational research and personalized medicine, as they can be used to test many relevant treatments on many different solid tumor types. Chapter 6 describes the first steps towards functional *ex vivo* testing of organotypic tissue slices from small core needle biopsies, making the technique more useful as a drug screening tool in the clinic. Functional *ex vivo* assays may be the ultimate selection method when unique genetic markers have not been identified for particular drugs or do not suffice (e.g. in metastatic setting or after multiple lines of therapy).

Future perspectives

The studies presented in this thesis have generated new insights in functional tissue based therapy prediction. The first step towards clinical implementation of functional diagnostics is to determine and validate whether the assays predict *in vivo* response to relevant therapies. Therefore, we have recently initiated two clinical proof-of-concept trials specifically powered to determine the predictive value of i. the RECAP test [Functional selection of advanced breast cancer patients for Talazoparib treatment Using the REpair capacity test (FUTURE) study, [Trialregister.nl/trial/8099](https://www.trialregister.nl/trial/8099)], and ii. sensitivity assays that use organotypic slices from histological biopsies [Breast cancer *Ex vivo* Anthracycline Sensitivity Test (BREAST) study, [trialregister.nl/trial/5588](https://www.trialregister.nl/trial/5588)]. Both the RECAP test and *ex vivo* chemotherapy sensitivity testing (for example for anthracyclines) could be applied in the neoadjuvant as well as the advanced setting.

The aim of the FUTURE study is to assess the predictive potential of the RECAP test for *in vivo* response to PARP inhibitor therapy (Talazoparib) among high grade ER positive/HER2 negative or triple negative BC patients by investigating the percentage of patients

with HRD breast tumors, as determined by the RECAP test, with PFS on Talazoparib monotherapy of 4 months or longer.

The aim of the BREAST study is to determine the concordance between the *ex vivo* anthracycline sensitivity test and *in vivo* response to anthracycline-based neoadjuvant chemotherapy. Also, optimal cut-off values for the *ex vivo* anthracycline sensitivity assay are determined to carefully predict *in vivo* anthracycline response. Patients with primary BC, who are scheduled to be treated with anthracycline-based neoadjuvant chemotherapy are scheduled for a study-specific pre-treatment tumor biopsy for the *ex vivo* sensitivity test. The primary end point is the concordance between the *ex vivo* anthracycline sensitivity test and the *in vivo* response to anthracycline-based NAC on MRI.

Besides the translation and implementation of tissue based *ex vivo* assays to and in the clinic, it is important to extend the use of these assays. Functional diagnostics is a broadly applicable method, that can be used for many different types of drug sensitivity screening and has applicability beyond BC to many different solid tumor types. *Ex vivo* tissue slices have been generated and successfully cultured for many different tumor types, however drug sensitivity screening is performed seldom on tissue slices. In our lab, the chemotherapy sensitivity assay using BC tissue slices has been employed for predicting response to anthracyclines and cisplatin therapy. Currently, we are adapting the assay to more specifically predict response to taxane-based chemotherapies.

Since only a limited number of tissue slices can be obtained from one core needle biopsy, future research should be focussed on how to generate as much knowledge as possible from limited material. Until now, analyses of tissue slices included traditional morphologic assessment by haematoxylin and eosin staining as well as immunofluorescence, requiring a tissue slice to be fixed after a certain amount of cultivation time. In the future, technical improvements in the microfluidics and cancer-on-chip field might facilitate high-throughput cultivation and analysis of tissue slices. Nevertheless, cancer tissue is heterogeneous and a tumor biopsy is not comprised solely of tumor cells, neither are these tumor cells distributed equally in the entire biopsy. Therefore, dividing the biopsy into many smaller pieces for separate analyses reduces the chance of obtaining interpretable results. Moreover, advances in live-imaging microscopy and the use of fluorescent probes, could facilitate a single tissue slice to be analysed at multiple time points. Fluorescent probes are already available to assess several cellular processes, such as apoptosis and fibrosis. New developments in the laboratory are continuing to complement the toolkit necessary for fresh tissue analyses. However, to develop functional diagnostics further, more clinical trials should include a biopsy to generate tissue slices and allow correlation between tissue-based sensitivity screening and therapy responses of patients. This clinical validation is required before fresh tissue-based functional diagnostics can be implemented in the routine clinical diagnostic process.



Appendices

- Nederlandse samenvatting
- Curriculum Vitae
- List of Publications
- PhD portfolio
- Dankwoord

Nederlandse samenvatting

Dit proefschrift beschrijft hoe bij borstkanker patiënten door middel van functionele weefsel-gebaseerde testen het effect van behandeling met specifieke geneesmiddelen beter voorspeld kan worden. Voor de keuze van de behandeling, of dit nu geavanceerde toegespitste therapieën ('targeted therapies') of klassieke chemotherapie is, is het noodzakelijk om specifieke tumor of patiënt kenmerken ('biomarkers') te identificeren die voorspellen of een patiënt zal reageren op de betreffende therapie. Behandeling met een specifieke doelgerichte behandeling (te weten PARP remmers) wordt momenteel toegepast bij borst- of eierstokkanker patiënten met een kiembaan mutatie in het *BRCA1* of *BRCA2* gen. Echter, door patiënten te selecteren op basis van de homologe recombinatie (HR) status van de tumor, in plaats van *BRCA1/2* kiembaan mutatie status, kunnen meer patiënten geïdentificeerd worden die mogelijk baat hebben bij deze behandeling. Behandeling met klassieke chemotherapie blijft de hoeksteen van borstkanker behandeling, terwijl ondanks jarenlang onderzoek nog steeds geen standaard biomarker beschikbaar is voor deze therapie. Traditionele biomarkers worden bepaald in gefixeerde weefsels of door middel van genetische testen, maar omdat deze informatie niet altijd het gedrag van de tumor reflecteert, is het belangrijk om nieuwe methoden te ontwikkelen om patiënten voor behandelingen te selecteren op basis van het fenotype van hun tumor in plaats van het genotype. Het voorspellen van de individuele therapie respons van een patiënt is mogelijk met behulp van functionele *ex vivo* testen. Functionele testen worden over het algemeen vooral uitgevoerd op primaire cel culturen of in diermodellen (zogenoemde patient derived xenografts). In dit proefschrift wordt een nieuwe aanpak voor biomarker ontwikkeling getoond: het meten van de respons van een individueel borstkanker weefselplakje op *ex vivo* chemotherapie behandeling of bestraling.

Allereerst, wordt er in **hoofdstuk 2** een overzicht gegeven van verschillende *ex vivo* tumor kweeksystemen om functioneel therapierespons te testen. In dit review beschrijven we de voor- en nadelen van de verschillende systemen die over het algemeen gebruikt worden om tumoren *ex vivo* te kweken, zoals: primaire cel culturen, sferoïden, organoïden en weefselplakjes. De hoofdboodschap van dit hoofdstuk is dat weefselplakjes het beste de intratumor heterogeniteit en tumor-stromale interacties behouden. Weefselplakjes kunnen toegepast worden in zowel translationeel onderzoek als in patiëntenzorg bij het voorspellen van individuele therapie responsen van patiënten, aangezien bijna elk relevant middel op deze manier getest kan worden. In de toekomst kunnen dit soort weefsel gebaseerde *ex vivo* sensitiviteitstesten bijdragen aan het individualiseren van therapierespons voorspelling voor patiënten in de dagelijkse klinische praktijk.

In **hoofdstuk 3** beschrijven we de REpair CAPacity (RECAP) test, een functionele test die homologe recombinatie deficiënte (HRD) tumoren identificeert. Daarbij wordt gebruik gemaakt van ophoping van het RAD51 eiwit in prolifererende cellen na *ex vivo* bestraling van vers borstkanker weefsel. We laten in een groot cohort van primaire borstkankers zien dat deze test reproduceerbaar is. We beschrijven de grootste set (n=125) van verse

borstkanker weefsels waarop een functionele bepaling van de HR status werd uitgevoerd, die in de overgrote meerderheid van de gevallen (74%) succesvol bleek. Ongeveer tweederde van de HRD tumoren hadden een mutatie in een van de *BRCA* genen. De overige niet *BRCA* gemuteerde HRD tumoren lieten soms ook 'BRCAness' mutatie profielen zien. Door de grootte van dit cohort, konden we HRD associëren met hoge aantallen tumor infiltrerende lymfocyten (TILs) en microsatelliet instabiliteit (MSI). De voornaamste klinische implicatie van deze studie is het feit dat de RECAP test 50% meer patiënten kan identificeren die mogelijk baat hebben bij PARP remmers dan kiembaan *BRCA1/2* mutatie analyse en dat een deel van deze patiënten mogelijk ook baat hebben bij immunotherapie.

De functionele HR bepaling door middel van de RECAP test produceert een unieke 'real-time' maat van de HR status, zoals beschreven wordt in **hoofdstuk 4**. HRD werd gevonden in 13 van de 41 geanalyseerde biopten (32%). Van deze 13 HRD biopten bevatten slechts vijf een kiembaan mutatie in *BRCA1/2*, wat aangeeft dat de RECAP test ongeveer 60% meer patiënten kan identificeren die baat kunnen hebben bij PARP remmers. In deze studie waren er drie patiënten met een kiembaan *BRCA1/2* mutatie, bij wie zowel voor als na therapie met dubbel strengs breuk inducerende chemotherapie een biopt was afgenomen. Door het bestuderen van dit weefsel ontdekten wij dat er een reversie van de HR status was opgetreden (van HR deficiënt naar HR proficiënt/intermediair), wat de behoefte voor functionele testen, gebaseerd op het tumor fenotype, zoals de RECAP test voor het voorspellen van tumor respons extra benadrukt. Bij één van deze drie patiënten werd een specifieke oorzaak van de reversie gevonden: er was sprake van een secundaire mutatie in *BRCA1* waardoor er weer functioneel *BRCA1* eiwit geproduceerd kon worden. Voor de andere twee patiënten is het resistentie mechanisme onbekend. De RECAP test herkent dus resistentie binnen *BRCA* gemuteerde tumoren, zonder dat de daadwerkelijke onderliggende oorzaak bekend hoeft te zijn. De RECAP test heeft daarom potentie om gevoeligheid voor dubbelstrengs breuk inducerende chemotherapie en PARP remmers te voorspellen in patiënten met gemetastaseerd borstkanker, die al met meerdere lijnen chemotherapie behandeld zijn, wat mogelijk HR reversie tot gevolg heeft gehad.

In **hoofdstuk 5**, werden in een groot cohort (n=71) van borstkanker patiënten de reeds bekende functionele HR status, bepaald door de RECAP test, vergeleken met de resultaten van HRD testen gebaseerd op "genomische littekens" als teken van HR deficiëntie (*BRCA1/2*-like classificatie en CHORD). Voor een deel van de tumoren (n=54) werd de sequentie van het gehele genoom bepaald om het HRD fenotype, en met name de niet *BRCA* gemuteerde HRD tumoren, verder te onderzoeken. Het bleek dat slechts de helft van de niet *BRCA* gemuteerde RECAP-HRD tumoren ook HRD werd bevonden door een andere HRD test. *In vivo* therapie respons was bekend voor enkele tumoren. De belangrijkste conclusie van dit hoofdstuk is dat verschillende HRD testen niet precies dezelfde populatie patiënten identificeren (60-70% concordantie tussen de testen). In de toekomst zullen meerdere HRD testen toegepast moeten worden in klinische studies om te bepalen hoe goed zij *in vivo* respons van patiënten

kunnen voorspellen, aangezien er op basis van de huidige gegevens nog niet één ultieme HRD test gekozen kan worden.

Hoofdstuk 6 beschrijft de ontwikkeling van een gevoeligheidstest voor een ander antikanker middel, te weten cisplatine, door *ex vivo* behandelingen uit te voeren op weefselplakjes van biopten van gemetastaseerde borstkanker laesies. Dit heeft zowel technische als klinische implicaties. Ten eerste, dit hoofdstuk beschrijft dat *ex vivo* gevoeligheidstesten ook op weefselplakjes van kleine histologische biopten technisch haalbaar is en niet alleen op grotere stukken resectiemateriaal zoals in eerdere studies. Ten tweede, de *ex vivo* gevoeligheden werden vergeleken met *in vivo* respons van patiënten. De cisplatine *ex vivo* gevoeligheidstest meet de respons van de tumor van een individuele patiënt op een bepaalde behandeling, in plaats van het voorspellen van de respons op basis van predictieve factoren die over het algemeen correleren met een betere uitkomst.

De resultaten van een functionele homologe recombinatie (HR) screen in 54 borst- en 38 ovariumkanker cellijnen worden gepresenteerd in **hoofdstuk 7**. HRD werd gevonden in 19% (10/54) van de borst- en in 8% (3/38) van de ovariumkanker cellijnen. In deze cellijnen werd HRD in 77% (10/13) niet veroorzaakt door een BRCA defect. Eén niet BRCA gerelateerde cellijn bevatte een *EXO1* mutatie die mogelijk het intermediaire HR fenotype verklaart. Omgekeerd bleek van de BRCA gemuteerde cellijnen 56% van de borst- (5/9) en 38% van de ovariumkanker cellijnen OC (3/8) niet HRD. In vier van deze cellijnen werd een mogelijke oorzaak voor de discrepantie gevonden, zoals verlies van *SHLD2*. Verder onderzoek is onderweg om de discrepanties tussen BRCA mutatie status en functionele HR status te verklaren. BRCA deficiënte en/of HRD cellijnen kunnen onderling erg verschillen en niet elke BRCA gemuteerde cellijn vertegenwoordigt BRCA deficiënte of HRD tumoren. Aangezien deze cellijnen voor veel verschillende soorten experimenten gebruikt worden als modelsystemen in alle mogelijke onderzoeksvelden, is het erg belangrijk dat men zich realiseert dat de specifieke cellijn die gebruikt wordt de conclusies van het experiment enorm beïnvloedt.

In conclusie, de studies in dit proefschrift maken gebruik van functionele testen op tumor weefsel om zo bij borstkanker patiënten beter de respons op chemotherapie of PARP remmers te verbeteren. Dit is een nieuwe vorm van biomarker ontwikkeling: de daadwerkelijk respons van een individueel borstkanker weefselplakje op *ex vivo* behandeling met geneesmiddelen of bestraling wordt gemeten. In de toekomst kunnen deze weefsel gebaseerde *ex vivo* gevoeligheidstesten therapierespons voorspelling individualiseren voor patiënten in de dagelijkse praktijk.

Curriculum Vitae

Name: Titia Geertje Meijer
 Address: Bentincklaan 330, 3039 KK, Rotterdam,
 The Netherlands
 Telephone: +31-6-34866811
 E-mail: titia.meijer@gmail.com
 Date of birth: 22 November 1989
 BIG-number: 89919163101



Education

- 2015-2019 Arts-onderzoeker (PhD-student) 'Ex vivo assays for selection of breast cancer patients for PARP inhibitor treatment'
Promotor: Prof. Dr. R. Kanaar, Co-promotoren: Dr. D.C. Van Gent, Department of Molecular Genetics and Dr. A. Jager, Department of Medical Oncology, Erasmus Medisch Centrum, Rotterdam
- 2010-2015 MSc Molecular Medicine
Erasmus Medisch Centrum, Rotterdam
- 2011-2014 MSc Medicine
Erasmus Medisch Centrum, Rotterdam
- 2008-2011 BSc Medicine
Erasmus Medisch Centrum, Rotterdam
- 2007-2008 Fulbright Campus Scholarship Program
 'Letter of mastery in International business communication'
University of Oregon, Eugene, USA
- 2001-2007 Grammar school (cum laude)
 Profiles: Nature & Health and Nature & Technology
Gymnasium Coleanum, Zwolle

List of publications

First author publications

RECAP identifies homologous recombination deficiency in breast cancers undetected by DNA-based BRCAness tests **Titia G. Meijer**, Luan Nguyen, Arne van Hoeck, Kirsten Ruigrok-Ritstier, Anieta M. Sieuwerts, Nicole S. Verkaik, Carolien H.M. van Deurzen, Harmen J. G. van de Werken, Esther Lips, Sabine C. Linn, Roland Kanaar, John Martens, Edwin Cuppen, Agnes Jager and Dik C. van Gent. (submitted for publication)

Functional RAD51 based HRD screen of breast and ovarian cancer cell lines **Titia G. Meijer**, Antoinette Hollestelle, Corine Beaufort, Saskia Wilting, Marcel Smid, Nicole S. Verkaik, Roland Kanaar, Agnes Jager, Dik van Gent, John W.M. Martens. (in preparation)

Ex vivo tissue-based cisplatin sensitivity testing on metastatic breast cancer biopsies, **Titia G. Meijer**, Nicole S. Verkaik, Carolien H.M. van Deurzen, Michael A. den Bakker, Marieke van de Ven, Jos Jonkers, Roland Kanaar, Dik C. van Gent and Agnes Jager. (in preparation)

Direct ex vivo observation of homologous recombination defect reversal after DNA damaging chemotherapy in metastatic breast cancer patients, **Titia G. Meijer**, Nicole S. Verkaik, Carolien H.M. van Deurzen, Hendrikus-Jan Dubbink, T. Dorine den Toom, Hein F.B.M. Sleddens, Esther Oomen-De Hoop, Winand N.M. Dinjens, Roland Kanaar, Dik C. van Gent and Agnes Jager, JCO Precision Oncology, doi: 10.1200/PO.18.00268 JCO Precision Oncology. Published online March 11, 2019

BRCA en BRCAness, **T.G. Meijer**, S. Vlieg, D.C. van Gent, S.C. Linn, A. Jager, NTVO, December 2018

Functional ex vivo assay reveals homologous recombination deficiency in breast cancer beyond BRCA gene defects, **Titia G. Meijer**, Nicole S. Verkaik, Anieta M. Sieuwerts, Job van Riet, Kishan A.T. Naipal, Carolien H.M. van Deurzen, Michael A. den Bakker, Hein F.B.M. Sleddens, Hendrikus-Jan Dubbink, T. Dorine den Toom, Winand N.M. Dinjens, Esther Lips, Petra M. Nederlof, Marcel Smid, Harmen J. G. van de Werken, Roland Kanaar, John W. M. Martens, Agnes Jager and Dik C. van Gent, Clin Cancer Res. 2018 Dec 15;24(24):6277-6287. doi: 10.1158/1078-0432.CCR-18-0063. Epub 2018 Aug 23.

Ex vivo tumor culture systems for functional drug testing and therapy response prediction, **Titia G. Meijer**, Kishan A.T. Naipal, Agnes Jager and Dik C. van Gent, Future Science OA, May 2017, 3(2), pp:FSO190

Other publications

Ex vivo treatment of prostate tumor tissue recapitulates in vivo therapy response, Zhang W, van Weerden WM, de Ridder CMA, Erkens-Schulze S, Schönfeld E, **Meijer TG**, Kanaar R, van Gent DC, Nonnekens J, Prostate. 2019 Mar;79(4):390-402. doi: 10.1002/pros.23745. Epub 2018 Dec 5.

Identification of novel determinants of resistance to lapatinib in ERBB2-amplified cancers, D Wetterskog, K-K Shiu, I Chong, **T Meijer**, A Mackay, M Lambros, D Cunningham, J S Reis-Filho, C J Lord and A Ashworth, Oncogene, Feb 2014;33(8):966-76

Down-staging (<pT2) of urothelial cancer at cystectomy after the diagnosis of detrusor muscle invasion (pT2) at diagnostic transurethral resection (TUR): is prediction possible? W. Beukers, **T. Meijer**, C. Vissers, J. Boormans, E. Zwarthoff en G. van Leenders, Virchows Archive, Aug 2012;461:149-56

PhD Portfolio

Summary of PhD training and teaching

Name:	Titia Geertje Meijer
Erasmus MC department:	Molecular Genetics
Research School:	Medical genetics Center (MGC)
Promotor:	Prof. dr. R. Kanaar
Co-promotors:	Dr. D.C. van Gent and Dr. A. Jager
PhD period:	2015-2019

1. PhD training / courses (13.8 ECTS)

	Date	Workload (ECTS)
Biomedical English Writing and Communication A1	Fall 2018	3 ECTS
Biostatistical Methods I: Basic Principles Part A	September 2017	2 ECTS
Research Integrity	August 2017	0.3 ECTS
BROK cursus: Certificate Good Clinical Practice for Clinical Investigators, CPO board certificate	December 2016	1.5 ECTS
Genetics course (PhD Teaching Program of Biomedical Sciences)	May 2016	3 ECTS
Special topic course on Chromatin (PhD Teaching Program of Biomedical Sciences)	December 2015	0.3 ECTS
Stralingsbescherming deskundigheidsniveau 5B (Radiation protection level 5B)	November 2015	1 ECTS
Veilig Werken in laboratoria (Laboratory Safety course)	November 2015	0.3 ECTS
OIC Course Functional Imaging and Super Resolution	October 2015	1 ECTS
Next Generation Sequencing (NGS) data analysis (Medical Genetics Centre South-West Netherlands)	September 2015	1.4 ECTS

2. Symposia and conferences (18.5 ECTS)

Oral presentations	Date	Workload (ECTS)
<i>De ex vivo CDDP gevoeligheidstest: van bench to bedside</i> , Borstkanker Behandeling Beter symposium, Rotterdam	September 2019	0.3 ECTS
<i>De RECAP test, klaar voor de kliniek?</i> , Borstkanker Behandeling Beter symposium, Rotterdam	September 2018	0.3 ECTS
Invited lecture: <i>Detection of homologous recombination deficiency in breast cancer</i> , Joint Meeting of the British Division of the International Academy of Pathology and the Pathological Society of Great Britain & Ireland, Maastricht	June 2018	1.5 ECTS
<i>De RECAP test, klaar voor de kliniek?</i> , Regionale Borstkanker research meeting, EMC, Rotterdam	May 2018	0.2 ECTS
<i>RECAP test: ready for the clinic?</i> , EORTC Gynecologic Cancer Group, Amsterdam	March 2018	0.3 ECTS
<i>RECAP test: ready for the clinic?</i> , Cancer Genomics Center Annual Scientific meeting, Utrecht	January 2018	0.3 ECTS
<i>Ex vivo validation of PET imaging for response assessment of NSCLC tumors</i> , Research Day Radiation Oncology, EMC, Rotterdam	June 2017	0.2 ECTS

<i>RECAP test: ready for the clinic?</i> , Scientific meeting Medical Oncology / Wetenschapsmiddag, EMC, Rotterdam	June 2017	0.3 ECTS
<i>Homologous recombination deficiency (HRD) test in breast cancer</i> , Oncology research meeting, UMCG, Groningen	January 2017	0.5 ECTS
<i>Bringing the RAD51 IRIF assay (HRD test) into the clinic</i> , MCG meeting of DNA repair group, LUMC, Leiden	February 2016	0.3 ECTS
Multiple Alpe d'Huzes consortia meetings, Breast Cancer Research meetings, work discussions and journal clubs		1 ECTS

Poster presentations	Date	Workload (ECTS)
<i>Ex vivo tissue-based cisplatin sensitivity testing on metastatic breast cancer biopsies</i> , Benzon Symposium 65 – Targeting Breast and Ovarian Cancers: From Basic Research to Novel Treatment Strategies, Copenhagen, Denmark	September 2019	1.5 ECTS
<i>Direct ex vivo observation of homologous recombination defect reversal after DNA damaging chemotherapy in metastatic breast cancer patients</i> , San Antonio Breast Cancer Symposium (SABCS), USA	December 2018	1.5 ECTS
<i>Functional homologous recombination REpair CAPacity (RECAP) test in metastatic breast cancer biopsies</i> , EACR25 congress, Amsterdam	July 2018	1.5 ECTS
<i>Breast Cancer Ex vivo Anthracycline Sensitivity Test (BREAST) using organotypic tissue slices from core needle biopsies</i> , Joint Meeting of the British Division of the International Academy of Pathology and the Pathological Society of Great Britain & Ireland, Maastricht	June 2018	0.5 ECTS
<i>Functional homologous recombination REpair CAPacity (RECAP) test in metastatic breast cancer biopsies</i> , San Antonio Breast Cancer Symposium (SABCS), USA	December 2017	1.5 ECTS
<i>Functional homologous recombination REpair CAPacity (RECAP) test in metastatic breast cancer biopsies</i> , KWF Cancer Biology meeting, Lunteren	October 2017	0.7 ECTS
<i>Neoadjuvant BREAST study – Breast cancer ex vivo anthracycline sensitivity test</i> , MGC PhD workshop (Leuven)	June 2017	0.5 ECTS
<i>Functional ex vivo drug sensitivity assays on breast cancer tumor and biopsies slices</i> , NC3Rs Workshop: Human tissue models for cancer research, London	March 2017	1.5 ECTS
<i>Functional ex vivo assays for selection of breast cancer patients for PARP inhibitor treatment</i> , 10th Quinquennial conference, Responses to DNA damage: from molecule to disease, Egmond aan Zee	April 2016	0.7 ECTS

Attendance	Date	Workload (ECTS)
Oncode annual scientific meeting, Amsterdam	January 2019	0.3 ECTS
17e NABON-BOOG symposium, Driebergen-Zeist	April 2018	0.3 ECTS
Symposium BRCAdemy, Dordrecht	April 2018	0.2 ECTS
Cancer Genomics Center Annual Scientific meeting, Utrecht	January 2017	0.3 ECTS
Borstkanker Behandeling Beter symposium, Rotterdam	September 2017	0.2 ECTS
MGC PhD workshop, Dortmund	June 2016	0.3 ECTS
Research Day Radiation Oncology, EMC, Rotterdam	June 2016	0.3 ECTS
Cancer Genomics Center annual meeting, Amsterdam	November 2015/2016	0.6 ECTS



2nd transatlantic conference on personalized medicine, EMC, Rotterdam	October 2015	0.3 ECTS
26 th /27 th /28 th MGC symposium, Rotterdam/Leiden	September 2016/2017/2018	0.9 ECTS
<hr/>		
Grants and awards	Date	
Travelgrant 'Simons Foundation Fund' 800€	December 2018	
Selected to speak with Her Majesty Queen Máxima at the official launch of the Onco Institute	February 2018	
Travelgrant 'Erasmus MC Trustfund' 500€	December 2017	
Best presentation at Scientific meeting Medical Oncology, EMC, Rotterdam	June 2017	
<hr/>		
3. Teaching activities (4.2 ECTS)		
<hr/>		
Supervision during practicals	Date	Workload (ECTS)
BSc Nanobiology – assistance during practicals	October 2016, 2017 and 2018	1 ECTS
'Vaardigheidsonderwijs Klinische Casus: Fanconi Anemie' for medical students	November 2016	0.5 ECTS
<hr/>		
Supervision of students	Date	Workload (ECTS)
MSc Biotechnology	2017	2 months (0.5 ECTS)
MSc Molecular Medicine/Medical school	2017	6 months (1.0 ECTS)
BSc Nanobiology	2017	4 months (0.7 ECTS)
MSc Technical Physics	2015	3 months (0.5 ECTS)
<hr/>		

Total 2015-2019 (36.5 ECTS)

Dankwoord

In de wetenschap, streven we altijd naar zo veel mogelijk 'exposure'. We presenteren liever voor een volle zaal, we hopen dat er veel mensen naar onze poster komen kijken en het is van belang dat onze papers zo veel mogelijk gelezen en geciteerd worden. De laatste pagina's van dit proefschrift zijn misschien de minst wetenschappelijke, maar hoogstwaarschijnlijk wel de meest gelezen en daarom zeker niet minder belangrijk. De eindstreep is in zicht en de tijd is aangebroken om aan een nieuw avontuur te beginnen, maar niet voordat ik iedereen bedankt heb die op wat voor wijze dan ook geholpen heeft met het tot stand komen van dit proefschrift.

Allereerst wil ik mijn promotor bedanken, prof. Dr. Kanaar. Beste Roland, hartelijk dank voor de gelegenheid om een promotietraject te starten op de afdeling Moleculaire Genetica. Ik heb met veel plezier aan dit onderzoek gewerkt. Ik wil je bedanken voor al je kritische vragen en opmerkingen tijdens werkbesprekingen. Ik heb me altijd verbaasd over hoe snel je feedback op een manuscript kon geven. Ook heb je mij enorm geholpen om focus te houden tijdens mijn onderzoek. Ik hoop ook in de toekomst met je te kunnen samenwerken.

Dan volgt co-promotor Dr. Van Gent. Beste Dik, bedankt voor de vrijheid die je mij gegeven hebt om binnen de kaders van het promotieonderzoek mijn weg te vinden en invulling te geven aan het project. Je stond altijd voor me klaar als ik iets wilde overleggen of vragen. Daarnaast kon ik er ook altijd op vertrouwen dat jij bij werkbesprekingen nieuwe, innovatieve ideeën zou opperen. Ik waardeer het ook zeer dat ik ons onderzoek breder kenbaar heb mogen maken door verschillende buitenlandse congressen te bezoeken. Heel veel dank!

En natuurlijk co-promotor Dr. Jager. Beste Agnes, bedankt voor jouw steun en begeleiding! Het was erg leerzaam om onder jouw begeleiding protocollen te schrijven voor de verschillende studies die nu lopen. Bij het schrijven van artikelen of voorbereiden van presentaties, houd ik altijd de tips in mijn achterhoofd die je mij door de jaren heen gegeven hebt. Het hoogtepunt van mijn promotietraject was denk ik toch ons overleg met Pfizer tijdens de SABCS in 2017, waar de eerste stap werd gezet richting de FUTURE studie, die ons hopelijk de lang verwachte antwoorden gaat geven over de klinische waarde van onze test. Verder ben ik je dankbaar voor de gelegenheid die je mij geboden hebt om onze onderzoeksresultaten te presenteren op verschillende symposia. Ik waardeer jouw manier van werken, efficiënt, maar met oog voor detail. En altijd met het belang van de patiënt voorop. Ik heb jou tijdens mijn gehele promotietraject als voorbeeld gezien. Ik hoop uiteindelijk ook, net als jij, onderzoek te kunnen combineren met de werkzaamheden als arts. Bedankt voor de kansen die je mij gegeven hebt!

Beste leden van de leescommissie, Prof. Dr. Martens, prof. Dr. Van Vugt en Dr. Van Deurzen, veel dank voor het zorgvuldig lezen van mijn proefschrift.

Prof. Dr. Martens, beste John, ik heb voor mijn master stage jouw lab gekozen en daarna is het contact gebleven. Ik wil je bedanken voor de prettige samenwerking en het feit dat ik altijd met mijn vragen bij je terecht kon. Tijdens mijn onderzoek heb ik voor verschillende projecten nog met collega's uit jouw lab samen mogen werken. Kirsten, Antoinette, Corine, Lindsay, Marcel en Saskia, heel veel dank voor jullie hulp met vriesweefsels, cellijnen, analyses en andere praktische zaken. In het bijzonder wil ik ook mijn dank betuigen aan Anieta, jouw plotselinge overlijden aan het einde van mijn PhD traject was een grote schok, ik heb veel van je geleerd en heb onze samenwerking altijd als zeer prettig ervaren.

Zonder goede samenwerking met vele klinici zou ons onderzoek nooit mogelijk zijn geweest. Daarom wil ik hier graag alle artsen bedanken die betrokken zijn geweest, in het bijzonder: Carolien van Deurzen, Michael Den Bakker, Linetta Koppert en Cecile de Monye. Daarnaast wil ik ook graag alle pathologen en medewerkers van de uitsnijkamer van de afdeling pathologie, zowel in het Erasmus MC als in het Maasstad ziekenhuis bedanken voor de hulp bij het verzamelen van studiemateriaal. Ook alle radiologen en laboranten die betrokken zijn geweest bij het afnemen van studiebiopten, ontzettend bedankt! Bovenal wil ik de patiënten bedanken die deel hebben willen nemen aan onze studies.

Dit project maakt deel uit van het Alpe d'Huzes consortium "Ex vivo assays for selection of breast and ovarian cancer patients for PARP inhibitor treatment", alle betrokken collega's uit Leiden, Amsterdam en Groningen wil ik graag bedanken voor de prettige samenwerking. In het bijzonder Maaïke, Harry en Lise, bedankt voor de vele vruchtbare overleggen en Maaïke, bedankt dat ik altijd met mijn vragen over VUSen bij je terecht kon.

Voor meerdere hoofdstukken in dit proefschrift zijn we afhankelijk geweest van de expertise van de Moleculaire Pathologie. Beste Winand, Erik Jan, Dorine en Hein, hartelijk dank voor jullie hulp en de enthousiaste samenwerking. Zonder Dorine hadden we nooit DNA analyses kunnen uitvoeren op samples waarvan er maar heel weinig materiaal beschikbaar was.

Medewerkers van het clinical trial center, beste Nelly en Loes, dankjulliewel voor het behouden van het overzicht van onze bioptenstudies. Jullie oog voor detail blijft ongeëvenaard en is essentieel bij dit soort studies. Medewerkers van het secretariaat, beste Jasperina, Sonja, Rachel, Marcella en Rosita, hartelijk dank voor al jullie hulp bij verschillende praktische zaken door de jaren heen. Beste Koos, Leo, Nils en Sjozef, bedankt voor de technische ondersteuning.

Dan wil ik natuurlijk mijn collega's van lab 663, ofnee 702, bedanken voor de hulp met verschillende experimenten, maar vooral voor de gezellige werksfeer en initiatieven om altijd wel wat leuks te ondernemen! Natuurlijk Anja, Hanny en Nicole, Danny en Marjolijn, maar ook nieuwkomers Ben en Thom, veel dank! Ontzettend veel dank voor jullie praktische hulp en kennis, maar natuurlijk vooral voor jullie gezelligheid! Hanny, je hebt mij enorm geholpen met de BRCA western blots, zonder jou had ik dat niet zo snel lopend kunnen krijgen. Je bent altijd zo behulpzaam en lief, je staat voor iedereen klaar. Ontzettend bedankt!

En ook mijn hok-genoten: Janette, Alex, Sanjiban, Maayke en Stefan. De samenstelling is door de jaren heen wel wat veranderd, dus ik wil ook graag oud-collega's: Joyce, Nathalie, Kishan en Wenhao bedanken! Wenhao en Stefan, we zijn zo'n beetje tegelijk begonnen. Wenhao heeft het spits afgebeten en nu mag ik volgen, Stefan veel succes met de laatste loodjes! Julie, jij telt ook als oud-hokgenoot! Ik wil je ook ontzettend bedanken voor alle gesprekken die wij hebben gevoerd. Ik vind het knap hoe jij het moederschap combineert met het opbouwen van een wetenschappelijke carrière! Ik kan alleen maar hopen dat het mij ook gaat lukken!

Dan wil ik nog graag de mensen van de verschillende labs op de 7^e bedanken voor advies en praktische zaken door de jaren heen, en specifiek ons buur-lab met Nicole van Vliet, Cecile, Yanto en Nathalie.

Levi, Winnie, Nikita, Diego en Edgar, ik heb jullie tijdens verschillende stages in het lab (mede-) mogen begeleiden. Dankjulliewel voor jullie enthousiasme en inzet! Levi en Winnie, heel veel succes met jullie PhD!

Dan rest mij natuurlijk nog mijn paranimfen te bedanken: Nicole en Marjolijn. Beste Nicole, heel veel dank voor de intensieve samenwerking de afgelopen jaren! We vormden een goed team en volgens mij hebben we samen mooie resultaten bereikt! Zonder jouw ervaring en expertise had ik dit project nooit zo soepel kunnen overnemen van Kishan. Je bent altijd zo heerlijk enthousiast en ik heb met veel plezier met je samengewerkt. Ik hoop dat je nog vele jaren met plezier werkt, ook al is dat niet meer volledig op het borstkankerproject. Beste Marjolijn, we hebben ongeveer 2 jaar samen aan dit project mogen werken. Ik wil je bedanken voor je toewijding en voor onze gezamenlijke reflectiemomentjes en gezellige babbels. Ik wens je heel veel succes en vooral plezier bij het afronden van je PhD. Ik ben ontzettend benieuwd wat er in de FUTURE voor ons in het verschiet ligt ;).

Lieve familie en vrienden, de laatste paragrafen zijn voor jullie. Het afgelopen jaar is een bijzondere geweest, met weinig tijd voor andere zaken dan zorgen dat dit proefschrift op tijd af kwam en zorgen dat Krijn groter werd. Dit proefschrift is nu af en Krijn al aanzienlijk groter, dus langzaam komt er weer meer tijd vrij voor gezelligheid! Sahar, Rob, Floor & Martijn, Burc, Debbie en Fatma, oftewel Co-groep Lingo: wat hebben we altijd een lol samen. Dankjulliewel voor alle gezellige momenten met spinazieflapjes, barbecuemasters, borek en pannenkoeken!! Natasja en Boukje, dankjulliewel voor onze mooie vriendschap die in de collegebanken is ontstaan. Ik waardeer dat jullie altijd interesse hebben getoond in mijn onderzoek en ik hecht veel waarde aan onze gezellige momenten samen. Celeanummeiden, Marijke, Lianne, Marloes, Eline, Anna, Eleonore en Hanne, wat kennen wij elkaar al lang! Als we elkaar zien is het altijd als vanouds gezellig! Dankjulliewel voor jullie vriendschap!

Lieve Mirjam, papa en mama, dankjulliewel voor jullie oneindige steun en toeverlaat. Jullie staan altijd voor ons klaar en ook op momenten dat ik door de bomen het bos niet meer zie, weten jullie alles altijd weer te relativiseren. Jullie hebben mij het belang van een positieve instelling en hard werken meegegeven. Richard, Anita en Wendy, ik wil jullie bedanken voor jullie steun. Ik voel me altijd thuis bij jullie en waardeer jullie hulp ontzettend. It takes a village to raise a child, toch? Corrie en Juno, dank voor jullie belangstelling tijdens mijn promotietraject en steun bij mijn ontdekkingsreis in het moederschap. Oma Lum en opa Leo, wat ben ik trots dat ik nog een oma heb en dat Krijn zelfs nog een overgrootoma én overgrootopa heeft! Lieve Tim en Krijn, mijn mannen. Tim, je bent mijn rots in de branding en ik wil niets liever dan samen gelukkig oud worden. Nu is dat het afgelopen jaar al goed gelukt, dat ouder worden dan;) Krijn, je bent mijn kleine lachebek. Wat herken ik al veel van mijzelf in jou! Jullie zijn mijn alles.

